



# DIPLOMARBEIT

Titel der Diplomarbeit

„Synthesis and Biological Evaluation of Novel  
Combretastatin A-4 Analogs“

Verfasserin

Rita Fürst

angestrebter akademischer Grad

Magister der Naturwissenschaften (Mag. rer. nat.)

Wien, März 2009

Studienkennzahl lt.  
Studienblatt:

A 419

Studienrichtung lt.  
Studienblatt:

Diplomstudium Chemie

Betreuerin / Betreuer:

O.Univ.-Prof. Dr. Johann Mulzer



## Danksagung

An erster Stelle möchte ich meinem Diplomarbeitsbetreuer Dr. Uwe Rinner für seine fachliche Beratung und finanzielle Unterstützung während meiner Diplomarbeit danken. Mein Dank gilt auch Herrn Professor Johann Mulzer für das Aufzeigen neuer fachlicher Perspektiven.

Meine Kollegen und deren Ratschläge, wie die Chemie vielleicht besser funktionieren könnte, haben die Arbeit im vergangenen Jahr um vieles erleichtert. Besonders danke ich meinem Laborkollegen Mag. Christoph Lentsch, Mag. Christian Aichinger, Mag. Tina Nowikow, Jale Özgür und Martin Himmelbauer für die angenehme Arbeitsatmosphäre und den Spaß den wir hatten.

Doch viele andere Personen haben mit ihren Tipps meine Ergebnisse zu verbessern zum Fortschritt meiner Diplomarbeit beigetragen. Mein Dank gilt der gesamten Arbeitsgruppe Mulzer, Dr. Tanja Gaich, Mag. Kathrin Prantz, Mag. Thomas Magauer, Dipl.-Ing. Harald Weinstabl, Dipl.-Ing. Konrad Tiefenbacher, Dipl.-Ing. Andreas Gollner, Dipl.-Ing. Jürgen Ramharter, Dipl. Chem. Alexej Gromov, Mag. Stefan Marchart, Dr. Harry Martin, Dr. Peter Siengalewicz und Ing. Martina Drescher.

Vielen Dank auch der NMR-Abteilung, Dr. Hanspeter Kählig, Dr. Lothar Brecker und Susanne Felsinger sowie dem HPLC-Team Sabine Schneider und Dipl.-Ing. Fikret Nasufi.

Doch ohne meine Eltern, deren Unterstützung bei all meinen Vorhaben und Möglichkeiten die sie mir bis heute gegeben haben, wofür ich ihnen herzlich danke, wäre ich heute nicht da wo ich bin.

Zu guter Letzt danke ich meinem Bruder und Gertraud für aufbauende Worte wann immer sie notwendig waren und Ablenkung vom Unialltag sowie all meinen Freunden und Robert für die schöne Zeit und viel Verständnis, das er gegenüber meiner Arbeit aufgebracht hat.



## Table of contents

Table of contents .....	i
List of Figures .....	iii
List of Schemes .....	iv
List of Tables .....	vii
List of abbreviations .....	viii
1. General Part .....	1
1.1. Introduction.....	1
1.2. Aim of the synthetic work.....	3
1.3. Isolation .....	3
1.4. Structural related compounds.....	5
1.4.1. Phenanthrenes .....	5
1.4.2. Colchicine .....	7
1.5. Biological background .....	8
1.5.1. Tumorigenesis .....	8
1.5.2. The Cytoskeleton – Microtubules .....	10
1.5.3. Microtubules – their important role in mitosis .....	13
1.5.4. Antimitotic drugs .....	15
1.5.5. Microtubule-destabilizing agents .....	16
1.5.6. Microtubule-stabilizing agents .....	23
1.5.7. Antivascular effects .....	25
1.6. Combretastatins – Structure-Activity Relationship.....	27
1.7. Combretastatin analogs.....	28
1.8. Cyclopropane and cyclobutane synthesis .....	31
1.9. Cyclopropanes – a theoretical consideration.....	31
1.9.1. Synthesis of cyclopropane.....	32
2. Results and discussion.....	51
2.1. Synthesis of CA-4.....	51
2.1.1. Retrosynthetic analysis.....	51
2.1.2. Synthesis of the two aromatic fragments.....	51
2.1.3. Suzuki-Miyaura coupling reaction.....	52
2.2. Synthesis of CA-4-phosphate.....	54
2.3. Synthesis of the amino derivative AVE8062.....	55
2.4. Synthesis of cyclopropane derivative (268).....	57

2.5.	Synthesis of the cyclobutane derivative.....	60
2.5.1.	First approach – [2+2]-cycloaddition.....	60
2.5.2.	Second approach – Squaric acid.....	63
3.	Biological evaluation.....	65
3.1.	Results – HeLa cells.....	66
3.2.	Results – MCF 7 cells.....	68
4.	Conclusion and Outlook.....	71
5.	Experimental part.....	73
5.1.	General.....	73
5.2.	Procedures.....	75
References	.....	107
Abstract.....		113
Zusammenfassung.....		114
Curriculum Vitae.....		115

## List of Figures

Figure 1: Antineoplastic agents in clinical use .....	1
Figure 2: Structure of Combretastatin A-4 .....	2
Figure 3: Derivatives in clinical studies .....	2
Figure 4: Synthesis of CA-4 derivatives .....	3
Figure 5: Combretastatin family .....	4
Figure 6: Phenanthrene core structure .....	5
Figure 7: Examples of isolated phenanthrenes .....	6
Figure 8: Phenanthrenes isolated from <i>Combretum cafferum</i> .....	6
Figure 9: Colchicine .....	7
Figure 10: Colchicine derivatives .....	8
Figure 11: Atropisomers of colchicine .....	8
Figure 12: Microtubule formation <sup>36</sup> .....	12
Figure 13: Cell cycle .....	14
Figure 14: Vinca alkaloids used in clinical therapy .....	17
Figure 15: Derivatives of the vinca alkaloids in clinical use .....	18
Figure 16: Compounds binding on the vinca domain I .....	20
Figure 17: Compounds binding on the vinca domain II .....	20
Figure 18: Compounds binding on the vinca domain III .....	21
Figure 19: Compounds binding on the vinca domain IV .....	21
Figure 20: Structure of colchicine .....	22
Figure 21: Compounds binding at the colchicine binding site .....	23
Figure 22: The epothilones and derivatives in clinical use .....	25
Figure 23: Vascular disrupting agents (VDAs) .....	27
Figure 24: CA-4 analogs for SAR-studies .....	28
Figure 25: CA-4 analogs I .....	29
Figure 26: CA-4 analogs II .....	30
Figure 27: Coulson-Moffitt model of cyclopropane .....	32
Figure 28: Walsh model of cyclopropane .....	32
Figure 29: Chiral ligands for asymmetric Simmons-Smith reaction .....	45
Figure 30: Biologically active compounds synthesized within this work .....	71
Figure 31: Cyclobutane- and cyclopentane derivative of CA-4 .....	72

## List of Schemes

Scheme 1: Semisynthetic route of taxol and docetaxel .....	24
Scheme 2: 1,3-Elimination of two heteroatoms I.....	33
Scheme 3: 1,3-Elimination of two heteroatoms II.....	33
Scheme 4: 1,3-Elimination of two heteroatoms III.....	33
Scheme 5: 1,3-Elimination of two heteroatoms IV .....	34
Scheme 6: 1,3-Elimination of two heteroatoms V .....	34
Scheme 7: 1,3-Elimination of two heteroatoms VI .....	34
Scheme 8: 1,3-Elimination of two heteroatoms VII .....	34
Scheme 9: 1,3-Elimination of two heteroatoms VIII .....	35
Scheme 10: Cyclopropane synthesis <i>via</i> S <sub>N</sub> 2 displacement I.....	35
Scheme 11: Cyclopropane synthesis <i>via</i> S <sub>N</sub> 2 displacement II.....	36
Scheme 12: Cyclopropane synthesis by intramolecular epoxide opening .....	36
Scheme 13: Synthesis of chrysanthemic acid derivative .....	37
Scheme 14: Substitution initiated ring-closure reaction (SIRC) .....	37
Scheme 15: Michael initiated ring closure reaction (MIRC) .....	38
Scheme 16: Hyperconjugation in MIRC reactions .....	38
Scheme 17: Dichlorocarbene formation.....	39
Scheme 18: Reaction of dichlorocarbene .....	40
Scheme 19: Reaction of dibromocarbene.....	40
Scheme 20: Reaction of triplet carbenes .....	40
Scheme 21: Cyclopropanation with diazomethane .....	41
Scheme 22: Diastereoselective cyclopropanation with diazomethane I.....	41
Scheme 23: Diastereoselective cyclopropanation with diazomethane II.....	42
Scheme 24: Asymmetric cyclopropanation of $\alpha,\beta$ -unsaturated aldehydes .....	42
Scheme 25: Furukawa modification of the Simmons-Smith reaction .....	43
Scheme 26: Cyclopropanation reaction of (Z)-allylic secondary alcohols .....	43
Scheme 27: Cyclopropanation reaction of (E)-allylic secondary alcohols.....	43
Scheme 28: Cyclopropanation of $\alpha,\beta$ -unsaturated acetals .....	44
Scheme 29: Asymmetric cyclopropanation of 1-alkenylboronic esters .....	44
Scheme 30: Cyclopropanation of allylic alcohols in presence of chiral ligands.....	44
Scheme 31: Cyclopropane synthesis <i>via</i> elimination of a one-atom fragment.....	45
Scheme 32: Cyclopropane synthesis by rearrangement of cyclobutyl cations I.....	46
Scheme 33: Cyclopropane synthesis by rearrangement of cyclobutyl cations II.....	46



Scheme 34: Cyclopropane synthesis in presence of an electron-donating and a leaving group .....	46
Scheme 35: Ring contraction of 2,2-dihalocyclobutanols .....	46
Scheme 36: Ring contraction in steroid synthesis .....	47
Scheme 37: Deazetization of 4,5-dihydro-3 <i>H</i> -pyrazoles.....	47
Scheme 38: Synthesis of optically active cyclopropanes.....	48
Scheme 39: Synthesis of optically active amino acid derivatives .....	48
Scheme 40: Cyclopropane synthesis <i>via</i> a cyclohexyl cation .....	48
Scheme 41: Photochemical <i>meta</i> -addition of anisole with cyclopentene.....	49
Scheme 42: Photochemical [2+2]-cycloaddition .....	49
Scheme 43: Orbitals of ketene and isocyanate for a thermal [2+2]-cycloaddition .....	50
Scheme 44: Dichloroketene formation from dichloroacetyl chloride .....	50
Scheme 45: [2+2]-cycloaddition of a cyclopentene derivative with dichloroketene.....	50
Scheme 46: Retrosynthesis of CA-4.....	51
Scheme 47: Corey-Fuchs reaction .....	51
Scheme 48: Synthesis of terminal alkyne 249 <i>via</i> a variation of the Bestmann-Ohira-sequence .....	52
Scheme 49: Synthesis of the aromatic fragment 250 .....	52
Scheme 50: Suzuki-Miyaura coupling reaction.....	52
Scheme 51: Synthesis of CA-4.....	54
Scheme 52: Synthesis of CA-4-P .....	54
Scheme 53: Coupling reaction to generate the precursor of AVE8062 .....	55
Scheme 54: Synthesis of AVE8062.....	56
Scheme 55: Cyclopropanation reaction.....	57
Scheme 56: Synthesis of cyclopropane derivative 268 .....	58
Scheme 57: Synthesis of the cyclopropane derivative of AVE8062 (273).....	59
Scheme 58: Synthesis of the cyclobutane derivative <i>via</i> [2+2]-cycloaddition .....	60
Scheme 59: [2+2]-cycloaddition on <i>trans</i> -stilbene .....	60
Scheme 60: [2+2]-cycloaddition on styrol .....	61
Scheme 61: [2+2]-cycloaddition on trimethoxystyrol .....	62
Scheme 62: [2+2]-cycloaddition on MOM-protected CA-4.....	62
Scheme 63: Retrosynthetic analysis of the squaric acid approach.....	63
Scheme 64: Squaric acid approach.....	63
Scheme 65: HeLa screen .....	66

Scheme 66: IC <sub>50</sub> value for CA-4 (HeLa cells).....	67
Scheme 67: IC <sub>50</sub> -value for the cyclopropane derivatives 1651 and 1654 (HeLa cells) .....	67
Scheme 68: MCF 7 screen .....	69
Scheme 69: IC <sub>50</sub> value for CA-4 (MCF 7 cells) .....	69
Scheme 70: IC <sub>50</sub> -value for the cyclopropane derivatives 1651 and 1654 (MCF 7 cells) .....	70

## List of Tables

Table 1: GI <sub>50</sub> -values of combretastatins <sup>86</sup> .....	27
Table 2: Synthesis of chrysanthemic acid derivative – cis/trans ratio .....	37
Table 3: Reaction conditions for the coupling reaction of CA-4 .....	53
Table 4: Reaction conditions for coupling reaction of AVE8062 synthesis .....	55
Table 5: Reaction conditions for the cyclopropanation reaction.....	57
Table 6: Reaction conditions [2+2]-cycloaddition, trans-stilbene .....	61
Table 7: Reaction conditions [2+2]-cycloaddition, styrol .....	61
Table 8: Reaction conditions [2+2]-cycloaddition, trimethoxystyrol .....	62
Table 9: Reaction conditions [2+2]-cycloaddition, MOM-protected CA-4.....	62
Table 10: Tested compounds .....	65
Table 11: IC <sub>50</sub> -concentrations, HeLa cells .....	68
Table 12: IC <sub>50</sub> -concentrations, MCF 7 cells .....	70

## List of abbreviations

ABC-proteins	ATP – binding Cassette Proteins
aq.	aqueous
ASG	Anion-Stabilizing Group
ATP	Adenosine Triphosphate
Boc	Di- <i>tert</i> -butyl dicarbonate
CA-4	Combretastatin A-4
CA-4-P	Combretastatin A-4 Phosphate
CAN	Ceric Ammonium Nitrate
<i>de</i>	Diastereomeric Excess
DIC	N,N'-Diisopropylcarbodiimide
DIPA	Diisopropylamine
DIPEA	N,N-Diisopropylethylamine (Hünig's base)
DMAP	4-(Dimethylamino)pyridine
DME	Dimethoxyethane
DMF	Dimethylformamide
DMSO	Dimethyl sulfoxide
dr	Diastereomeric Ratio
<i>ee</i>	Enantiomeric Excess
eq, equiv.	Equivalent
<i>et al</i>	Et alii (and others)
Et <sub>2</sub> O	Diethylether
Fmoc	Fluorenylmethyloxycarbonyl
GDP	Guanosindiphosphate
GTP	Guanosintriphosphate
HOAc	Acetic acid
HPLC	High Performance Liquid Chromatography
Hz	Hertz
IARC	International Agency Research on Cancer
IR	Infrared
LDA	Lithium diisopropylamine
LG	Leaving Group
MDR	Multi Drug Resistant
MIRC	Michael Initiated Ring-Closure

MOM	Methoxymethyl
MsCl	Mesylchloride
MTOC	Microtubule Organizing Center
NBS	N-Bromosuccinimide
<i>n</i> -BuLi	<i>n</i> -Buthyllithium
NCI	National Cancer Institute
NSCLC	Non-Small-Cell Lung Cancers
ppm	parts per million
QSAR	Quantitative Structure-Activity Relationship
r.t.	Room temperature
R <sub>f</sub>	Ratio of fronts (TLC)
SAR	Structure-Activity Relationship
sat.	Saturated
SIRC	Substitution Initiated Ring-Closure
SM	Starting Material
TBS	<i>t</i> -Butyldimethylsilyl
<i>t</i> -BuLi	<i>t</i> -Buthyllithium
TEA	Triethylamine
THF	Tetrahydrofuran
TLC	Thin Layer chromatography
TMS	Trimethylsilyl
TS	Transition State
VDA	Vascular-Disrupting Agents
VEGF	Vascular Endothelial Growth Factor
WHO	World Health Organization



# 1. General Part

## 1.1. Introduction

Today cancer is accountable for about 25% of deaths in developing countries and for 15% of all deaths worldwide and therefore, cancer is one of the leading health problems in our society.<sup>1</sup> According to statistics of the International Agency Research on Cancer (IARC) of the World Health Organization (WHO) 12.4 million incident cases of cancer were expected in 2008.<sup>2</sup> These impressive statistical data suggest that anti-tumor therapy is a very important research field today.

Cancer therapy includes surgery, radiotherapy and systematic chemotherapy. Chemotherapeutic drugs, so called cytostatic or cytotoxic agents, prevent cell division of malignant cancer cells and as a result lead to the death of these cells. Chemotherapeutics developed in the past 50 years have different points of action in human cells, show different biological effects, and have diverse chemical structures.<sup>1</sup>

One very important class of anti-tumor agents are natural products, so called antineoplastic agents, which combat the development of neoplasms. Structurally different natural products are in clinical use, for example the vinca alkaloids vinblastine (1) and vincristine (2), or taxol (3) (Figure 1) and the epothilones.<sup>3</sup>

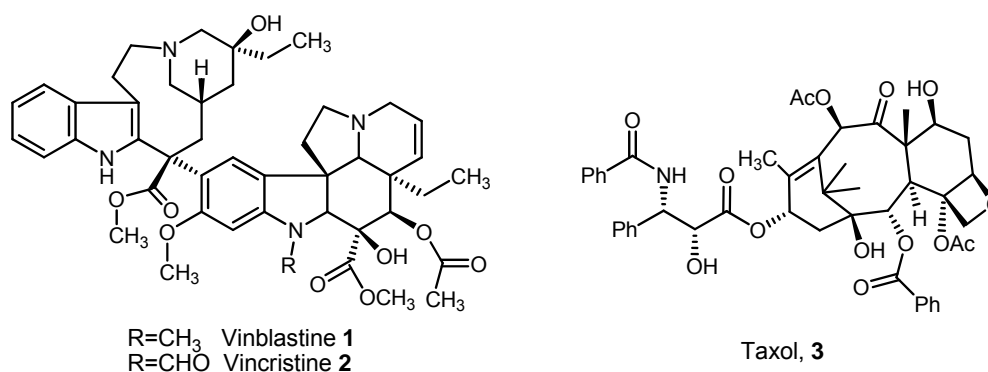
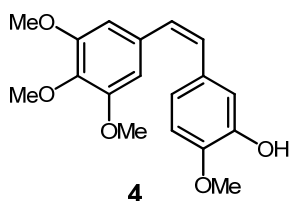


Figure 1: Antineoplastic agents in clinical use

In 1982 Pettit and co-workers isolated the *cis*-stilbene derivative combretastatin A-4 (CA-4, 4, Figure 2) from the bark of the African willow tree *Combretum caffrum*, which was found to be biologically most potent.<sup>4-6</sup>



**Figure 2: Structure of Combretastatin A-4**

The natural product shows cytotoxicity against a wide range of human cell lines, including multi drug resistant (MDR) cell lines. CA-4 binds to tubulin at the colchicin binding-site and inhibits microtubule-polymerization which leads to cell cycle arrest at the transition from meta- to anaphase and finally to apoptotic cell death.

In the past years several structure-activity relationship (SAR) studies were carried out and they all came to the same result, that CA-4 is only active in cis-form. Furthermore, the oxygenation pattern on the two aromatic ring systems is necessary for biological activity. Due to isomerization to the thermodynamically more stable trans-isomer and high lipophilicity, CA-4 shows low *in vivo* activity.<sup>7,8</sup>

Structural modifications are possible and several derivatives were synthesized, which show better *in vivo* activities than the natural product. Some derivatives used in clinical studies are shown below (**5-8**, Figure 3).<sup>9-12</sup>

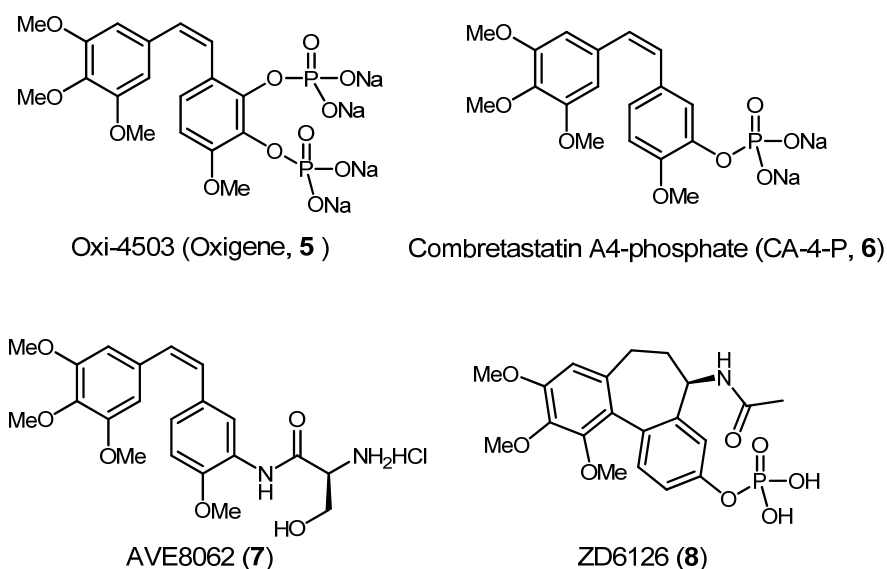


**Figure 3: Derivatives in clinical studies**



## 1.2. Aim of the synthetic work

The aim of our synthetic work is to increase the biological activity of the natural product CA-4 by modifying the *cis*-double bond. The incorporation of three- and four-membered carbocycles (**9**, **10**, Figure 4) prevents the *in vivo* isomerization of the *cis*-stilbene derivative to the thermodynamically more stable *trans*-isomer.

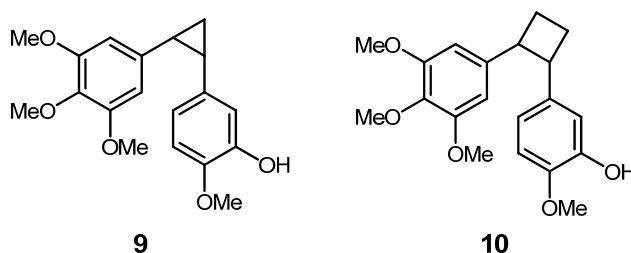
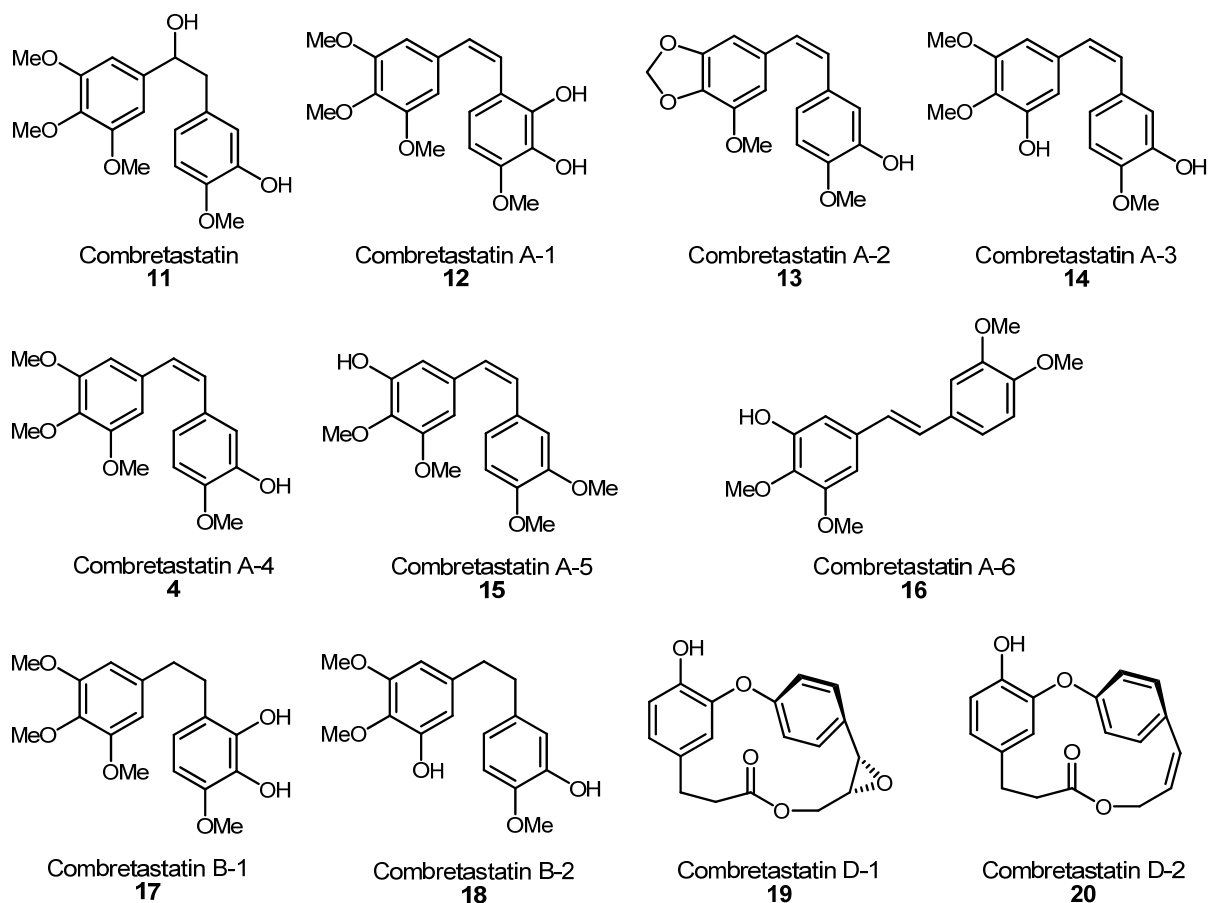


Figure 4: Synthesis of CA-4 derivatives

In the experimental part the syntheses of several biologically interesting cyclopropane derivatives *via* cyclopropanation with diazomethane are described in detail. Initial studies towards the synthesis of corresponding cyclobutane derivatives were carried out. However the approaches described herein could not be completed to date. Two later described approaches *via* [2+2]-cycloaddition and over the squaric acid cyclobutane building block did not come to an end.

## 1.3. Isolation

The *Combretaceae* plant family comprehends 20 genera and more than 600 species which are growing in tropical and subtropical regions as shrubs and trees. The genus *Combretum* was known centuries ago for its medicinal properties and was used in the primitive medical practice in Africa and India. In 1979 Pettit and co-workers started an investigation on the cytotoxic effects of compounds isolated from the bark of the African willow tree *Combretum cafrum* which are active against murine P-388 lymphocytic leukaemia.<sup>13,14</sup> In the following years natural compounds known as combretastatins were isolated from the bark of this African willow tree.<sup>4,6,13-17</sup>



**Figure 5: Combretastatin family**

Figure 5 shows the members of the combretastatin family (4, 11-20). All combretastatins except Combretastatin (11), A-6 (16), D-1 (19) and D-2 (20) have a *cis*-stilbene core structure. They show different substitution patterns of phenol- and methoxy-functionalities on the two aromatic ring systems which are connected over a two-carbon-bridge, with or without a double bond. Combretastatin D-1 and D-2 possess more complex structures; these are 17-membered macrocyclic lactones.

The combretastatins were all isolated following the same procedure. The isolation of CA-4, CA-5 and CA-6 is discussed below. First 77 kg of dry bark of *Combretum caffrum* was extracted with a methylene chloride-methanol mixture. This extraction was followed by a solvent partition sequence and a gel filtration of the methylene chloride extract through Sephadex LH-20. Subsequent column chromatography and further purification by HPLC gave a seemingly pure fraction. However, the data of  $^1\text{H}$ - and  $^{13}\text{C}$ -NMR pointed out that this fraction was a mixture of the three above-named stilbene derivatives. This mixed fraction was treated with TBS-Cl to get the silyl-ethers of the three components which could be separated by preparative thin layer chromatography.<sup>4,15</sup>

The combretastatins all show antimetabolic activity. Their presence in a cancer cell blocks the microtubule polymerization dynamics by binding on the colchicine binding site. Some members of this natural product family also show antivascular effects in tumor cells. These compounds are of additional interest because of their structural simplicity, and therefore can be easily prepared by synthetic means. CA-4 shows the most potent antitubulin effects. If CA-4 is used as an inhibitor of colchicine in an equimolar ratio, binding of colchicine at its binding site is inhibited by over 95% by CA-4.<sup>6</sup>

## 1.4. Structural related compounds

### 1.4.1. Phenanthrenes

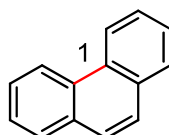
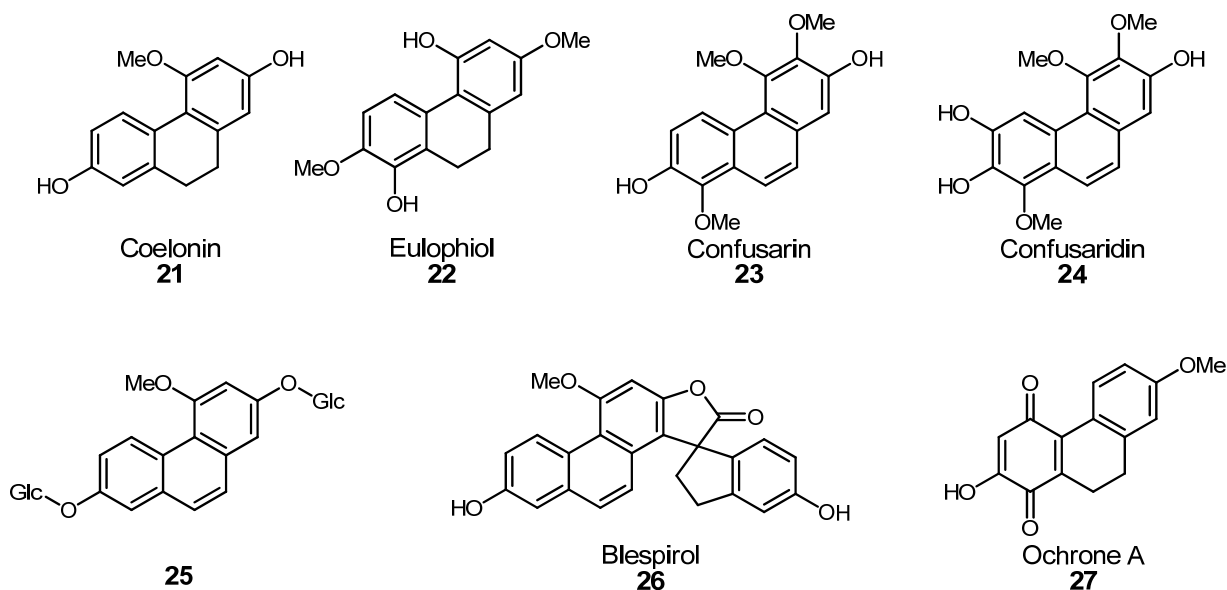


Figure 6: Phenanthrene core structure

Phenanthrenes and CA-4 show the same core-structure. Two aromatic ring systems are connected over a two-carbon-bridge. The only difference is that in phenanthrenes the two aromatic rings are stabilized over a single bond on ortho-position of the connecting bridge (Figure 6, structural motif 1)

The phenanthrenes isolated so far can be divided into three groups: mono- di- and triphenathrenes. Monophenathrenes can be subdivided according to different substitution patterns on the ring systems. Because of different connectivity of the phenanthrene subunits, diphenanthrenes can also be additionally classified. Up to this date only one isolated triphenanthrene is described in literature. Compounds without a double bond on the connecting carbon bridge are called dihydrophenanthrenes. Figure 7 shows only a few examples of known phenanthrenes and dihydrophenanthrenes (**21-29**).

Monophenanthrenes:



Di- and triphenanthrenes

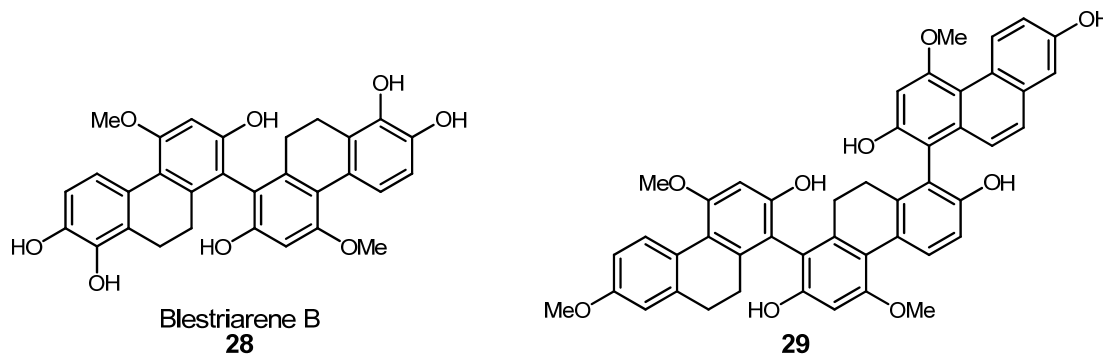


Figure 7: Examples of isolated phenanthrenes

In the past years a large number of phenanthrenes were isolated from higher plants, almost all from the *Orchidaceae* plant family and several dihydrophenanthrenes were also found in the African willow tree *Combretum caffrum*, (30-32, Figure 8). Their cytotoxicity was tested on murine P388 lymphocytic leukaemia cell lines representing  $IC_{50}$  values of an average of 2  $\mu\text{g/mL}$ .

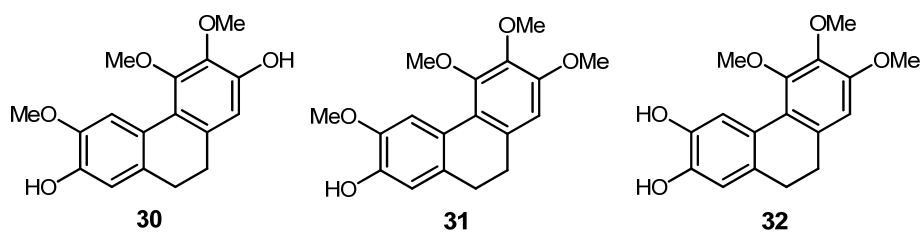
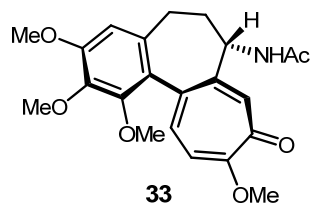


Figure 8: Phenanthrenes isolated from *Combretum caffrum*

Phenanthrens show different biological activities: anticancer effects, antimicrobial effects, spasmolytic effects, antiallergic- and anti-inflammatory activities.<sup>18</sup>

### 1.4.2. Colchicine



**Figure 9: Colchicine**

Colchicine (**33**, Figure 9) was isolated first in 1820 from the poisonous plant meadow saffron (*Colchicum autumnale L.*), also known as autumn crocus, by Pelletier and Caventou. The poisonous plant was known for more than 2000 years and was used in naturopathy in the treatment of acute gout. Up to present colchicine is applied in the therapy of gout and familial Mediterranean fever, but its high toxicity reduces its use in other therapies.<sup>19</sup>

Colchicine acts as an antimetabolic agent and binds to tubulin at the colchicine binding site. More precisely it interacts with the spindle microtubules during cell division. This interaction causes the destruction of the tubulin/microtubule polymerization dynamics and as a consequence mitosis is arrested in metaphase. This point of action in a living cell is a very interesting approach in cancer therapy because such compounds can be used for the selective damage of rapidly proliferating cancer cells.<sup>20</sup>

As mentioned above, colchicine cannot be used as a chemotherapeutic agent because of the high toxicity. In the past years several derivatives were synthesized with the fundamental goal to increase the biological activity of the natural product.<sup>21</sup>

Several QSAR (quantitative structure-activity relationship) studies were carried out but the toxicity could only scarcely be minimized. Thiocolchicine (**34**) and demecolcine (**35**), two colchicine derivatives (Figure 10), show similar activity and are employed in medical application.<sup>19</sup>

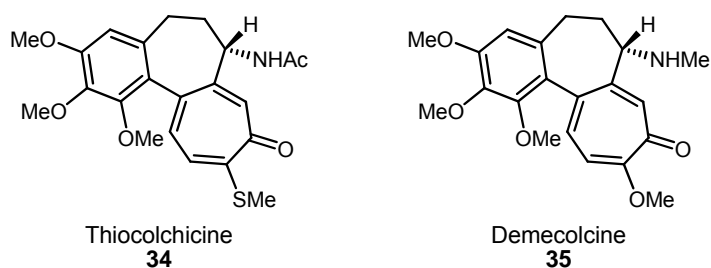


**Figure 10: Colchicine derivatives**

The development of new drugs that act in the same manner as colchicine is additionally complicated because the binding site and the mechanism which leads to the disruption of the microtubule polymerization dynamics is not completely elucidated.<sup>22</sup> It is known that colchicine binds irreversibly at a binding site at the  $\beta$ -tubulin subunit which leads to a partial unfold of the carboxy-terminus. This change in the secondary structure prohibits microtubule formation.<sup>23</sup> Also, the helical twist within the colchicine core structure is necessary for tubulin-binding. Berg *et al.* isolated the atropisomers of desacetamidocolchicine (*aR*-**36**, *aS*-**37**, Figure 11) and this research group was able to show that only the *aR* enantiomer is active and interacts with tubulin at the characteristic binding site.<sup>24</sup>

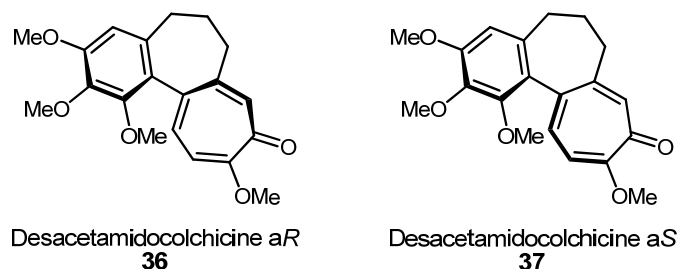


**Figure 11: Atropisomers of colchicine**

## 1.5. Biological background

### 1.5.1. Tumorigenesis

Tumorigenesis is a complex multistep process and starts with a single mutation in a single cell. The development of cancer can be considered as a microevolutionary process. The whole process is based on the Darwinian principles of evolution; mutations and natural selection have advanced the evolution of living organisms for billions of years.<sup>25</sup>

Cancer cells show two heritable characteristics: (1) reproduction is not stopped by the confinements of cell growth, which are common in a healthy cell. Tumor cells evolve mechanisms for uncontrolled cell division and (2) they invade and occupy areas normally arranged for other cells. Such aberrant cells that proliferate without consideration of cell growth signals give rise to a tumor or neoplasm. Cells at that cellular state are called neoplastic cells.<sup>26</sup> As long as these cells stay in their area or tissue the neoplasm is called benign tumor. A tumor is classified as cancer from the time when cells have achieved the ability to migrate into surrounding tissue; the tumor is called malignant. The competence to invade into other tissues is a crucial characteristic of cancer cells. They aim at the possibility to enter blood or lymphatic vessels and form secondary tumors at another area in the body, so called metastases. At that state of tumorigenesis, cancer is hard to be kept under control and metastases often kill the cancer patient.<sup>27,28</sup>

Cancer always starts with a primary tumor but a single mutation is not enough to cause cancer. There must be an appreciable number of independent genetic incidents during the lifetime of a single cell. Living organisms could not survive if just one mutation would transform a healthy cell into a rapidly proliferating tumor cell. Tumor progression is a multistep process, at each stage a cell gains a further mutation which affords a benefit over its neighbouring cells and an advance to invade in its environment. Repeated rounds of mutation and cell division follow, finally presenting a clone of malignant cancer cells. Each of these steps either enhances cell proliferation or decreases cell death in a single cell, so its progeny become the dominant clone in the tumor.<sup>29</sup>

When a tumor has reached a certain size it must create possibilities for an adequate blood supply to get the required oxygen and nutrients for its survival. This process is called angiogenesis. It is necessary to transmit angiogenetic signals. Within the cell pro-angiogenetic factors such as the *vascular endothelial growth factor* (VEGF) are activated and transcribed. The transcribed proteins are secreted out of the tumor cell, attract endothelial cells and start stimulation for the growth of new blood vessels. These newly formed blood vessels accommodate the tumor with nutrients and oxygen but they are also a possibility for the cancer cells to migrate from the original tissue to other regions of the organism. This is one way for tumor metastasizing.<sup>27,30</sup>

The human genome comprehends cancer-critical genes, which prevalently contribute to the development of cancer. These cancer-critical genes can be divided into two groups.

Genetic instability of proto-oncogenes leads to a gain-of-function mutation; too much activity of the gene product drives a cell toward cancer. The mutated and overexpressed forms of these genes are called oncogenes. The second class are tumor suppressor genes. A loss-of-function mutation can indicate the evolution of cancer.

One of the most important tumor-suppressor genes, which is mutated in nearly all human cancers, is the gene p53. This gene was named after the molecular mass of its protein product. The protein p53 is a cell cycle control protein and the loss of its activity is usually dangerous because it permits a cell with DNA-damage to pass through cell cycle and undergo mitosis. The second crucial point is that p53 mutated cells gain the ability to escape apoptosis. As a result of these two points cell division affords two genetically unstable daughter cells, where further cancer-promoting mutations can occur. These cells, because of an accumulation of mutation, often develop a resistance against anticancer drugs.<sup>31,32</sup>

The first known human oncogene was the mutated form of the proto-oncogene Ras. This gene is mutated in about one of five human cancers. Ras-proteins are monomeric GTPases, which are a part of the cell-signaling system and transmit signals from the cell surface to the cell interior. GTP-binding proteins are switched “on” when GTP is bound (actively signalling) and remain in “off” state when GDP is bound. Ras, and therefore all GTP-binding proteins, with bound GTP has an intrinsic GTPase activity and shuts itself off by hydrolyzing the bound GTP to GDP. The Ras oncogenes which were isolated from human tumors mostly possess point mutations. These mutations cause the overactive Ras protein, which is not able to hydrolyse the bound GTP to GDP, to inactivate itself.

Mutations in oncogenes are dominant, because they make the protein hyperactive and the change of only one of the two gene copies leads to the described effect. On the other hand mutations in tumor-suppressor genes are usually recessive. Both gene copies must be deleted, inactivated or silenced epigenetically to achieve the effects which are common in cancer cells.<sup>32,33</sup>

### **1.5.2. The Cytoskeleton – Microtubules**

In a living eukaryotic cell some crucial processes such as cell division, maintenance of cell shape, motility, physical robustness, interaction with the environment and correct internal structure must be organized. All these abilities necessary for optimal function of



a cell are arranged by diverse functions of the cytoskeleton which comprehends three types of protein filaments: (1) intermediate filaments, which are responsible for the mechanical strength of a cell, (2) microtubules determine the optimal position of membrane-enclosed organelles. These protein filaments also arrange the transport of vesicles, organelles and proteins within the cell and they play a crucial role at the transition from meta- to anaphase during the cell cycle, when the sister chromatids are pulled towards the spindle poles. And (3), the last class of protein filaments of the cytoskeleton are the actin filaments, also known as microfilaments. They are responsible for the stability of the cell shape, necessary for the definition of cell polarity and cell migration and they also form the contractile ring to form two daughter cells during cytokinesis.<sup>34</sup>

The whole cytoskeletal system would not work without the hundreds of accessory proteins that link the filaments to other cell components, as well as to each other. The optimal function of the cytoskeleton is essential during cell cycle. It can be imagined that because of the fast reorganization of a cell in all sections of the cell cycle the three protein filaments must be dynamic polymers. Each type of cytoskeletal filament is assembled from small soluble subunits. These small subunits diffuse rapidly within the cytoplasm so structural reorganizations and reassembling can be performed quickly.<sup>35</sup>

Microtubules are built of protein subunits called tubulin. The tubulin subunit itself is a heterodimer composed of closely related globular proteins known as  $\alpha$ - and  $\beta$ -tubulin, held together *via* noncovalent interactions. The polymerization process starts with the relatively slow formation of a small microtubule nucleus. Nucleation is followed by rapid elongation at both sides of the microtubule nucleus and finally a hollow cylindrical structure built from 13 parallel protofilaments is formed (Figure 12).<sup>20</sup>

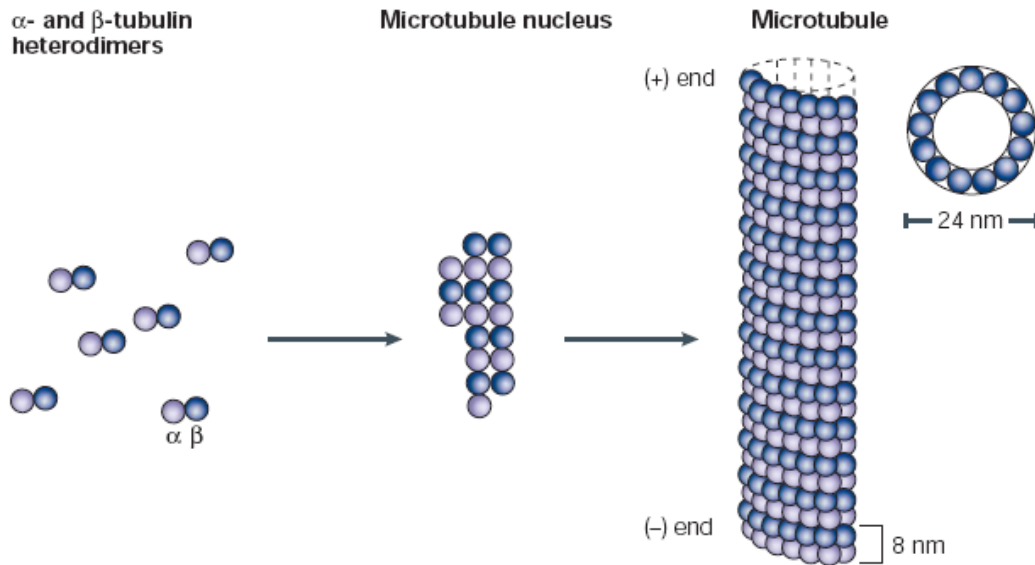


**Figure 12: Microtubule formation**<sup>36</sup>

Microtubules have two different ends, one is the so called plus-end where  $\beta$ -subunits are exposed and the second is the minus-end where  $\alpha$ -subunits are facing the solvent. Elongation from the plus-end proceeds faster than from the minus-end.<sup>36</sup>

This nucleation-elongation process is very complex and requires energy. Both,  $\alpha$ - and  $\beta$ -monomer have a GTP-binding site. Hydrolysis of bound GTP to GDP at the time of polymerization when tubulin with bound GTP adds to the microtubule end makes the energy available which is needed for this dynamic process. The free phosphate moiety is split off from GTP, but the hydrolyzed nucleoside diphosphate remains at the binding site within the filament structure. It can easily be differentiated between two forms of subunit structures. The first is the "T-form" with bound GTP and the second is known as the "D-form" interacting with GDP after hydrolysis of the triphosphate. In living cells most of the free subunits are usually in the T-form, because the free concentration of GTP is about tenfold higher than that of GDP. The subunit on the end of a filament can exist in T- or D-form. The hydrolysis state is determined by the rate of hydrolysis in comparison to the rate of subunit addition. When the filament is growing rapidly, hydrolysis can be too slow and a new subunit will be added at the polymer end before GTP has been cleaved in the previously added subunit. The tip of the polymer is existent in the T-form and forms a so called GTP-cap. However if the addition rate is slow, GTP-hydrolysis occurs before the next tubulin-subunit is added to the microtubule end and the filament end is available in D-form.<sup>34,37</sup>

The function of microtubules in a living cell is predominantly determined by their polymerization dynamics. Two forms of non-equilibrium dynamics can be differentiated. The so called “dynamic instability” means that a microtubule end undergoes alternating periods of slow growth and rapid shrinkage. Subunits are added and lost at the same end of the microtubule.

The second form of dynamic behaviour is filament treadmilling. At a particular subunit concentration in the cytoplasm, the filament growth at the plus-end exactly balances the filament shortening at the minus-end. In other words the subunits undergo a net assembly or net growth at the plus-end and a net disassembly or shrinkage at the minus-end at an identical rate. During the “steady state treadmilling” a constant rate of energy in form of GTP-hydrolysis is needed while the total length of the microtubule filament remains unchanged.<sup>36,38</sup>

Dynamic instability as well as treadmilling depends on the ratio of the free subunit concentration and the rate constant. While treadmilling the range of free subunit concentration is higher than the critical concentration of the T-form but lower than the critical concentration of the D-form. Subunits are added at the plus-end (in T-form) and at the same time at the minus-end tubulin-subunits in the D-form are lost. On the other hand during the dynamic instability status a constant free subunit concentration can be observed. A constant switch between growing, rescue state, and shrinking, also called the catastrophe situation, can occur.<sup>35,39</sup>

Microtubules have their origin and start nucleation at a specific intracellular location, the microtubule-organizing center (MTOC). In eukaryotic cells the MTOC is called the centrosome. Nucleation and polymerization, from the minus-end at the centrosome to the plus-end toward the cell periphery, occur in a star-like conformation.<sup>34</sup>

### **1.5.3. Microtubules – their important role in mitosis**

The cell cycle can be divided into two general sections, the interphase and the M-phase (M for mitosis). The interphase includes the S-phase (S for DNA synthesis), where the replication of the chromosomes and the duplication of the centrosomes occur, and the two gap phases (G<sub>1</sub>-and G<sub>2</sub>-phase). Cells have the possibility to enter a rest-phase, known as G<sub>0</sub>, if extracellular conditions are inappropriate for cell division. Cells can stay in this phase for a very long time, even years, before they restart cell proliferation. After completion of the interphase the chromosomes must be separated into two equivalent

daughter cells during M-phase. The M-phase includes two important processes: (1) nuclear division, or mitosis, the distribution of the sister chromatids and cytoplasmic division, and (2) cytokinesis where the two newly formed cells are constricted.

The M-phase is further divided into six phases: During prophase the replicated chromosomes are condensed and the mitotic spindles are formed outside of the nucleus. The starting signal for the prometaphase is the rapid breakdown of the nuclear envelope. The spindle microtubules start to interact with the kinetochores of the sister chromatids. During metaphase the chromosomes are forming the metaphase plate at the equatorial plane of the cell. The spindle microtubules are responsible for the transport of the chromosomes to their position at the equator of the cell. During anaphase the sister chromatids are separated and they are moving towards the spindle poles, pulled by microtubules. In telophase the separated chromosomes have reached the spindle poles and the division of the cytoplasm begins with the formation of the contractile ring. During cytokinesis the two daughter cells are formed by the contractile ring of actin and myosin (Figure 13).

This shows that microtubules are important in each sequence of the M-phase.

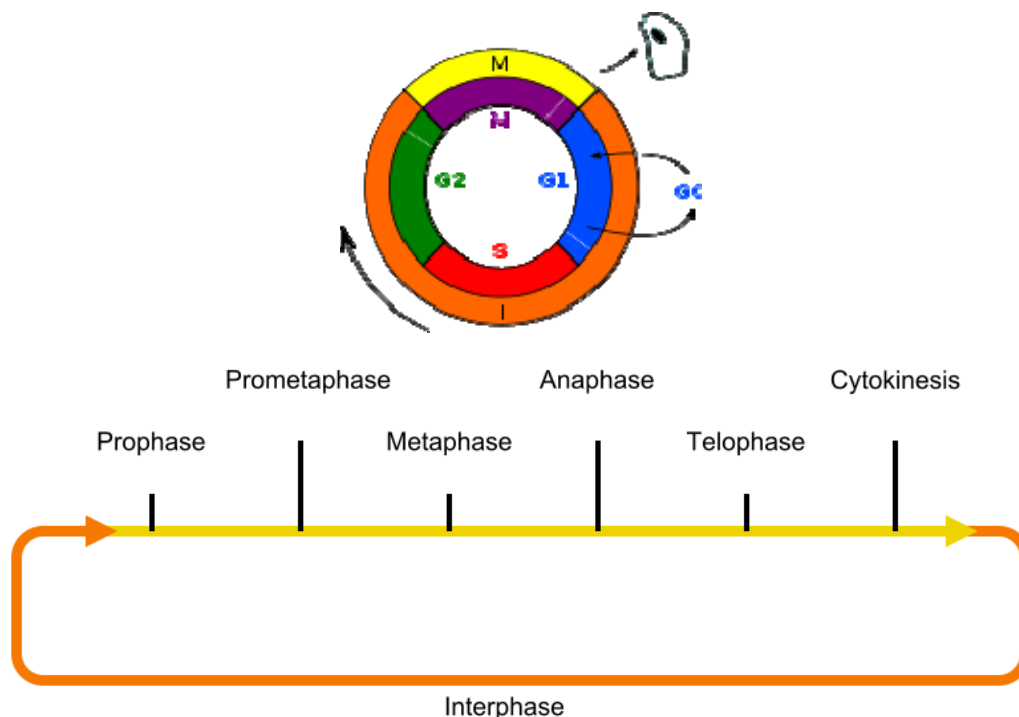


**Figure 13: Cell cycle**

The chromosome segregation depends on the optimal function of the mitotic spindle. The core of this mitotic spindle is a bipolar formation of microtubules. The minus-ends

are lying at the spindle poles, which are organized by centrosomes, and the plus-ends are reaching starlike into the cell periphery.

There are three different classes of mitotic spindle microtubules in an eukaryotic cell. The kinetochore microtubules build the connection between the sister chromatides and the spindle poles. The interpolar microtubules arise from both spindle poles and interlock at the equatorial plane over their plus-ends. The third group of spindle microtubules are the astral microtubules. Those radiate outward from the centrosomes and are interacting with the cortex for optimal position of the spindle poles during mitosis.<sup>34,40</sup>

The mitotic spindles would not be able to carry out their task without the support of two protein families called microtubule dependent motor-proteins. One family is called the kinesin-related proteins, which are moving from the spindle poles towards the plus-end of microtubules and the other family is known as the dyneins, moving in the opposite direction to the minus-end.<sup>41</sup>

#### **1.5.4. Antimitotic drugs**

A living cell would not be able to survive without an operating network of dynamic polymerizing microtubules. Antimitotic drugs are agents that distort the polymerization process of spindle microtubules and thereby mitosis is prohibited. The explanation why these drugs are effective against cell division is because the polymerization dynamics of spindle microtubules are much more active than cytoskeletal microtubules; 50% of the tubulin subunits of the filamentous spindle microtubules are exchanged with the soluble pool within 15 seconds.<sup>1</sup>

A large number of natural products with chemically diverse structures bind to soluble tubulin subunits and/or the filament form of the polymer. By binding to either the free form or filamentous form the microtubule formation is driven towards the toxin binding form. If the drug binds to soluble tubulin it prevents their assembly to filaments and *vice versa* while if the drug binds to tubulin incorporated into the microtubule lattice, depolymerization will not occur. Because of the different effectiveness of these agents, antimitotic drugs can be divided into two main groups: The first comprises microtubule-destabilizing agents, among those are the Vinca alkaloids (vinblastine, vincristine, vinorelbine, vindesine and vinflunine), colchicine and the combretastatins. The second

group is known as microtubule-stabilizing agents. Known representatives are paclitaxel (taxol), the epothilones, laulimalide and discodermolide.<sup>36</sup>

This classification of microtubule interacting drugs into microtubule-stabilizing and destabilizing agents can lead to confusion. It was found that some antimitotic agents which increase or decrease microtubule formation at high concentrations, suppress microtubule polymerization at 10-100-fold lower concentrations. It is believed, that the growth of tumors is inhibited predominately by suppression of spindle microtubule dynamics. As a result mitosis is slowed down or blocked at the transition from metaphase to anaphase and apoptotic cell death. All compounds named above bind to tubulin on specific binding sites. It can be distinguished between three main binding sites, which are named according to their best known ligands the Vinca-, colchicines-, and taxol-sites.<sup>42</sup>

Vinblastine binds to the  $\beta$ -tubulin subunit between amino acids 175 and 213.<sup>43</sup> Paclitaxel (taxol) has two interaction-sites on  $\beta$ -tubulin, an *N*-terminal unit and between amino acids 217-231. Colchicine binds between the taxol- and vinca binding site.<sup>44,45</sup>

### **1.5.5. Microtubule-destabilizing agents**

#### **Vinca alkaloids and their synthetic analogs**

The first natural products which were used in clinical therapy as antimitotic drugs were the Vinca alkaloids vinblastine (**1**) and vincristine (**2**, Figure 14). These complex compounds were isolated from the leaves of the periwinkle plant *Catharanthus roseus* (L.) G. Don, also known as *Vinca rosea*.<sup>46</sup> The leaves of *Vinca rosea* were used in naturopathy since the seventeenth century. The antimitotic effect and possible application as chemotherapeutic agent was discovered in the late 1950s by two independent research groups, one at Eli Lilly Research Laboratories and the second at the University of Western Ontario. These two compounds, vinblastine and vincristine, were introduced into clinical oncology in the late 1960s and remained in widespread clinical use up to present.<sup>1</sup>

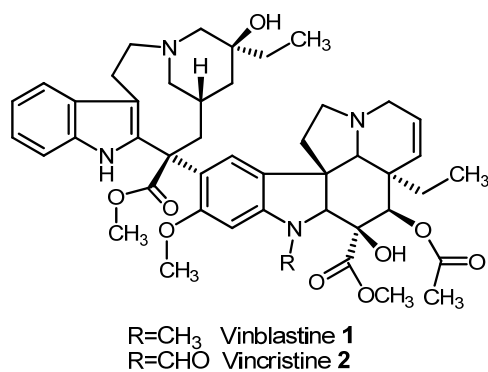


**Figure 14: Vinca alkaloids used in clinical therapy**

Vincristine and vinblastine show very similar structures and mechanisms of action in cancer cells but despite this fact they show different toxicological properties and application in chemotherapy. Vinblastine is used in the treatment of Hodgkin's disease and in combination therapy against metastatic testicular tumors while vincristine is used in the treatment of leukaemia and lymphomas.<sup>36</sup>

In search of related compounds with high biological activity which are effective in other cancer cell lines as well, several derivatives were synthesized and some of those semisynthetic analogs are also in clinical use (Figure 15). Vindesine (**38**) was the first derivative introduced in cancer therapy. It is used in combination therapy for treatment of leukaemia, lymphoma and non-small-cell lung cancers (NSCLC).<sup>47</sup> Vinorelbine (**39**) is used for NSCLC, metastatic breast cancer and ovarian cancer<sup>48-50</sup> whereas vinflunine (**40**), the fluorinated derivative, is in clinical development.<sup>51</sup>

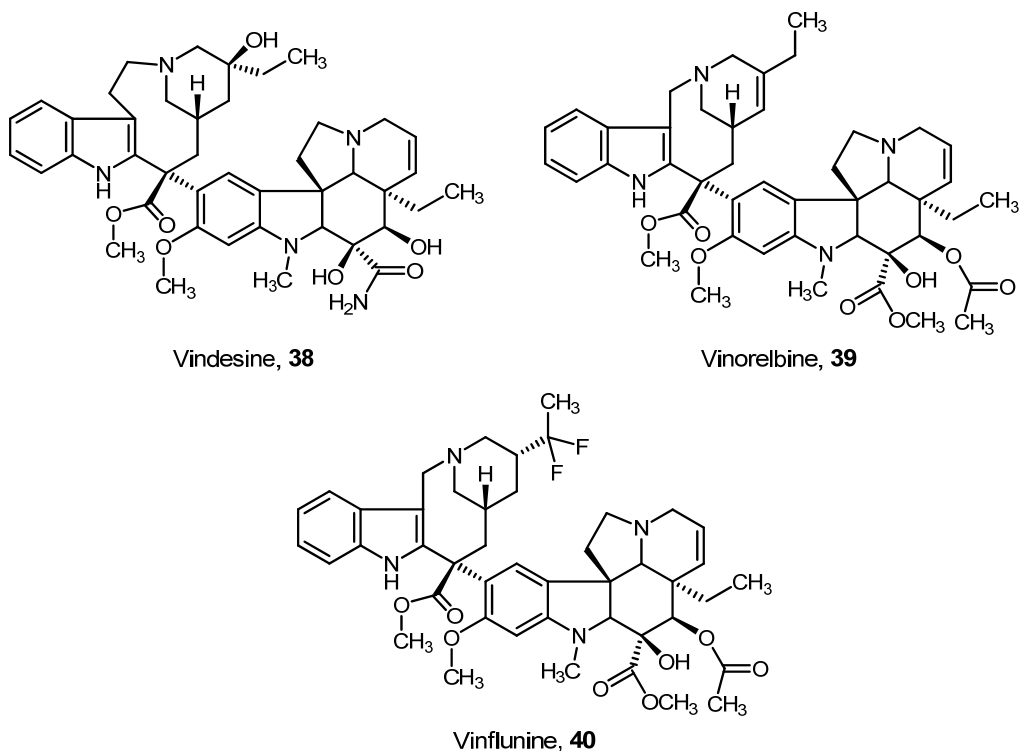


**Figure 15: Derivatives of the vinca alkaloids in clinical use**

The biological activity of the vinca alkaloids can be elucidated by effective binding to the  $\beta$ -subunit of tubulin dimers, in a region called the Vinca domain. They interact rapidly and reversibly with soluble tubulin, which induces a conformational change and leads to the formation of paracrystalline aggregates. The number of free tubulin dimers available for microtubule polymerization declines and the drug increases the affinity of tubulin for itself. The equilibrium is shifted toward disassembly and microtubule shrinkage. The described phenomena are noticed in cancer cells exposed to high drug concentration (for example, 10 - 100 nM in HeLa cells). As a result the dividing cancer cells are blocked in mitosis with condensed chromosomes. This mechanism was thought to be responsible for effecting apoptotic cell death for many years. However, recent investigations have shown that at low but clinically relevant concentrations (for example,  $IC_{50}$  0.8 nM in HeLa cells) depolymerization of the spindle microtubules does not happen; nevertheless, mitosis is blocked at metaphase and cells die by apoptosis.<sup>52</sup>

Several studies were performed to investigate if vinca alkaloids also bind directly to microtubules. It was found that vinblastine binds to the microtubule plus-ends with very high affinity at low drug concentration. It is very important, that the interaction of only one or two molecules of vinblastine per microtubule reduces both treadmilling and dynamic instability by about 50%. At those low drug concentrations microtubule

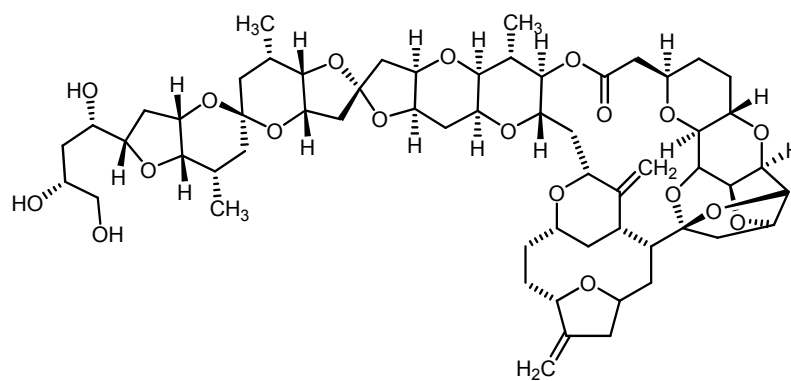


depolymerization does not occur. This disruption of spindle microtubule dynamics blocks mitosis.<sup>53</sup>

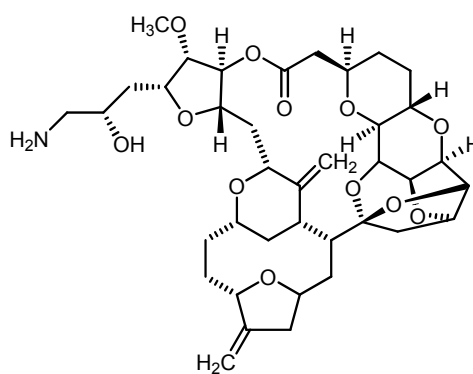
### **Marine natural products binding on the Vinca domain**

Marine organisms are a rich source of antitumor compounds. Many of these compounds are in preclinical or clinical stage of development.<sup>54,55</sup> They show different points of action in a living cell but several compounds were found binding at the Vinca domain, including the halichondrins, the dolastatins, the hemiasterlins, the cryptophycins, and the spongistatins among others. In this section just a few examples of the variety of marine natural products which bind on the Vinca domain will be described.

The macrolide polyether halichondrin B (**41**, Figure 16) was isolated from the marine sponge *Halichondria okadai* with remarkable *in vivo* antitumor activity.<sup>56</sup> The natural sources of this compound are not very high, so the development of the total synthesis<sup>57</sup> was a great progress and opened the doors for the preparation of structurally simpler analogs that show comparable potency as anticancer drugs. The truncated halichondrin B derivative eribulin mesylate (**42**, E7389) was found to act like its parent compound as an inhibitor of tubulin polymerization. Eribulin mesylate is in clinical phase III for the treatment of prostate, sarcoma, breast, NSCL and ovarian cancers.<sup>58</sup>



Halichondrin B, **41**



E7389, **42**

**Figure 16: Compounds binding on the vinca domain I**

Dolastatin 10 (**43**, Figure 17) was isolated first by Pettit and co-workers from the sea hare *Dolabella auricularia*.<sup>59</sup> This complex compound also inhibits tubulin polymerization by binding near the *Vinca* domain.<sup>60</sup> Dolastatin entered clinical phase I in the 1990s but the results were not encouraging.<sup>55</sup>

Many derivatives of the dolastatins were synthesized, among which TZT-1027 (auristatin PE, soblidotin, **44**) and tasidotin (**45**), a dolastatin 15 analog, have entered clinical trials.<sup>61</sup>

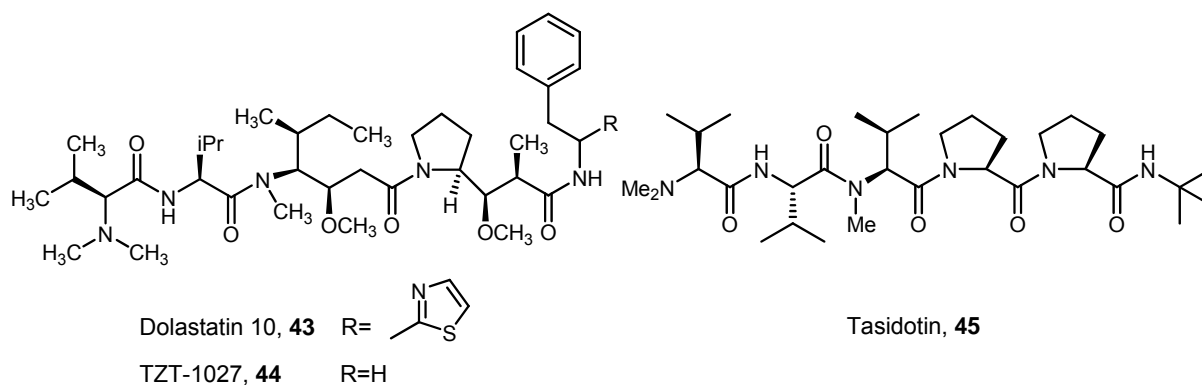


**Figure 17: Compounds binding on the vinca domain II**

Hemiasterlin (**46**, Figure 18) was isolated first by Kashman from the South African sponge *Hemiasterella minor*.<sup>62</sup> This tripeptidic compound interacts with the same tubulin binding site as the dolastatins. Many synthetic analogs have been prepared and HTI-286 (**47**) is under clinical trials.<sup>63</sup>

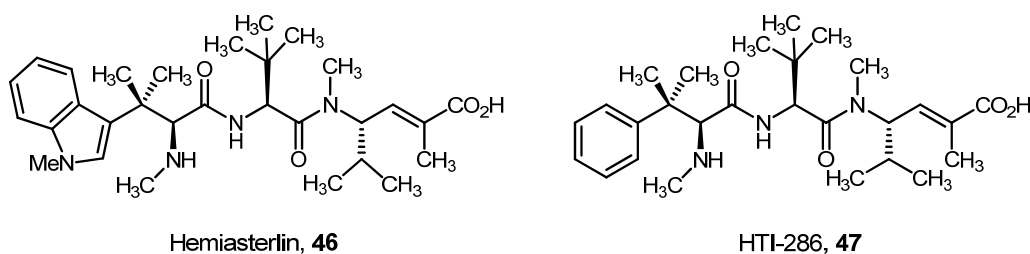


**Figure 18: Compounds binding on the vinca domain III**

Cryptophycin-1 (**48**, Figure 19) was isolated from the cyanobacterium *Nostoc sp.* and was first described as an antifungal drug.<sup>64</sup> After further investigations antimitotic and cytotoxic activity could be demonstrated. The cryptophycins are very potent antimitotic agents which bind very strongly and mainly irreversibly. These compounds also show activity against MDR-cancer cell lines.<sup>65</sup>

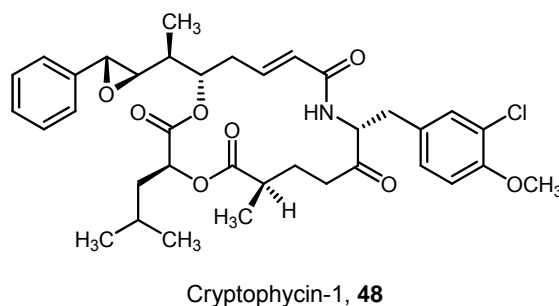


**Figure 19: Compounds binding on the vinca domain IV**

### Compounds binding at the colchicine site

Colchicine (**33**) has already been described in section 1.4.2. Up to present, the natural product is used in the treatment of acute gout. However, because of its high toxicity neither the natural product nor compounds that interact with the colchicine domain (for example the combretastatins) are used in clinical treatment of cancer. Colchicine acts in the same manner as described for the vinca alkaloids. It depolymerizes microtubules at high concentrations and stabilizes microtubule dynamics at low concentrations.<sup>36</sup>

Colchicine inhibits tubulin polymerization substoichiometrically. It forms a final-state tubulin-colchicine complex, which is mainly irreversible. This complex copolymerizes

into the microtubule lattice and microtubule dynamics are suppressed because the colchicine-tubulin complex binds more tightly to its tubulin neighbors than free tubulin subunits.<sup>66</sup>

The structural components within the colchicine skeleton required for the formation of the complex were analyzed by SAR studies. These studies came to the result, that the 9-keto functionality and the methoxy groups at C-1, C-2, and C-10 are necessary for effective tubulin binding. The acetamido function at position 7 is not required and can be substituted by other functional groups. However, the stereochemistry must be conserved. This fact is not clearly understood but it is thought, that the overall conformation of the molecule must be maintained. Ring B is responsible for irreversible tubulin binding and the general toxicity. The troponone ring C can be substituted by a similar substituted benzene ring without losing the antimitotic activity (Figure 20).<sup>1</sup>

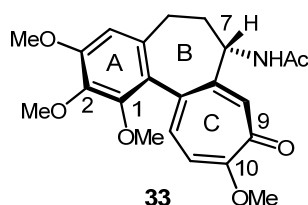


**Figure 20: Structure of colchicine**

The combretastatins described above bind to the colchicine binding domain. One of the shared functionalities is the trimethoxyphenyl ring. The troponone ring of colchicine is substituted by an aromatic ring system with different substitution patterns in the combretastatins and the most potent compound is CA-4. Structure-activity relationship is described in section 1.6. Two further compounds that also bind at the colchicine binding site are in clinical test phases. In addition to microtubule destabilizing effects, 2-methoxyestradiol (**49**, Figure 21) shows promising antiangiogenic activity and is in clinical phase I.<sup>67</sup> The second potent compound is methoxybenzene sulfonamide derivative ABT-751 (**50**). It is an orally active sulfonamide antitumor agent that is currently in a phase I clinical trial.<sup>68</sup>

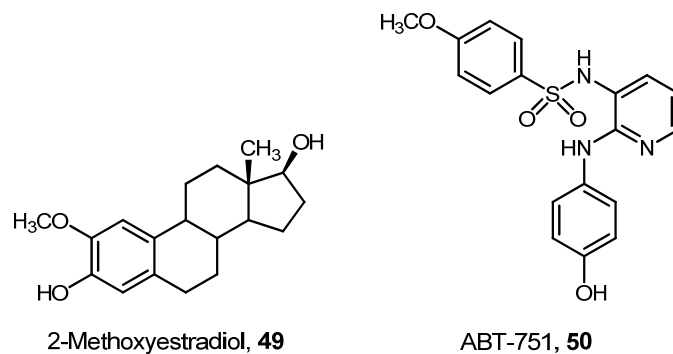


Figure 21: Compounds binding at the colchicine binding site

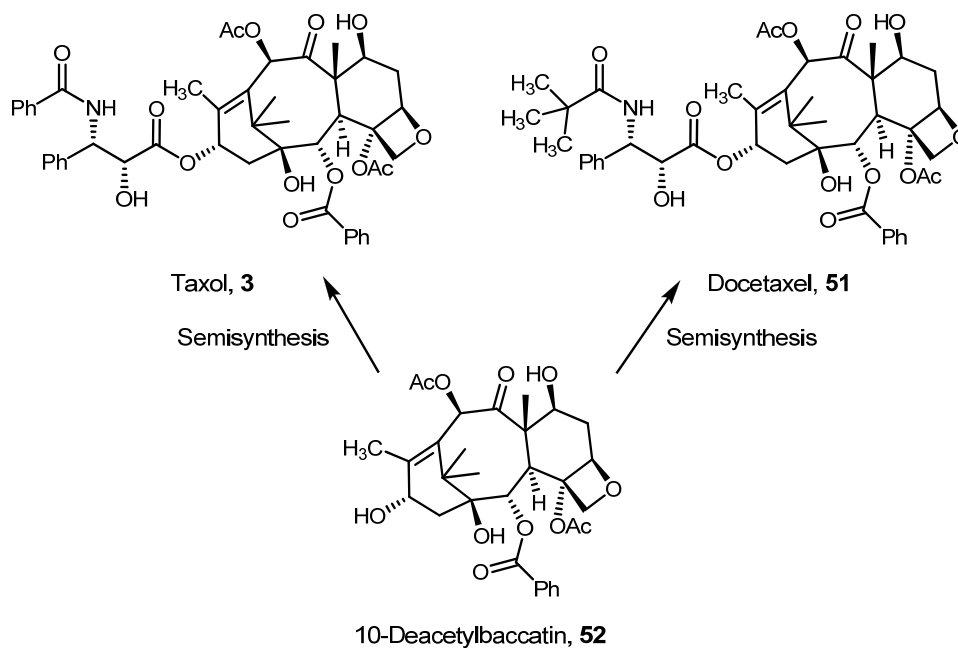
### 1.5.6. Microtubule-stabilizing agents

#### Compounds binding at the taxane site

##### Taxanes

Paclitaxel (Taxol, **3**) and its semisynthetic analog docetaxel (**51**) were the most important natural products introduced in cancer chemotherapy in the late twentieth century. Taxol was isolated first in 1967 by Monroe Wall and Mansukh Wani from the bark of the pacific yew tree *Taxus brevifolia*.<sup>69</sup> In 1979, Schiff et al. found that paclitaxel acts as an antimetabolic agent and disturbs the microtubule polymerization process.<sup>70</sup>

Enormous supply problems complicated the entering of the potent natural compound into clinical use. The concentration of taxol in the bark of *Taxus brevifolia* is very low and the extraction process is complex and expensive. The tree must be cut for isolation and it is a slow growing plant. It was found that a very similar natural product, 10-deacetylbaccatin III (**52**), could be isolated from the twigs and needles of the European yew, *Taxus baccata*. Through a semisynthetic route **52** can be transformed to taxol as well as to docetaxel (Scheme 1).<sup>71,72</sup>



**Scheme 1: Semisynthetic route of taxol and docetaxel**

The taxanes do not show strong interaction with soluble tubulin subunits, but they bind with high affinity to the  $\beta$ -subunit of tubulin, incorporated into the microtubule filament. More precisely, these important compounds bind to the interior face of the microtubule cylinder, stabilizing the microtubule and increasing microtubule polymerization. By binding to tubulin, taxol induces a conformational change in the subunit which leads to an increase in affinity for neighboring tubulin molecules.<sup>73</sup> The exact binding site is known because Nogales et al. were able to determine the crystal structure of tubulin complexed with paxlitaxel.<sup>74</sup>

The increase of microtubule polymerization induced by taxol binding on the interior surface of microtubules is associated with nearly stoichiometric binding of the natural product. This indicates a very high taxol concentration. In contrast to that phenomenon it was found that the binding of a substoichiometric number of taxol molecules stabilizes the polymerization dynamics without increasing microtubule polymerization.<sup>75</sup> The suppression of microtubule polymerization dynamics, or hyperstabilization of microtubules, leads to mitotic arrest and cytotoxicity in proliferating cells which die by apoptotic cell death.

In the last years several taxol derivatives were synthesized and some of them entered clinical trial.

## Epothilones

The epothilones A (**53**, Figure 22) and B (**54**) are 16-membered macrolides isolated first in 1993 from the myxobacterium *Sorangium cellulosum*. They show the same mechanism of action as taxol *in vitro* and also in cultured cells.<sup>76</sup> The epothilones show several advantages over the taxanes such as activity against taxol resistant cell lines, higher water solubility and simpler structures, so the synthesis of derivatives is much easier.<sup>77</sup>

On the other hand the natural epothilones show some limitations in clinical use. The most important confinement is their metabolic lability, because of the hydrolysis of their lactone ring by esterases in living cells. So the tendency goes towards the synthesis of metabolically more stable lactam analogs. Ixabepilone (BMS-247550, **55**) was already used in clinical trials in paclitaxel-resistant colorectal, metastatic breast, and non-small-cell lung cancer.<sup>1,78</sup> The second limitation is the poor water solubility, as an example the more water-soluble amino derivative of epothilone B, BMS-310705 (**56**) has entered clinical test phases.<sup>79</sup>

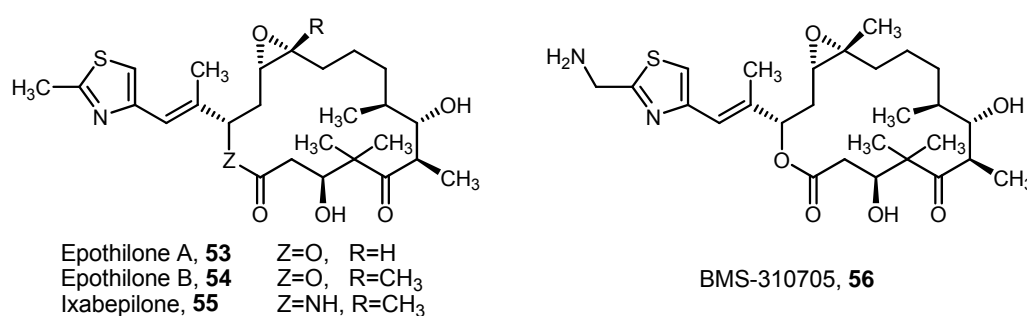


Figure 22: The epothilones and derivatives in clinical use

This was a short overview of the most important antimetabolic agents in clinical use or trial but it has to be pointed out that the list is far from being complete. The discussion of all these chemically diverse natural products should demonstrate that tubulin binding drugs are crucial in cancer therapy today.

### 1.5.7. Antivascular effects

For more than 50 years researchers are in search of chemotherapeutic agents that affect rapidly proliferating cancer cells with low levels of toxicity to healthy cells. Drugs with antivascular effects, also known as antiangiogenic drugs that cause the rapid and

selective shut down of tumor blood flow, could be the desired breakthrough in cancer chemotherapy.<sup>80</sup>

The tumor vasculature is an important target in cancer therapy, because many tumor cells are provided with oxygen and nutrients through that system, which is essential for cell survival. New blood vessels, built *via* angiogenesis, are also a possibility for tumor metastasis.<sup>81</sup>

Two different approaches exist to inhibit vascular function. One is the development of new agents that inhibit the accumulation of new blood vessels, disrupting angiogenesis. The second possibility is an antivasular approach using vascular-disrupting agents (VDA). The aim of both approaches is the rapid shut down of existing tumor vasculature. Especially tubulin-targeted compounds show antivasular activity. Several low-molecular-weight VDAs are in clinical trial or entered preclinical test phases, among those combretastatin A-4 phosphate (CA-4-P, **6**), combretastatin A-1-phosphate (CA-1-P, Oxi4503, **5**), ZD6126 (**8**), AVE8062 (**7**), flavone acetic acid (FAA, **57**), DMXAA (**58**).<sup>11,82</sup>

The antivasular effects of CA-4-P, AVE8062 and CA-1-P in ectopically (in an abnormal place, outside the tissue of origin) and orthotopically (within the tissue of origin) transplanted tumors, spontaneous tumors and vascularized metastases were proved partially at doses less than one-tenth of the maximum tolerated dose.<sup>81,83</sup> The primary effect of VDAs is a very fast reduction of tumor blood flow and extensive tumor cell necrosis (unnatural cell death). For example CA-4-P (**6**) can decrease the blood flow significantly within 5 minutes of drug exposure in animal systems. The complete vascular shut down is noticed within 20 minutes.<sup>84</sup>



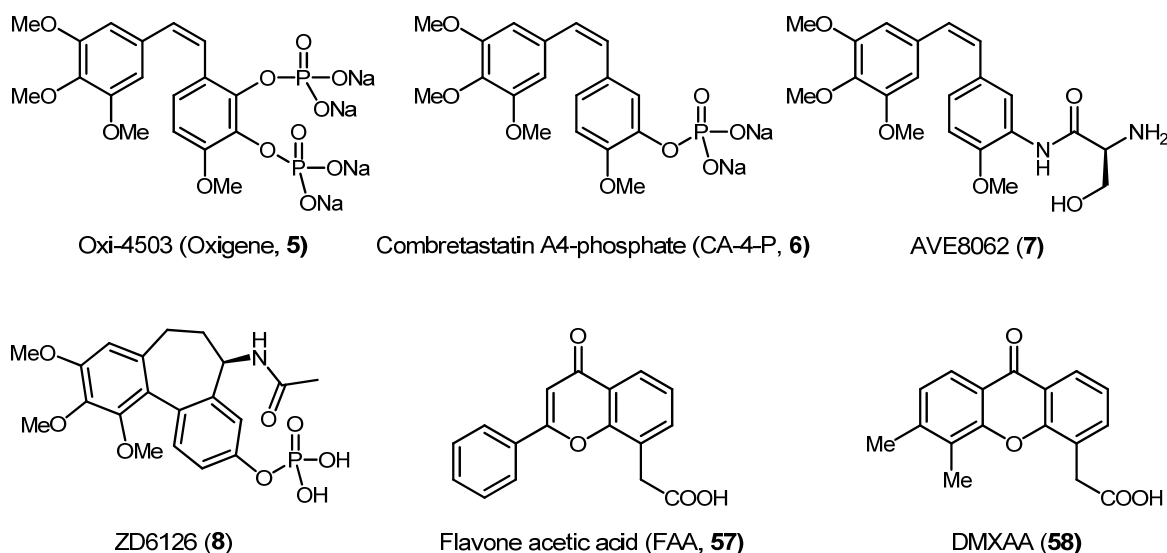


**Figure 23: Vascular disrupting agents (VDAs)**

All of the described compounds seem to damage the tumor vasculating system instead of normal, healthy blood vessels. It is most likely that morphological and functional changes in the endothelial cytoskeleton of cancer cells *in vivo* are responsible for the fast breakdown of tumor blood flow.<sup>85</sup>

### 1.6. Combretastatins – Structure-Activity Relationship

CA-4 (**4**) was found to be the biologically most potent compound within the combretastatin family.

CA-4 is capable of inhibiting microtubule assembly at nanomolar concentrations. Table 1 shows the mean value of 60 human tumor cell lines evaluated in the National Cancer Institute (NCI).<sup>86</sup> The GI<sub>50</sub>-value represents the 50% growth inhibitory concentration.

Combretastatins	Mean value GI <sub>50</sub> (x10 <sup>-8</sup> M)
A-1 ( <b>12</b> )	1.62
A-2 ( <b>13</b> )	3.16
A-4 ( <b>14</b> )	0.32
A-5 ( <b>15</b> )	165.00
A-6 ( <b>16</b> )	>10000

**Table 1: GI<sub>50</sub>-values of combretastatins<sup>86</sup>**

Hundreds of CA-4 derivatives have been synthesized up to present. Their screening has allowed to establish a detailed SAR profile,<sup>7,87-89</sup> which can be summarized as followed:

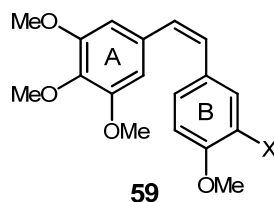


**Figure 24: CA-4 analogs for SAR-studies**

- CA-4 is only active in cis-form.
- The 3,4,5-trimethoxy substitution pattern on ring A is essential for antimitotic activity.
- The 4-methoxy-3-X-substituted phenyl ring B is indispensable for potent cytotoxicity. (X=H, OH, NH<sub>2</sub>, amino acid, phosphate or other moieties for better water solubility)
- The two aromatic ring systems must be separated by a two-carbon-bridge.

CA-4 shows potent cytotoxicity against a wide range of human cancer cell lines including multi-drug-resistant (MDR) cancer cell lines. MDR cancer cell lines show a resistance of antineoplastic agents, drugs that combat the growth of tumors. So-called ATP-binding cassette proteins (ABC-proteins) discharge cytotoxic molecules from the cancer cell. The intracellular drug concentration is always held below a cell-killing threshold.

### **1.7. Combretastatin analogs**

CA-4 does not show very strong *in vivo* efficacy. This is a consequence from, first, its high lipophilicity and poor water solubility and second, from the isomerization of the cis-double bond to the thermodynamically more stable trans-isomer.<sup>7,90</sup> Researchers in this field were challenged to synthesize better alternatives to the natural compound with the goal of disposing these negative properties. As a result innumerable CA-4 analogs have been synthesized in the past years, and some of them, for example Oxi-4503 (**5**), CA-4-P (**6**) and AVE8062 (**7**), as described earlier, have already entered clinical trials or preclinical test phases.

The following two figures (Figure 25, Figure 26) only show a small cutout of the variety of CA-4 analogs.

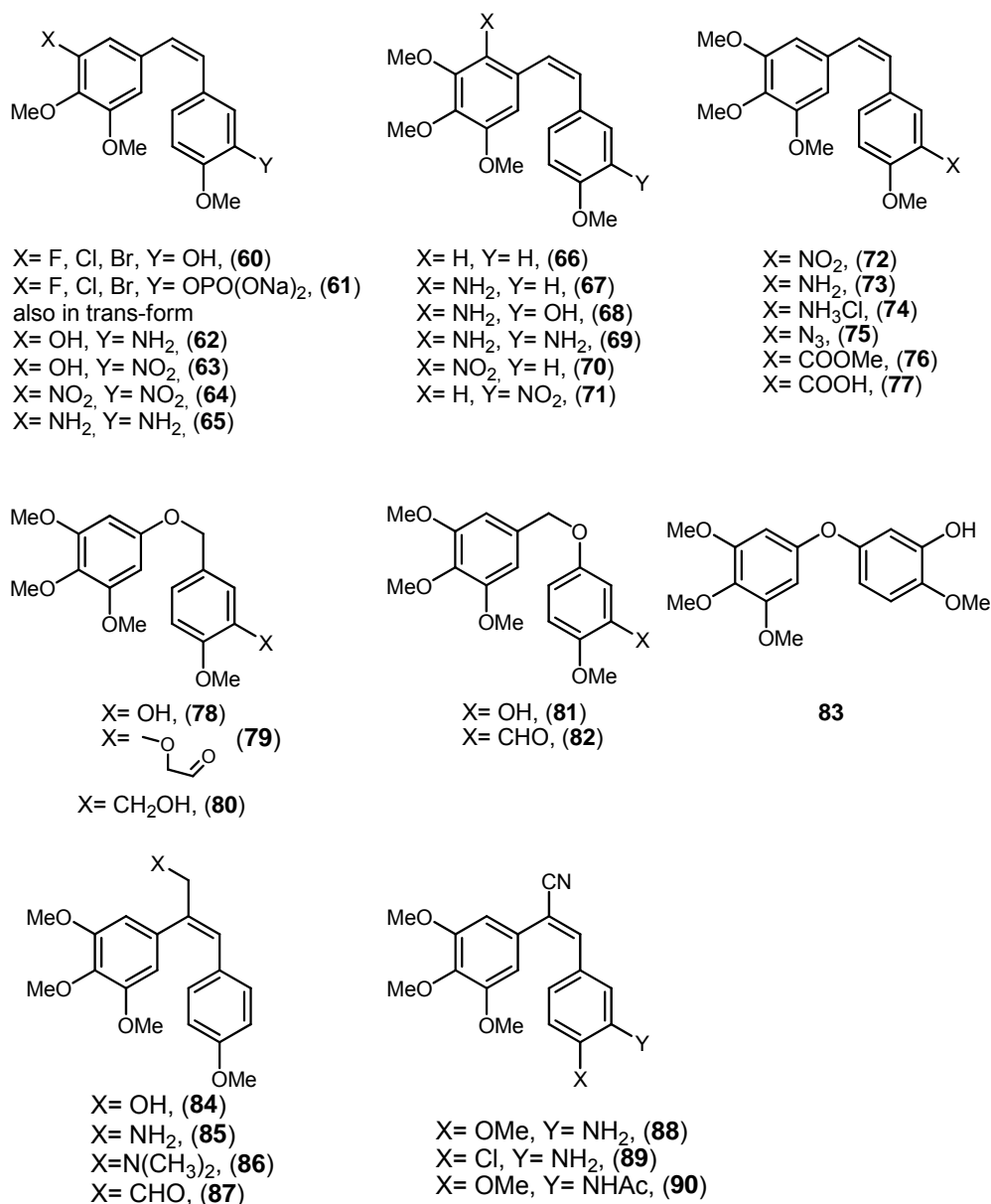
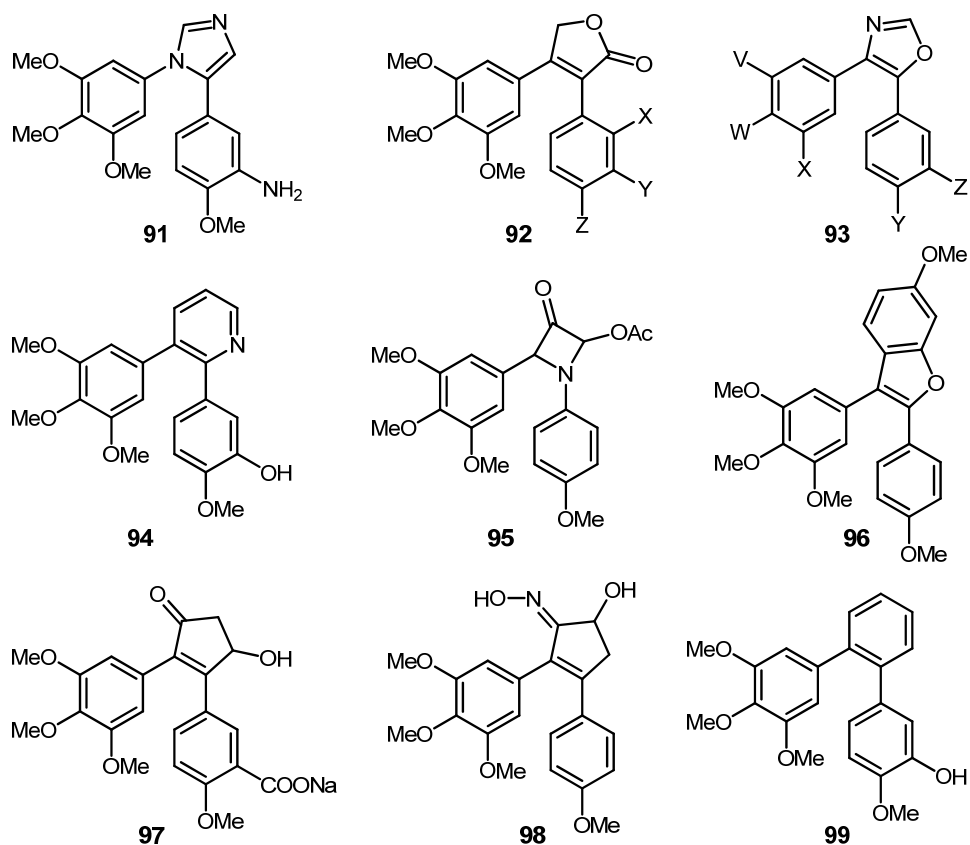


Figure 25: CA-4 analogs I

Figure 25 shows the incorporation of different moieties on the two aromatic ring systems, most of them for better water solubility (**60-90**). The connecting two-carbon bridge was substituted by a carbon-oxygen (**78-82**) respectively by an oxygen-connectivity (**83**), or one of the hydrogen atoms of the sp<sup>2</sup>-hybridized carbon atoms of the original connection were substituted by different functionalities (**84-90**).<sup>91-94</sup>



**Figure 26: CA-4 analogs II**

The incorporation of heterocycles (Figure 26, **91-96**) on the connecting carbon bridge prevents the system from cis-trans-isomerization, but the disadvantage of that approach is that the polarity of the whole molecule is changed compared to the natural product.<sup>95-</sup>

100

## **1.8. Cyclopropane and cyclobutane synthesis**

Small rings are common structural motifs of natural products and the synthesis of cyclopropanes or cyclobutanes is often an important task in total synthesis.

In the following section different cyclopropanation reactions will be discussed and the [2+2]-cycloaddition as one possibility for a cyclobutane synthesis will be described.

## **1.9. Cyclopropanes – a theoretical consideration**

Cyclopropanes are highly strained molecules. Most of this strain is a consequence of the deviation of the bond angles from the ideal tetrahedral angle of  $109.5^\circ$ . The internal angle in the planar cyclopropane is  $60^\circ$ , so the C-C bond energy is reduced and as a consequence the compound is more reactive than other cycloalkanes such as cyclohexane or cyclopentane. All C-H bonds are eclipsed which adds to the ring strain already present. Rotation around the C-C bonds is not possible and so all C-H bonds are forced in the eclipsed conformation.

The first detailed studies about the nature of cyclopropanes were published by Coulson and Moffit.<sup>101</sup> They came to the result that the C-C bonds of the cyclopropane ring are formed by the interaction of bond orbitals which are relatively rich in p-character leading to the minimization of the interorbital angle as well as the conventional bond angle. The reduction of the bond angles to  $60^\circ$  is possible because of the increase of p-character, but as a result the C-H bonds gain more s-character and are shortened. In cyclopropane the maximum electron density between two adjacent carbon atoms does not lie on the internuclear axis (Figure 27, shown in red) and such bonds are known as bent bonds. The interorbital angle in cyclopropane is  $104^\circ$ . The bending can be confirmed by X-ray crystallographic studies of cyclopropane derivatives. It could be demonstrated that the deformation density of the C-C bonds lies outside the cyclopropane triangle. Cyclopropane rings always have C-C bonds that are shorter than C-C single bonds in larger rings or in alkyl chains, which can be explained in terms of bent bonds.<sup>102</sup>

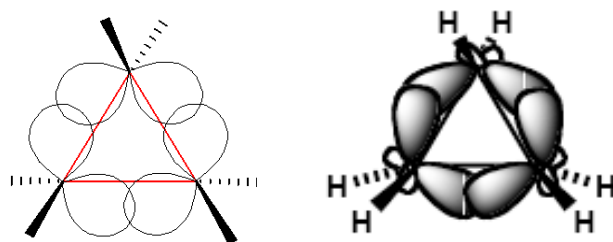


Figure 27: Coulson-Moffitt model of cyclopropane

A second model for cyclopropane was presented by Walsh.<sup>103,104</sup> He constructed a model of cyclopropane where  $sp^2$ -orbitals are directed toward the hydrogens and also toward the center of the three-membered ring. The remaining p-orbital lies in plane with the three-membered ring as shown in Figure 28. The C-C bonds result from the overlap of the  $sp^2$  orbitals showing towards the center of the cyclopropane ring and from the remaining p-orbitals outside the three-membered ring. It must be noted that this model also includes an antibonding overlap (Figure 28).

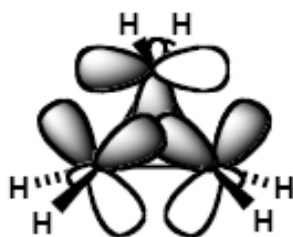


Figure 28: Walsh model of cyclopropane

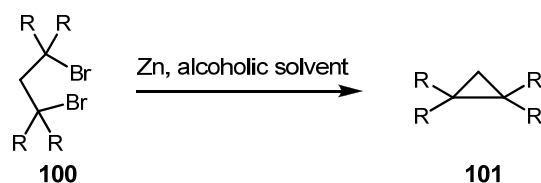
### 1.9.1. Synthesis of cyclopropane

Although the cyclopropane ring is a highly strained structure it is found in a wide range of natural products including terpenes, pheromones and fatty acid metabolites. The cyclopropanation reaction, especially the enantioselective synthesis of cyclopropane containing compounds is an interesting and important method in natural product synthesis. In the following section different cyclopropanation reactions are described.

#### 1,3-Elimination of two heteroatoms

Reductive elimination of 1,3-dihalides with metallic or organometallic reagents as reducing agents is a powerful method for the cyclopropane synthesis. The first intramolecular Wurtz-reaction was published in 1882. This was the reduction of 1,3-dibromopropane with sodium in an alcoholic solvent to afford cyclopropane. Varied

reaction conditions using zinc dust in methanol, ethanol or higher alcohols give substituted cyclopropanes (Scheme 2).

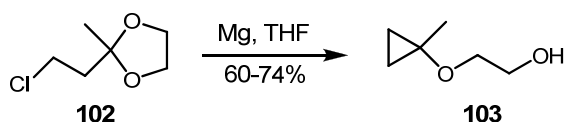


**Scheme 2: 1,3-Elimination of two heteroatoms I**

The reaction is a nonstereospecific process and not concerted. The formation of a carbanionic organometal compound *via* metal-halogen exchange is followed by the displacement of the halide ion by the organometal species in an  $\text{S}_{\text{N}}2$  reaction.<sup>105</sup>

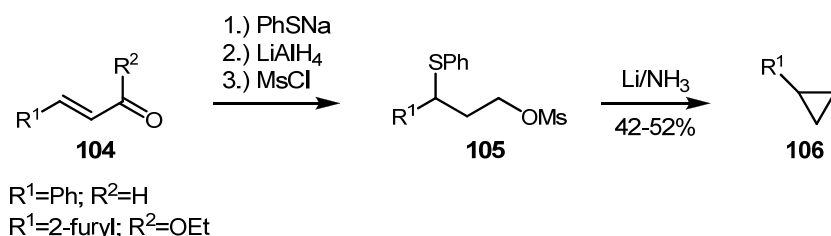
Various other reagents can be used for reductive debromination, cyclization reactions with chrome (II) perchlorate in dimethylformamide / water, lithium amalgam in THF, potassium-sodium alloy in THF, alkyllithium in THF are found in the literature among many others.

The following examples react all in the same manner:



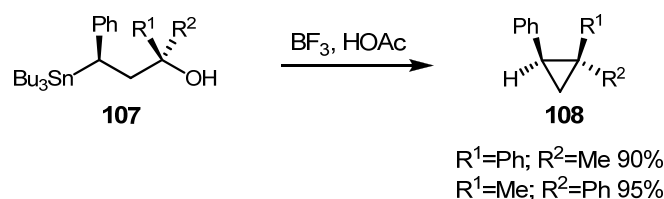
**Scheme 3: 1,3-Elimination of two heteroatoms II**

Scheme 3 demonstrates an example for a 1,3-elimination, the reaction of a chloroketal with magnesium to form the cyclopropyl derivative **103**.<sup>106</sup>



**Scheme 4: 1,3-Elimination of two heteroatoms III**

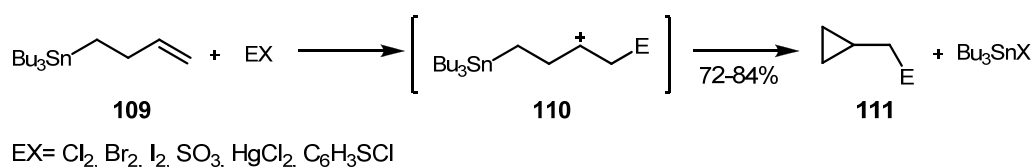
Scheme 4 shows a cyclopropanation by elimination of a sulfur and an oxygen atom. First the carbanion is formed by displacement of the phenylthio group.<sup>107</sup>



**Scheme 5: 1,3-Elimination of two heteroatoms IV**

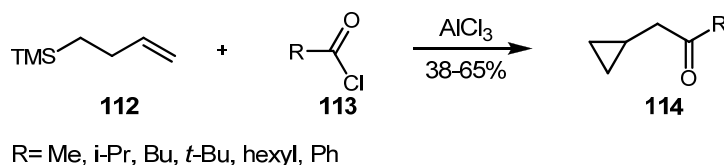
1,3-Deoxystannylation is a stereospecific reaction (Scheme 5) giving 1-methyl-1,2-diphenylcyclopropane (**108**).<sup>108</sup>

Scheme 6 shows a modification of this destannylation protocol, affording cyclopropane **111**.<sup>109</sup>



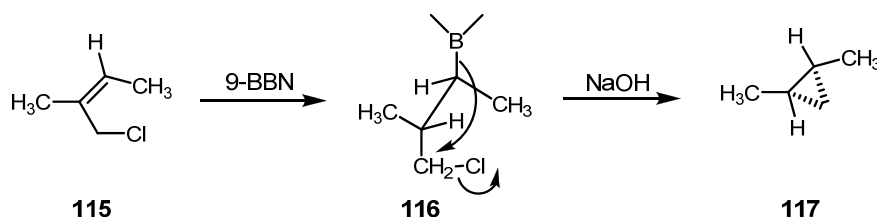
**Scheme 6: 1,3-Elimination of two heteroatoms V**

In a similar way (but-3-en-1-yl)trimethylsilane reacts with an acyl chloride to cyclopropyl ketone **114** (Scheme 7).<sup>110</sup>



**Scheme 7: 1,3-Elimination of two heteroatoms VI**

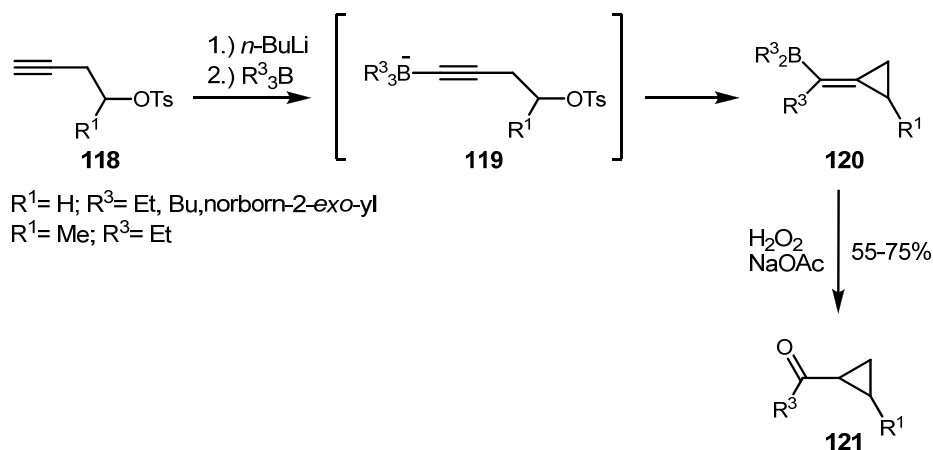
Hydroboration of an allylic chloride and subsequent treatment of the intermediately formed organoborane with aqueous sodium hydroxide gives cyclopropane **117**. The geometry in the alkene is retained in the resulting product (Scheme 8).<sup>105,111</sup>



**Scheme 8: 1,3-Elimination of two heteroatoms VII**



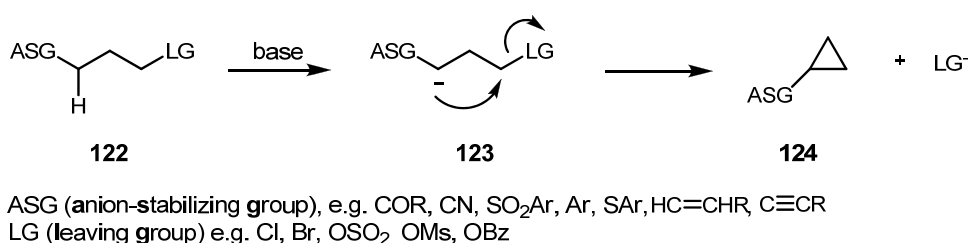
A possibility for a cyclopropyl ketone synthesis is the reaction of prop-2-ynyl 4-methylbenzenesulfonates (**118**) with trialkylborane and subsequent oxidative cleavage of the boron species with hydrogen peroxide and sodium acetate (Scheme 9).<sup>112</sup>



**Scheme 9: 1,3-Elimination of two heteroatoms VIII**

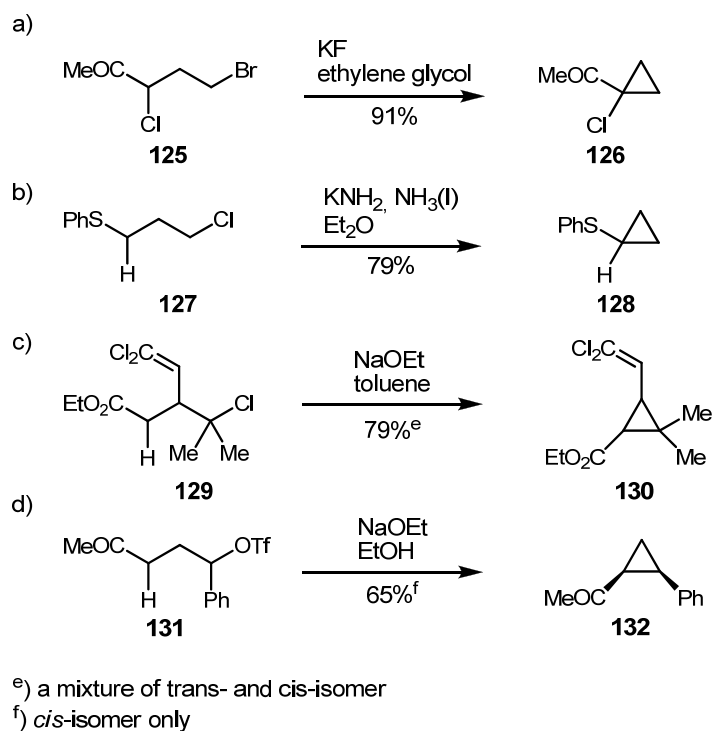
### Intramolecular $\text{S}_{\text{N}}2$ displacement

Another possibility to synthesize a cyclopropane ring is *via* an intramolecular  $\text{S}_{\text{N}}2$  displacement (Scheme 10).



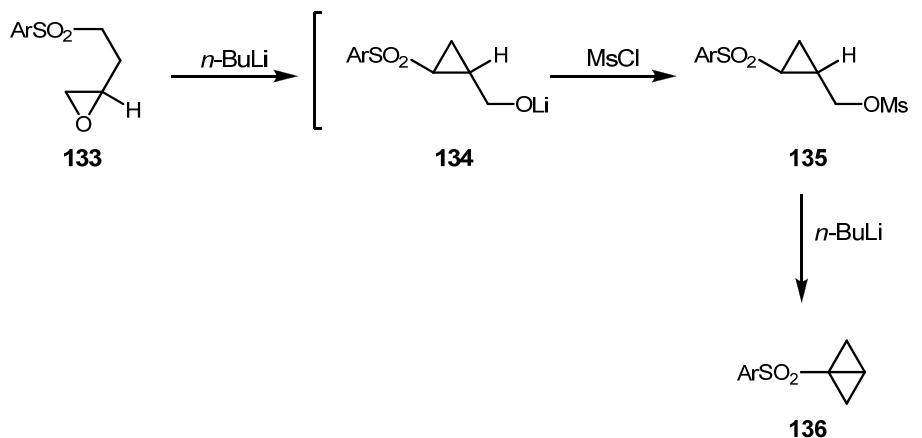
**Scheme 10: Cyclopropane synthesis *via*  $\text{S}_{\text{N}}2$  displacement I**

The anion can be generated next to different anion-stabilizing groups (ASGs) actually adjacent to an alkene or an arylthio group, which show only a reasonable stabilizing effect. The leaving group can be attached to a primary, secondary or tertiary carbon atom (Scheme 11, a-d).<sup>113-116</sup>



**Scheme 11: Cyclopropane synthesis via S<sub>N</sub>2 displacement II**

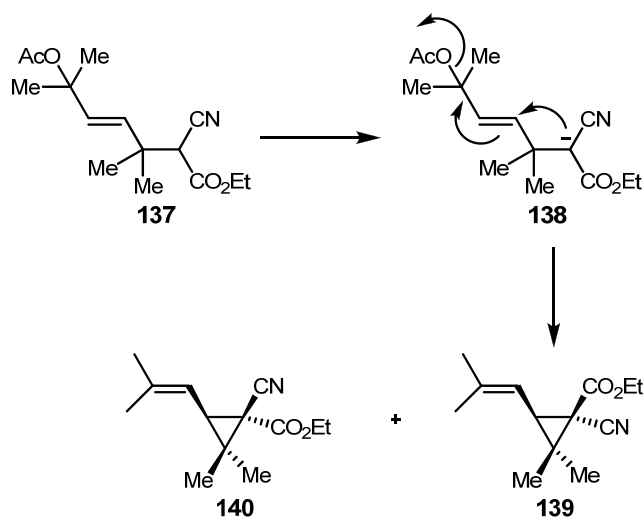
Cyclopropane synthesis is also possible by an intramolecular epoxide ring opening reaction. Scheme 12 demonstrates a double use of the 1,3-elimination reaction, affording bicyclo[1.1.0]butanes **136**.



**Scheme 12: Cyclopropane synthesis by intramolecular epoxide opening**

The geometry of the OMs- and arylsulfonyl groups in **135** is exclusively trans.<sup>117</sup>

Another possibility for a cyclopropanation is the intramolecular S<sub>N</sub>2-reaction from a  $\gamma,\delta$ -unsaturated carbonyl or nitrile compound with a leaving group at the  $\varepsilon$ -carbon atom.



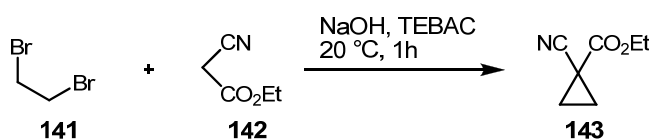
**Scheme 13: Synthesis of chrysanthemonic acid derivative**

Reaction conditions	140/139 ratio	Yield %
2.5 h, 65 °C	1:1	75%
1.5 h, 65 °C 5-10% Pd(PPh <sub>3</sub> ) <sub>4</sub>	19:1	70%

**Table 2: Synthesis of chrysanthemonic acid derivative – cis/trans ratio**

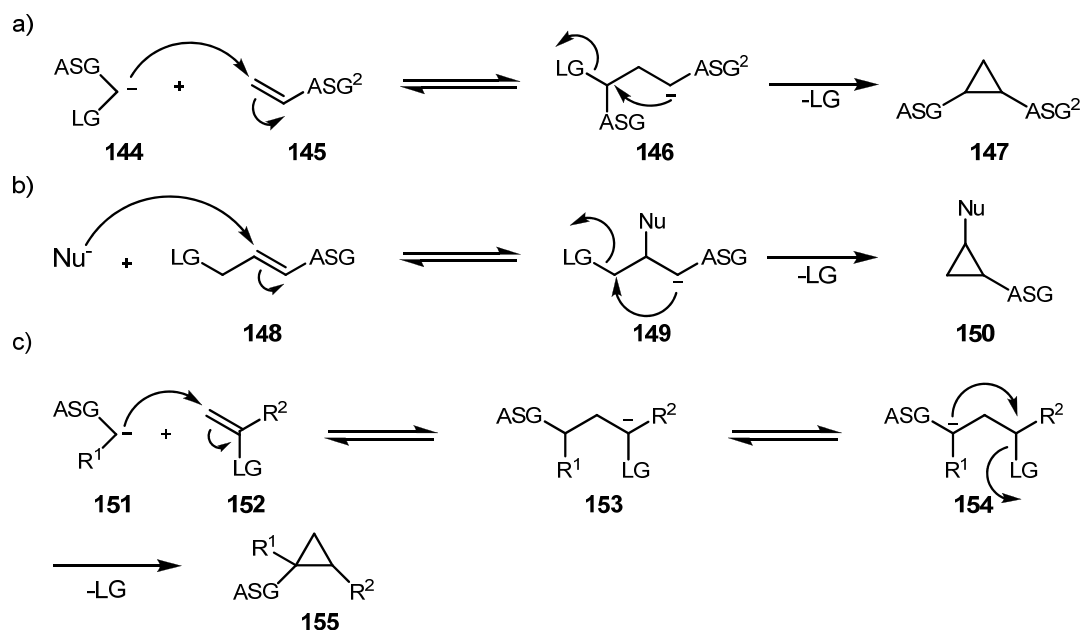
Scheme 13 shows a synthesis of a chrysanthemonic acid derivative. In the presence of a catalytic amount of tetrakis(triphenylphosphine)palladium(0), the cis-trans-ratio could be shifted toward the *cis*-chrysanthemonitrile derivative (Table 2).<sup>118</sup>

Another procedure for cyclopropane synthesis is a substitution initiated ring-closure reaction (SIRC). This is an alkylation followed by a cyclization of an activated methylene compound with 1,2-dihaloalkanes. One example is shown in the following Scheme 14.<sup>119</sup>



**Scheme 14: Substitution initiated ring-closure reaction (SIRC)**

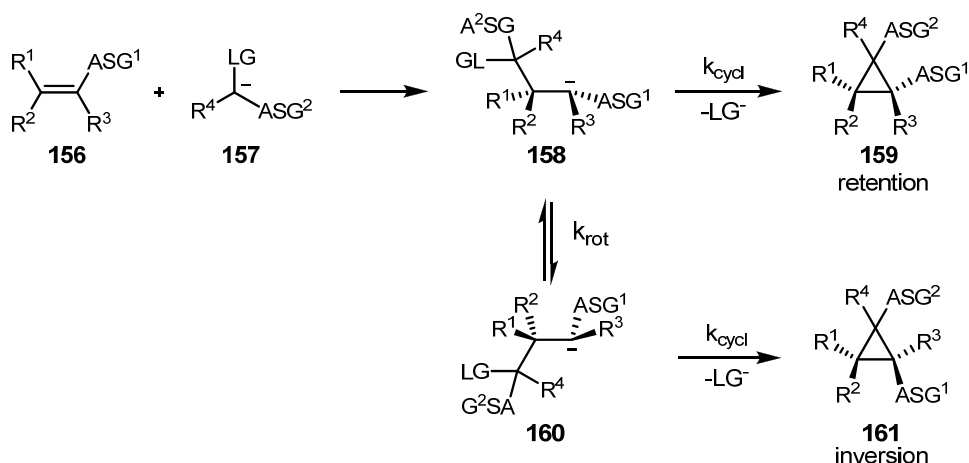
The Michael initiated ring-closure (MIRC) describes a ring closure reaction starting with a conjugate addition onto an electron-deficient alkene followed by the elimination of a leaving group (LG). The leaving group can be part of the nucleophile or can be incorporated into the Michael acceptor (Scheme 15).<sup>120</sup>



**Scheme 15: Michael initiated ring closure reaction (MIRC)**

Usually, MIRC reactions give racemic mixtures of cyclopropanes. The cis-trans-ratio and the stereoselectivity on the newly formed bond depends on different factors, the solvent polarity, the degree of anion-cation association and steric interactions.<sup>121</sup>

Due to hyperconjugation the carbanion intermediate has a relatively long lifetime; as a result rotation around the C-C bond is possible and inversion can be observed (Scheme 16).



**Scheme 16: Hyperconjugation in MIRC reactions**

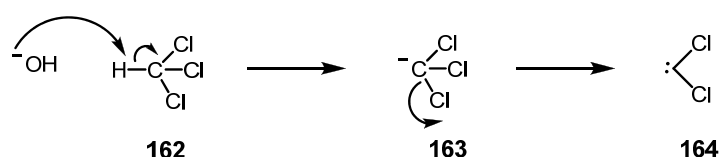
Stereospecificity can be observed when  $k_{cycl}$  is very high, which occurs with good leaving groups.

## Formation of cyclopropanes by the addition of carbenes to alkenes

Carbenes can be divided into two groups: so called triplet and singlet carbenes. Many carbenes exist in either state, but one may be more common. A  $sp^2$ -hybridized carbene has three  $sp^2$ -orbitals, which are low in energy, and one high-energy p-orbital, in which six electrons must be divided. There are two possibilities, all electrons can be paired in the  $sp^2$ -orbitals or two electrons can remain unpaired with one electron occupying the hybridized  $sp^2$ -orbital and the other the empty p-orbital. These two states describe the two classes of carbenes. The orbitals are the same in both cases. Triplet carbenes have two unpaired electrons and singlet carbenes have exclusively paired electrons in nonbonding  $sp^2$ -orbitals and an empty p-orbital.

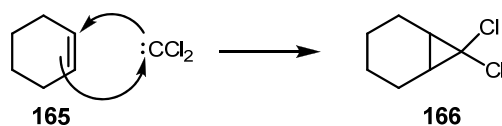
It depends on the substituents on the carbene in which of the two classes the reactive compound falls. For example the methyl carbene ( $:CH_2$ ) is a triplet carbene, which means that the triplet state is lower in energy than the singlet state and energy is necessary to pair the two electrons. When carbenes are formed during a chemical reaction it does not have to be formed in its most stable state, the ground state. Otherwise, dichlorocarbene ( $:CCl_2$ ) is a singlet carbene with the singlet state as most stable state, the ground state. Singlet carbenes all have electron-rich substituents carrying lone pairs which can interact with the free p-orbital of the carbene, forming a new lower-energy orbital.

The electronic structure of carbenes depends on how they are generated. Dichlorocarbene (**164**) is formed *via* an  $\alpha$ -elimination mechanism. Chloroform has exclusively paired electrons, in the first step of this elimination mechanism the C-H- $\sigma$ -bond breaks, both electrons move to the carbon atom to form the lone pair. The carbanion has also all paired electrons. In the following step two paired electrons from the C-Cl bond leave and the carbene is formed in the singlet state (Scheme 17).



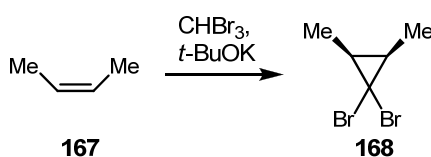
**Scheme 17: Dichlorocarbene formation**

Carbenes react with alkenes affording cyclopropanes. The mechanism of this reaction is different depending on whether the carbene is a singlet or a triplet. Singlet carbenes react in a concerted manner (Scheme 18).



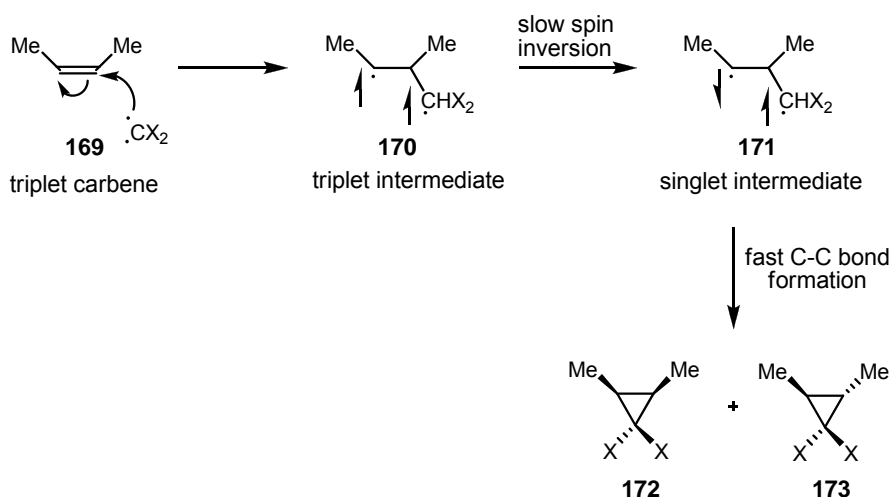
**Scheme 18: Reaction of dichlorocarbene**

The reaction is stereospecific, the geometry of the alkene is retained in the product (Scheme 19). The Z-alkene gives cis-cyclopropane, which is less stable than the trans-isomer.



**Scheme 19: Reaction of dibromocarbene**

For triplet carbenes the alkene insertion reaction is nonstereospecific and the reaction mechanism is not concerted. The carbene adds to the alkene in a radical reaction and a diradical (triplet) intermediate is formed. One of the spins must be inverted to form the second C-C bond. The intermediate is long living, C-C bond rotation can happen and the stereochemistry is lost (Scheme 20).



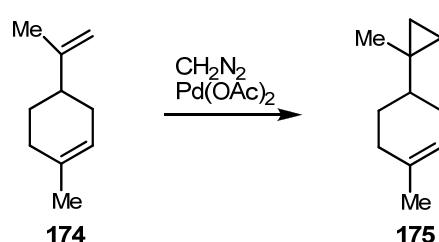
**Scheme 20: Reaction of triplet carbenes**

When a carbene is formed by  $\alpha$ -elimination it must be in singlet state, but nevertheless the triplet state is lower in energy. Most carbene reactions are very fast, carbenes with triplet ground states do not have the time for spin-flipping and react in the state they are

formed (singlet state). This fact can be observed for  $:\text{CH}_2$  produced from diazomethane. The addition of  $\text{CH}_2\text{N}_2$  to a double bond is stereospecific.

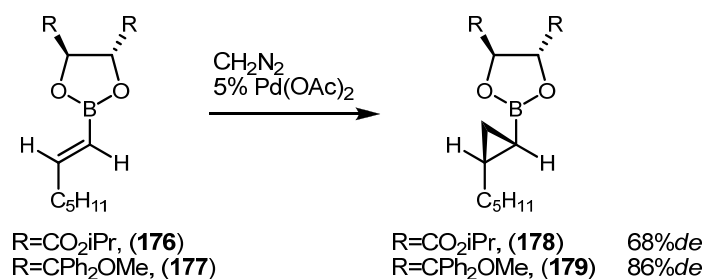
The reaction of a triplet carbene with an alkene can be classified as a radical reaction; otherwise, the concerted addition of a singlet carbene can be considered as a [1+2]-cycloaddition.

Photolysis of diazomethane generates the reactive carbene species. The photolytic decomposition can be catalyzed by metal salts. Palladium(II) acetate is a very effective catalyst for the cyclopropanation reaction.<sup>122</sup>



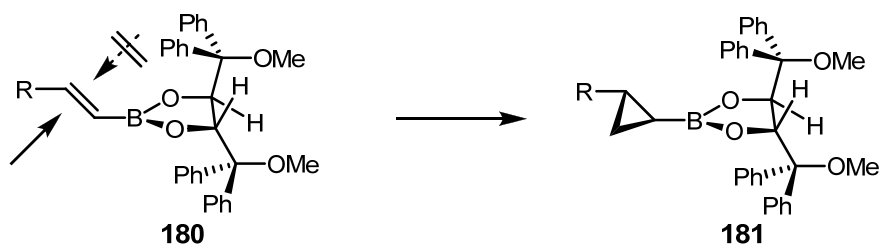
**Scheme 21: Cyclopropanation with diazomethane**

Scheme 21 shows the cyclopropanation on a cyclic olefin, the carbene species attacks the less hindered double bond.<sup>123</sup> The cyclopropanation with this method proceeds with low diastereoselectivity for acyclic olefins. Pietruszka *et al.* developed a method for diastereoselective cyclopropanation of alkenylboronic esters (Scheme 22).



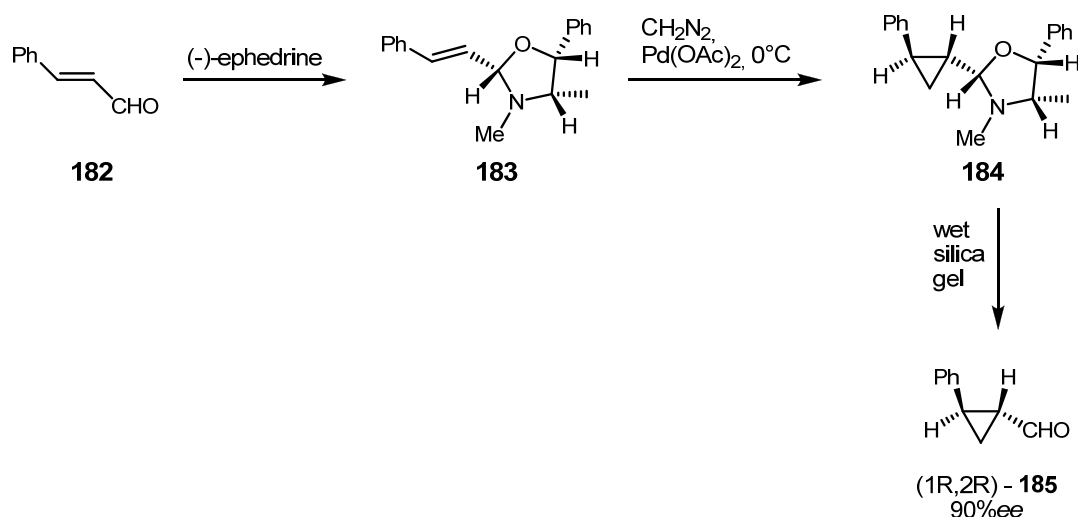
**Scheme 22: Diastereoselective cyclopropanation with diazomethane I**

The carbene attacks the double bond from the less hindered side without complexation to the bulky boronic ester group (Scheme 23).<sup>124</sup>



**Scheme 23: Diastereoselective cyclopropanation with diazomethane II**

Asymmetric cyclopropanation under the same reaction conditions could be arranged under the application of the chiral auxiliary (-)- or (+)- ephedrine and  $\alpha,\beta$ -unsaturated aldehydes (Scheme 24).<sup>125</sup>



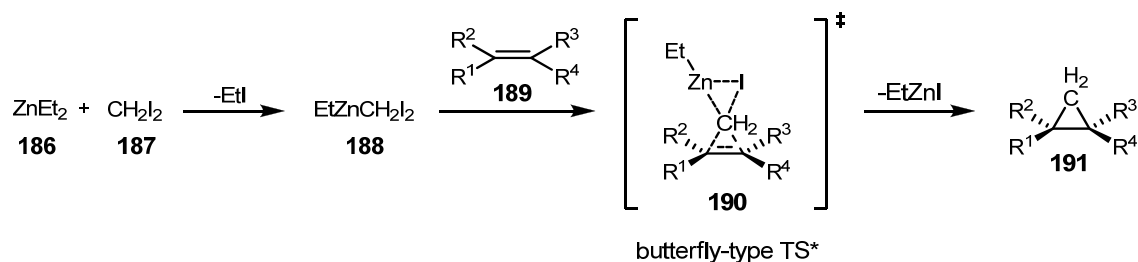
**Scheme 24: Asymmetric cyclopropanation of  $\alpha,\beta$ -unsaturated aldehydes**

## Simmons-Smith cyclopropanation

In 1958 Simmons and Smith published the stereospecific cyclopropanation of alkenes with diiodomethane and zinc-copper couple in high yield. The reactive intermediate is (iodomethyl)zinc iodide ( $\text{ICH}_2\text{ZnI}$ ) the product of the initial reaction of diiodomethane and zinc metal.<sup>126</sup> The Simmons-Smith reaction is a very powerful method for cyclopropane synthesis. The reaction is stereospecific, so the stereochemical information of the alkene is retained in the product. For chiral substrates the reaction is highly diastereoselective and the attack occurs from the less hindered side of the double bond. In the Furukawa modification diethylzinc and diiodomethane are used as reagents with high reproducible results.<sup>127</sup> The mechanism of this reaction is shown in Scheme 25. The so called Molander modification with iodo- or chloromethylsamarium

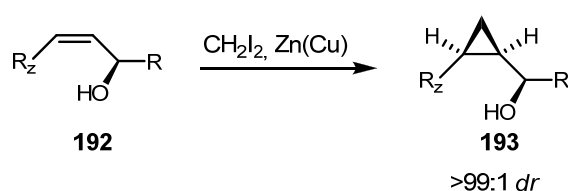


iodide is the method of choice for chemoselective cyclopropanation of allylic alcohols in the presence of other olefins.<sup>128</sup>



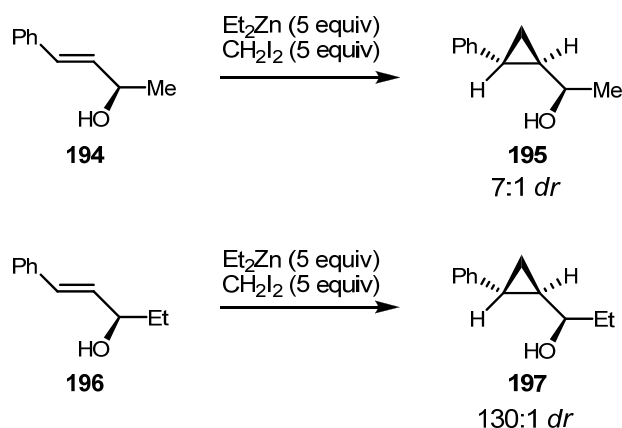
**Scheme 25: Furukawa modification of the Simmons-Smith reaction**

The diastereomeric selectivity of the Simmons-Smith reaction in cyclic and acyclic systems is strongly affected by allylic alcohol functionalities. The cyclopropanation reaction of (*Z*)-allylic secondary alcohols with zinc or samarium occurs with high diastereoselectivity (Scheme 26).<sup>123</sup>



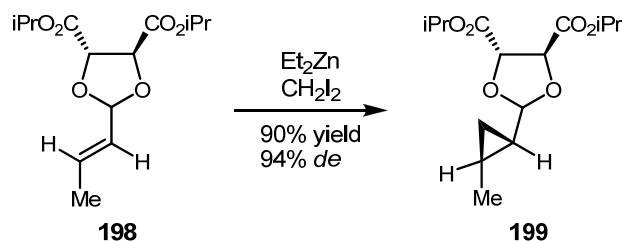
**Scheme 26: Cyclopropanation reaction of (*Z*)-allylic secondary alcohols**

The diastereomeric ratio (*dr*) can be explained by the directing influence of the allylic hydroxyl group which prevents allylic-1,3-strain. Cyclopropanation of the *trans*-isomer with  $\text{CH}_2\text{I}_2/\text{Et}_2\text{Zn}$  shows good *syn* selectivity. The diastereoselectivity depends on the steric bulk on the secondary alcohol (**194**, **196**, Scheme 27).<sup>129</sup>



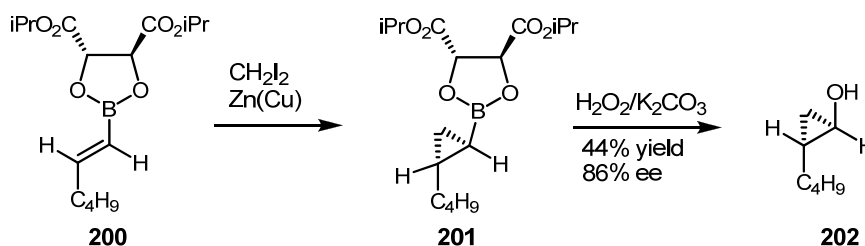
**Scheme 27: Cyclopropanation reaction of (*E*)-allylic secondary alcohols**

The cyclopropanation of  $\alpha,\beta$ -unsaturated acetals from tartrate esters was reported by Yamamoto (Scheme 28). The diastereoselectivity can be explained by the coordination of the Zn-species to the acetal as well as to the adjacent ester carbonyl.<sup>130</sup>



**Scheme 28: Cyclopropanation of  $\alpha,\beta$ -unsaturated acetals**

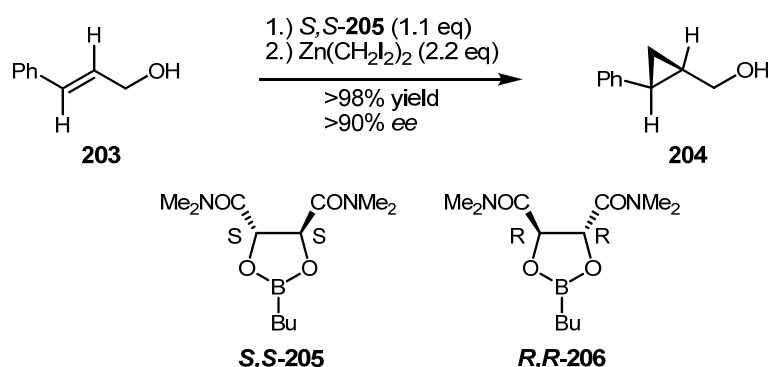
The asymmetric cyclopropanation of 1-alkenylboronic esters is also reported in literature. Subsequent oxidation affords cyclopropanols with high optical purity.<sup>131</sup>



**Scheme 29: Asymmetric cyclopropanation of 1-alkenylboronic esters**

The enantioselectivity for the Simmons-Smith cyclopropanation of **200** is opposite to that for the cyclopropanation with diazomethane (Scheme 29)

Cyclopropanation of allylic alcohols in presence of the chiral ligands *S,S*-**205**, *R,R*-**206** gives cyclopropylcarbinols in excellent yield and high *ee* (Scheme 30).<sup>132</sup>



**Scheme 30: Cyclopropanation of allylic alcohols in presence of chiral ligands**

A large number of chiral ligands were used for asymmetric Simmons-Smith cyclopropanation and were applied in the synthesis of cyclopropane containing natural products. Three examples of these chiral ligands are shown in Figure 29.<sup>133-135</sup>

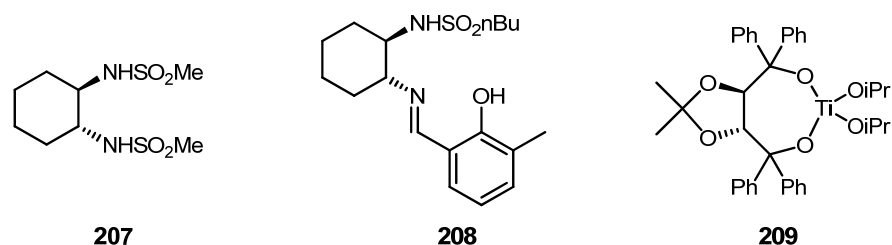
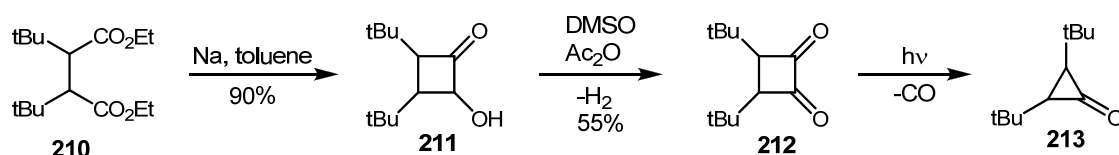


Figure 29: Chiral ligands for asymmetric Simmons-Smith reaction

## Cyclopropane synthesis *via* ring contraction

### 1) From four-membered rings

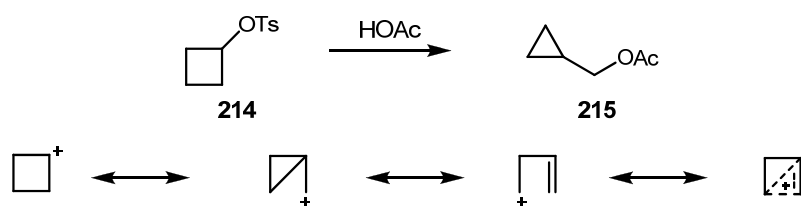
One possibility for cyclopropane synthesis from four-membered rings is the elimination of a one-atom fragment. The reactive intermediate of this reaction is a biradical. The cycloalkanone is irradiated with light of a certain wavelength which leads to  $\alpha$ -bond cleavage and an acyl-alkyl diradical which subsequently decarbonylates and forms the ring-contracted cycloalkane.



Scheme 31: Cyclopropane synthesis *via* elimination of a one-atom fragment

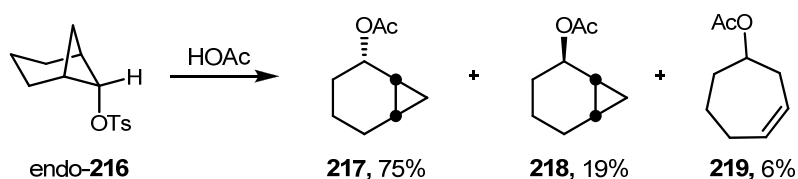
Acyloin-type cyclization and oxidation with activated DMSO (Albright-Goldman oxidation) is followed by irradiation of the resulting  $\alpha,\beta$ -diketone affording the desired cyclopropanone (Scheme 31).<sup>136</sup>

Another way of cyclobutane ring contraction is by rearrangement of cyclobutyl cations. Solvolysis of a tosylcyclobutane (**214**) occurs *via* a disrotatory ring opening which gives a cyclopropylmethyl cation as an intermediate and finally the cyclopropyl derivative is formed (Scheme 32).<sup>137</sup>



**Scheme 32: Cyclopropane synthesis by rearrangement of cyclobutyl cations I**

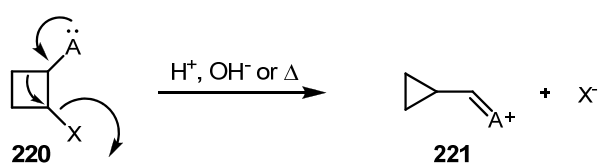
Under acidic conditions endo-**216** gives mainly 2-acetoxynorcaranes **217** and **218** (Scheme 33).<sup>137</sup>



**Scheme 33: Cyclopropane synthesis by rearrangement of cyclobutyl cations II**

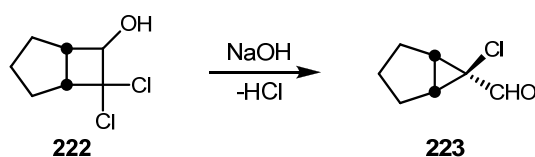
This reaction type often gives a mixture of a variety of products depending on the stabilized cation.

A very interesting class of ring contractions is the reaction of a substrate with an electron-donating group connected to one ring carbon atom and a leaving group, an electron-withdrawing group, on a neighboring carbon in the ring (Scheme 34). Known reactions that fall into this category are the acyloin and pinacol rearrangements, the benzilic acid and the quasi-Favorskii rearrangement.



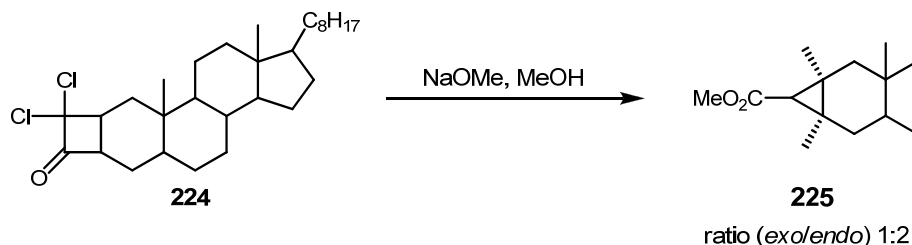
**Scheme 34: Cyclopropane synthesis in presence of an electron-donating and a leaving group**

Different examples are shown in the following schemes.



**Scheme 35: Ring contraction of 2,2-dihalocyclobutanols**

Scheme 35 shows the ring contraction of 2,2-dihalo-cyclobutanols with aqueous sodium hydroxide. The reaction is stereospecific: *exo*-alcohols give *endo*-aldehydes and *vice versa*. The chlorine atom trans to the hydroxyl functionality is displaced.<sup>138</sup>

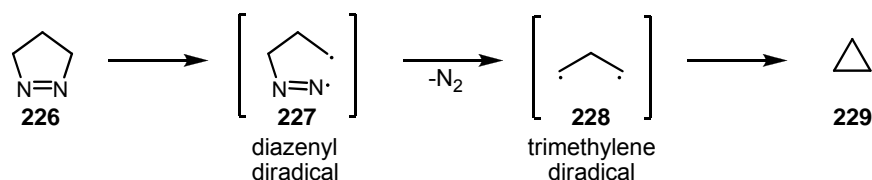


**Scheme 36: Ring contraction in steroid synthesis**

An example of a ring contraction in steroid synthesis is described in Scheme 36.<sup>139</sup>

## 2) From five-membered rings

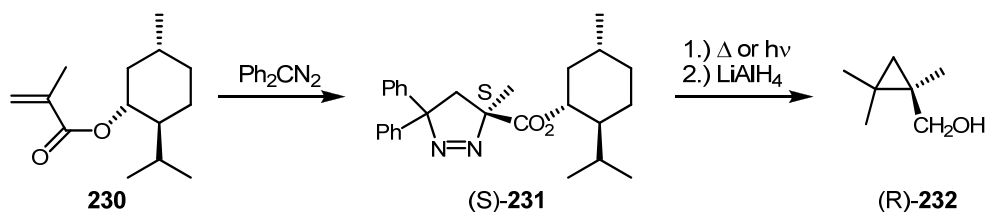
The thermal and photochemical deazetization of 4,5-dihydro-3*H*-pyrazoles is a very important method for cyclopropane synthesis. A simplified mechanism is shown in Scheme 37.



**Scheme 37: Deazetization of 4,5-dihydro-3*H*-pyrazoles**

The addition of diazoalkanes to alkenes to form 4,5-dihydro-3*H*-pyrazoles needs activating substituents, electron withdrawing groups such as trifluoromethyl, ester, nitrile, nitro substituents.

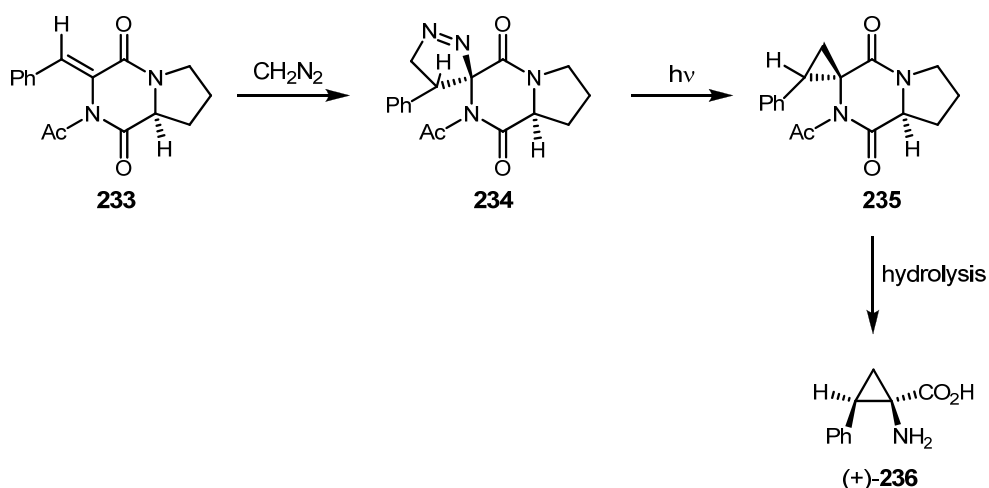
This method can be used for the synthesis of optically active cyclopropanes. One example, the reaction of diphenyldiazomethane with the corresponding (-)-menthyl ester, is demonstrated in Scheme 38.<sup>140</sup>



**Scheme 38: Synthesis of optically active cyclopropanes**

Diphenyldiazomethane reacts with (-)-menthyl ester to the diastereomer **231** (94% *de*). Pyrolysis or photolysis of the product and subsequent cleavage of the menthyl moiety with lithium aluminium hydride gave the desired product **232** with *R* configuration.

This route can be modified to give access to optically active amino acid derivatives (Scheme 39).<sup>141</sup>

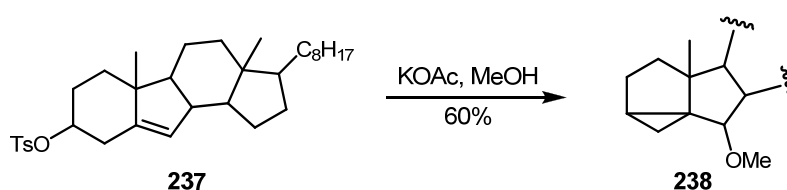


**Scheme 39: Synthesis of optically active amino acid derivatives**

The addition of diazomethane to **233** gave the spiro-pyrazoline **234** (diastereomeric ratio 95:5), after photolysis and subsequent hydrolysis (+)-**236** could be isolated.

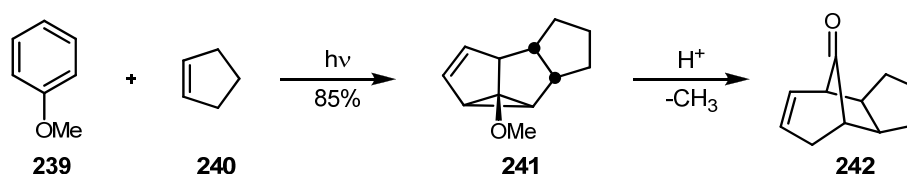
### 3) From six-membered rings

When a cyclohexyl cation is formed, a three-membered ring can be prepared (Scheme 40).<sup>142</sup>



**Scheme 40: Cyclopropane synthesis via a cyclohexyl cation**

Another possibility for cyclopropane synthesis from six-membered rings is the photochemical *meta*-addition of acyclic and cyclic alkenes with benzene.<sup>143</sup>



**Scheme 41: Photochemical *meta*-addition of anisole with cyclopentene**

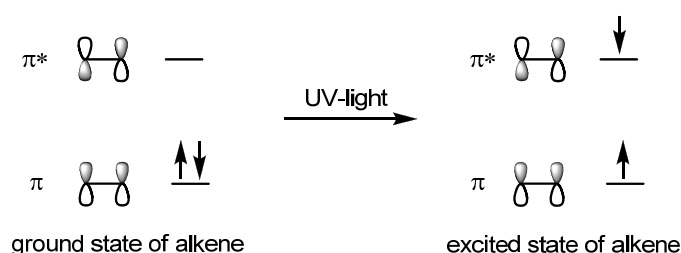
Scheme 41 shows the photochemical reaction of anisole (**239**) with cyclopentene (**240**) to tetracycle **241**. Subsequent acidic treatment allows the product to undergo a rearrangement affording **242**.<sup>144</sup>

## Cyclobutane

The C-C-C bond angle in cyclobutane is 90° in contrast to 109.5°, the tetrahedral angle in a linear butane molecule. Planar cyclobutane has exclusively eclipsed methylene groups, and such a conformation has a maximum torsional strain. The cyclobutane ring distorts from that planar conformation to decrease the negative eclipsed interactions, but otherwise at the same time the C-C-C dihedral bond angle is reduced resulting in an increase of the angle strain. The equilibrium geometry depends on those two competing strains. Cyclobutane shows a so called puckered or “wing-shaped” conformation.

## [2+2]-Cycloaddition

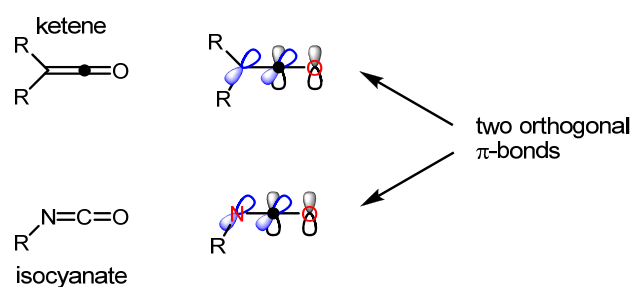
Cycloadditions with  $4n$   $\pi$ -electrons are allowed if the reaction is carried out photochemically. A thermal [2+2]-cycloaddition is symmetrically forbidden. The contradicting symmetry of two alkenes can be avoided if one electron is converted photochemically into the  $\pi^*$ -orbital (Scheme 42).



**Scheme 42: Photochemical [2+2]-cycloaddition**

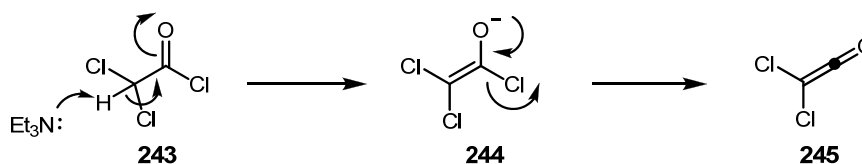
The symmetry problem is solved by the combination of one excited alkene with another in the ground state. The reaction is stereospecific and it proceeds *via* the least hindered transition state.

Thermal [2+2]-cycloadditions occur in the reaction of a simple alkene with an electrophilic alkene. The most important examples are ketenes and isocyanates. These compounds possess two perpendicular  $\pi$ -bonds which is the correct angle to allow a thermal reaction to occur (Scheme 43).



**Scheme 43: Orbitals of ketene and isocyanate for a thermal [2+2]-cycloaddition**

The very acidic proton on dichloroacetyl chloride can be removed with triethylamine. In a following  $E_1cB$  reaction a chloride anion is removed and the desired dichloroketene is formed.



**Scheme 44: Dichloroketene formation from dichloroacetyl chloride**

The cyclopentene derivative reacts with dichloroketene in a regio- and stereospecific manner (Scheme 45). The most nucleophilic atom in the alkene species is connected to the most electrophilic atom of the ketene in the resulting product **247**.<sup>145</sup>



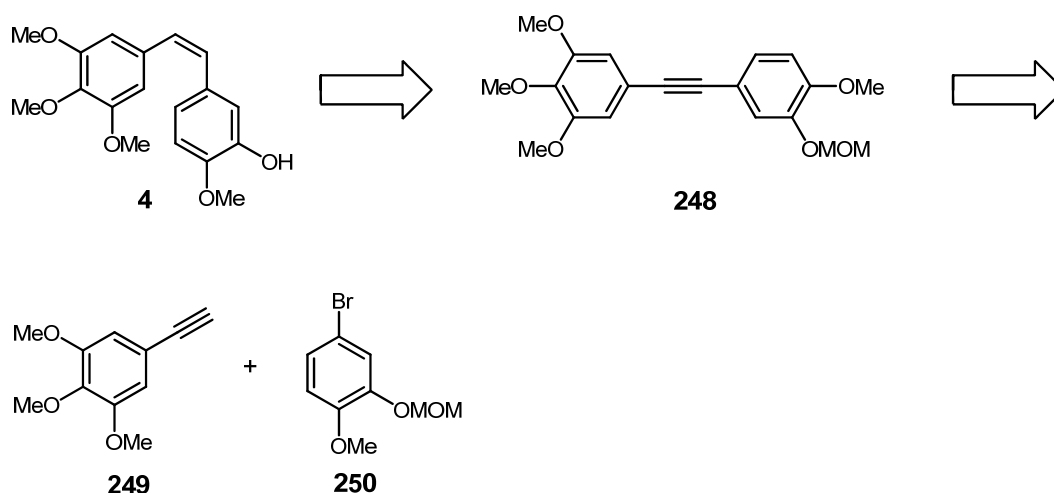
**Scheme 45: [2+2]-cycloaddition of a cyclopentene derivative with dichloroketene**



## 2. Results and discussion

### 2.1. Synthesis of CA-4

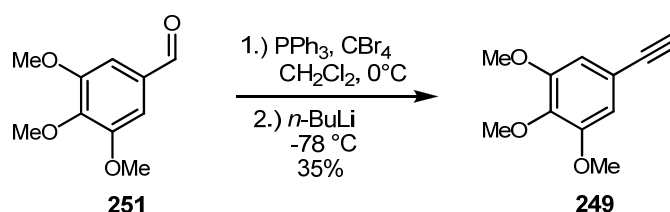
#### 2.1.1. Retrosynthetic analysis



Scheme 46: Retrosynthesis of CA-4

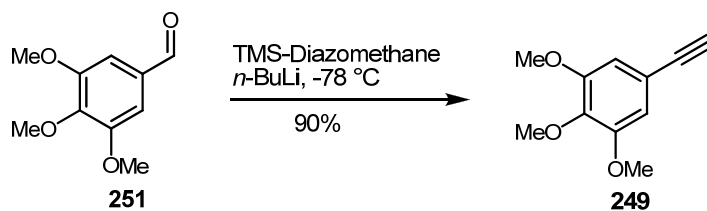
The synthetic strategy (Scheme 46) is based on the Suzuki-Miyaura palladium catalyzed coupling reaction between a alkynylboronic ester, generated *in situ* from acetylenic derivative **249**, and arylbromide **250**.<sup>146</sup> The coupling reaction is followed by the second key-step, the hydroboration or catalytic hydrogenation to afford natural product CA-4 (**4**).

#### 2.1.2. Synthesis of the two aromatic fragments



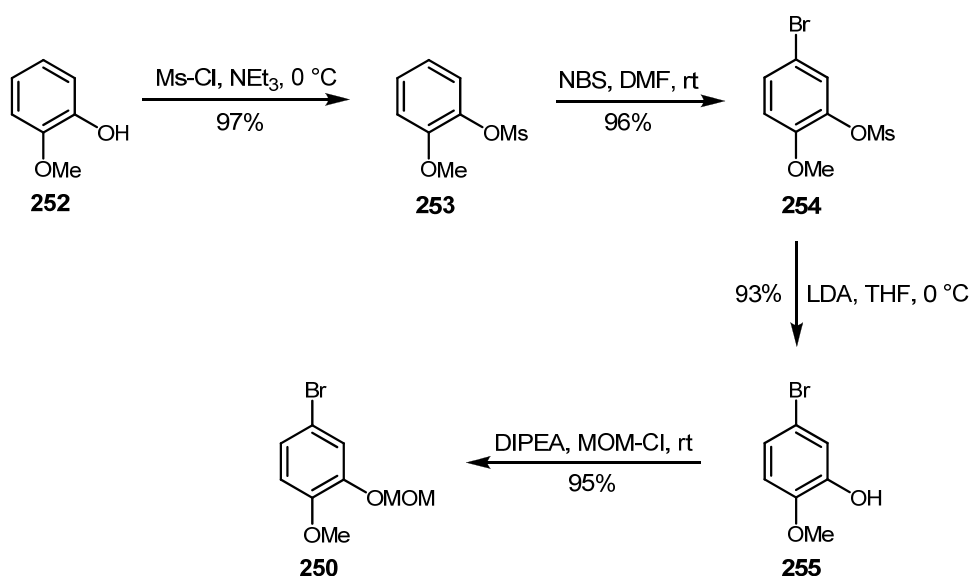
Scheme 47: Corey-Fuchs reaction

Initially, the alkyne was introduced *via* Corey-Fuchs reaction (Scheme 47),<sup>147,148</sup> of aldehyde **251**. However, the reaction afforded the desired alkyne in low yield and the method was replaced by a variation of the Bestmann-Ohira-sequence shown in Scheme 48. The aldehyde reacts in presence of  $n\text{-BuLi}$  and TMS-diazomethane to afford terminal alkyne **249**.<sup>149</sup>



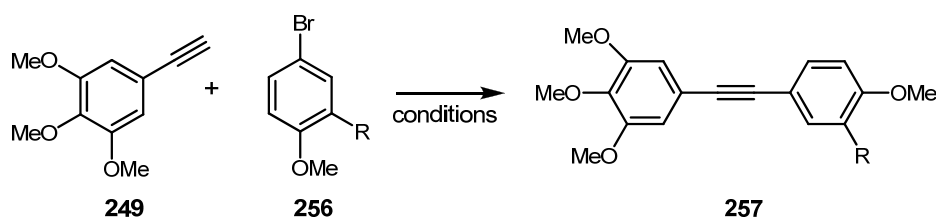
**Scheme 48: Synthesis of terminal alkyne 249 via a variation of the Bestmann-Ohira-sequence**

We were able to synthesize the aromatic fragment **250** in good yield over four steps as shown below (Scheme 49). Protection of guaiacol (**252**) with Ms-Cl under basic conditions gave aromatic derivative **253**, deactivated on the ortho-position of the methoxy functionality. The following selective bromination in para-position of the methoxy-group gave tri-substituted aromatic system **254**. In the next two steps **254** was deprotected (**255**) and the Ms-group was substituted by a MOM-group, affording the desired product **256**.<sup>150</sup>



**Scheme 49: Synthesis of the aromatic fragment 250**

### 2.1.3. Suzuki-Miyaura coupling reaction



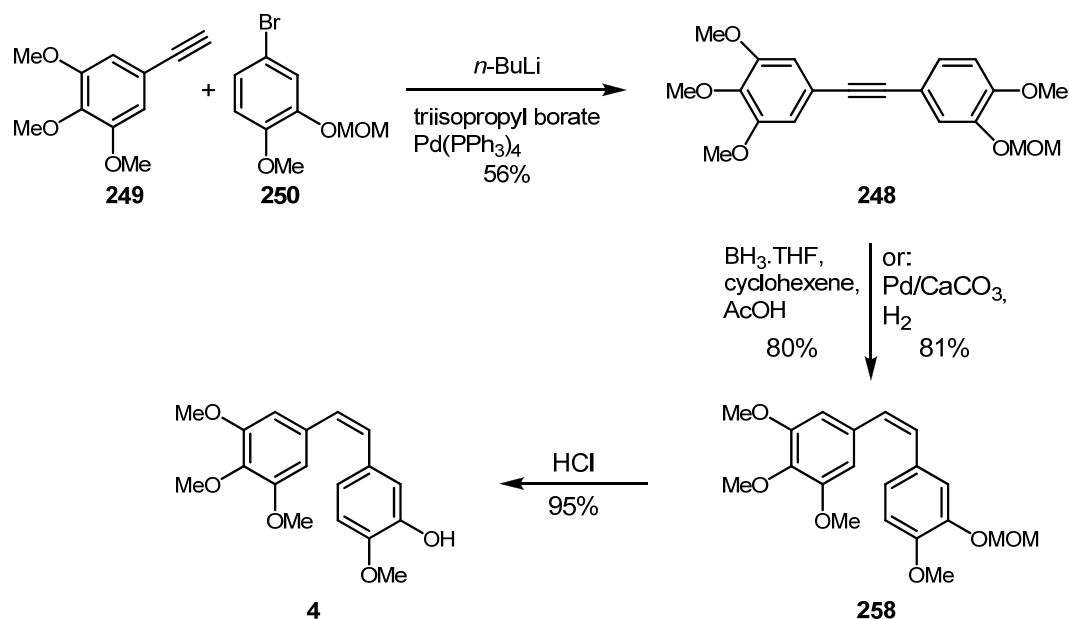
**Scheme 50: Suzuki-Miyaura coupling reaction**

The following step is the coupling reaction of the two before prepared aromatic fragments (Scheme 50). Finding reaction conditions which gave acceptable yield was tedious. Various conditions tried for that step are listed in Table 3.

R	reagents	catalyst	solvent	T	Reaction time	yield
OH	PPh <sub>3</sub> , <i>n</i> -BuLi <sup>151</sup>	Pd(OAc) <sub>2</sub>	pyrrolidine	90 °C	150 min	0%, SM reisolated
OH	triisopropylborate, <i>n</i> -BuLi <sup>151</sup>	Pd(PPh <sub>3</sub> ) <sub>4</sub>	DME	90 °C	14 h	0%, SM reisolated
OMs	triisopropylborate, <i>n</i> -BuLi <sup>146</sup>	Pd(PPh <sub>3</sub> ) <sub>4</sub>	DME	90 °C	14 h	0%, SM reisolated
OMOM	triisopropylborate, <i>n</i> -BuLi <sup>146</sup>	Pd(PPh <sub>3</sub> ) <sub>4</sub>	DME	90 °C	2 d	38%
OMOM	triisopropylborate, <i>n</i> -BuLi <sup>146</sup>	Pd(PPh <sub>3</sub> ) <sub>4</sub>	DME/THF 10:1	90 °C	1 week	0%, decomp.
<b>OMOM</b>	<b>triisopropylborate, <i>n</i>-BuLi<sup>146</sup></b>	<b>Pd(PPh<sub>3</sub>)<sub>4</sub></b>	<b>DME/THF 10:1</b>	<b>90 °C</b>	<b>2 d</b>	<b>56%</b>
OMOM	9-MeO-9-BBN, <i>n</i> -BuLi <sup>152</sup>	PdCl <sub>2</sub> (dpp)	THF	75 °C	6 h	33%
OMOM	9-MeO-9-BBN, <i>n</i> -BuLi <sup>152</sup>	PdCl <sub>2</sub> (dppf)	THF	75 °C	2 d	20%
OMOM	9-MeO-9-BBN, <i>n</i> -BuLi <sup>152</sup>	PdCl <sub>2</sub> (dppf)	DME/THF 10:1	90 °C	2 d	26%

**Table 3: Reaction conditions for the coupling reaction of CA-4**

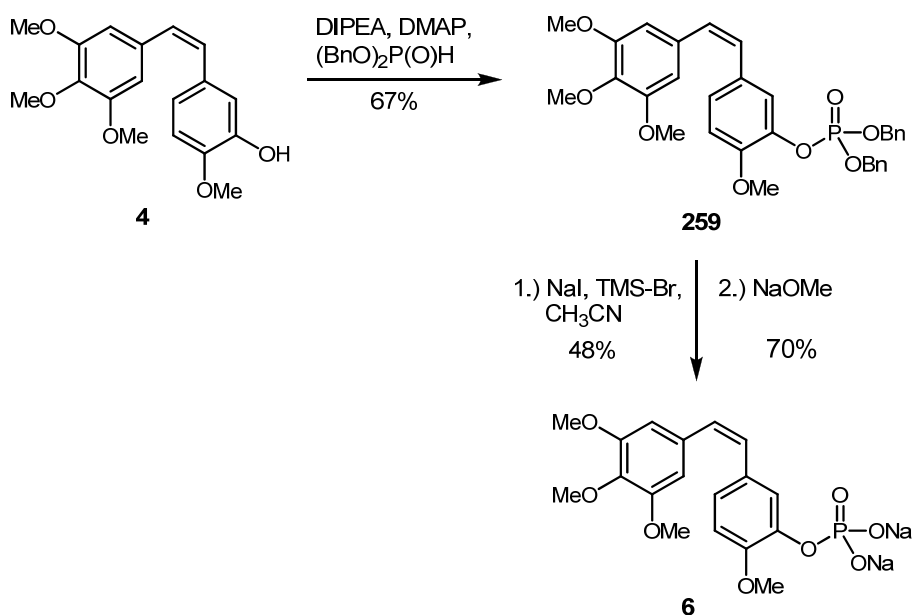
We found that protection of the phenolic hydroxy functionality as MOM-ether is essential for a positive result. The free and Ms-protected alcohol did not react under the reaction conditions shown in Table 3. For the most potent coupling condition triisopropylborate was used as the boron-species, tetrakis(triphenylphosphine)palladium(0) as catalyst and a solvent mixture DME/THF, 10:1.<sup>146</sup> The reaction mixture was heated to reflux for 2 days, leading to an acceptable yield (56%) of **248**.



Scheme 51: Synthesis of CA-4

As shown in Scheme 51 the palladium catalyzed coupling reaction was followed by hydroboration<sup>153</sup> or alternatively by catalytic hydrogenation. Both reactions afford the desired *cis*-stilbene derivative **258** in excellent yield. In the final step the MOM-protection-group was cleaved with a catalytical amount of hydrochloric acid affording the natural product CA-4.

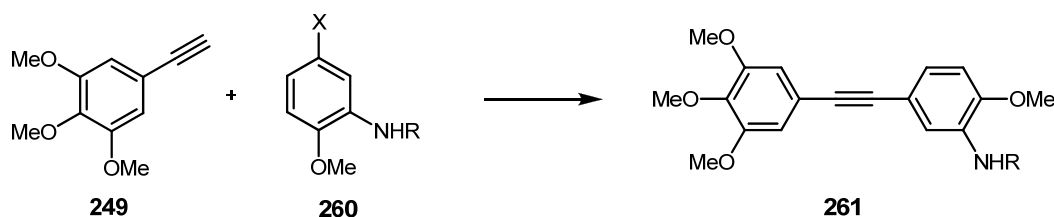
## 2.2. Synthesis of CA-4-phosphate



Scheme 52: Synthesis of CA-4-P

Scheme 52 shows the synthesis of combretastatin analog **6**. Derivatization of the phenol functionality with dibenzylphosphite and a catalytical amount of DMAP gave the dibenzylphosphate of CA-4 (**259**). Cleavage of the benzyl groups with NaI and TMS-Cl and subsequent transformation into the sodium salt for better water solubility, afforded CA-4-P (**6**).<sup>154</sup>

### 2.3. Synthesis of the amino derivative AVE8062



Scheme 53: Coupling reaction to generate the precursor of AVE8062

Again, key-step is the coupling reaction of the terminal alkyne (**249**) and aniline derivative **260** as shown in Scheme 53.

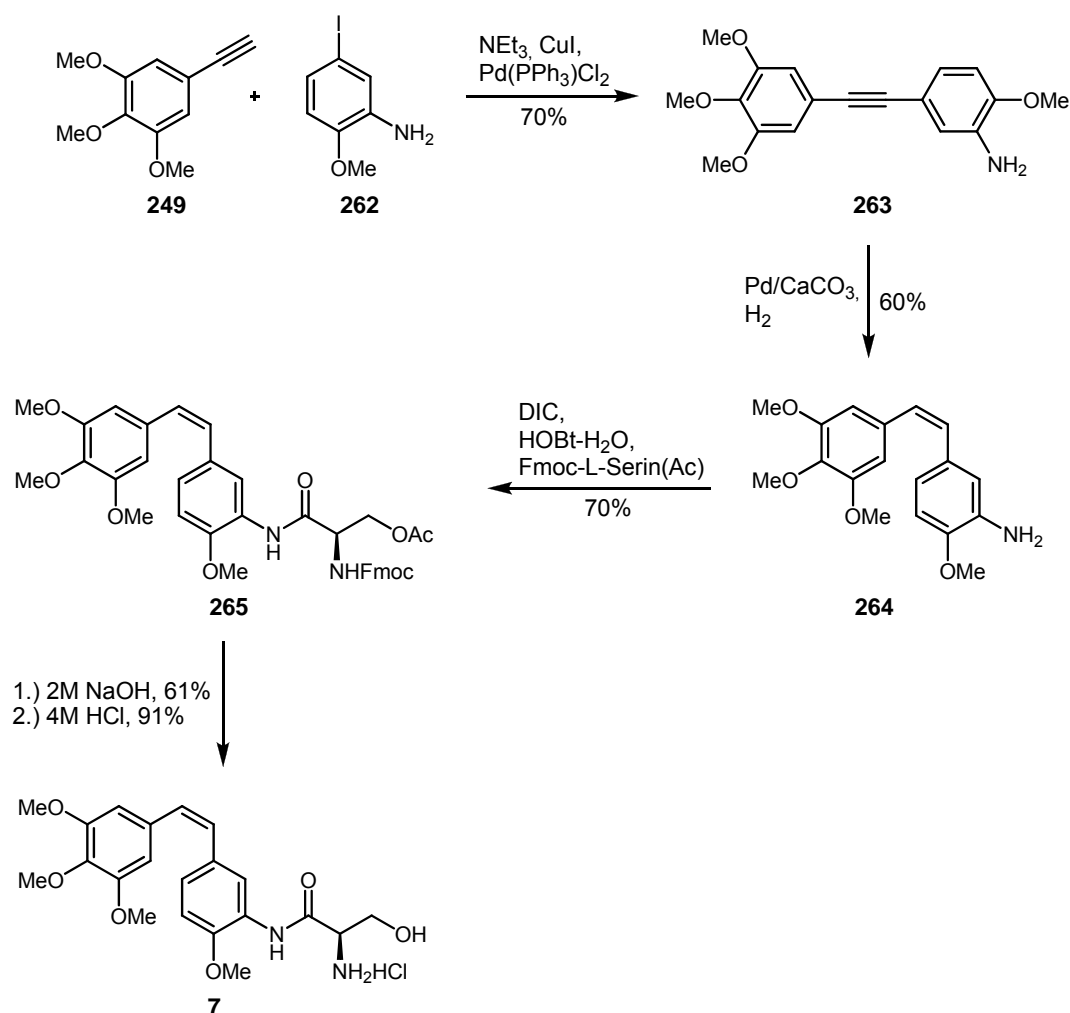
Table 4 demonstrates the various conditions tried to find the most efficient coupling conditions.

NHR	X	reagents	catalyst	solvent	T	Reaction time	yield
NHBoc	Br	Triisopropylborat, <i>n</i> -BuLi <sup>146</sup>	Pd(PPh <sub>3</sub> ) <sub>4</sub>	DME:THF 10:1	90 °C	14 h	0%, SM reisolated
NH <sub>2</sub>	Br	PPh <sub>3</sub> <i>n</i> -BuLi <sup>151</sup>	Pd(OAc) <sub>2</sub>	pyrrolidine	90 °C	5 h	0%, SM reisolated
NH <sub>2</sub>	Br	CuI <sup>155</sup>	Pd(PPh <sub>3</sub> ) <sub>4</sub>	piperidine	r. t.	1 day	0%, decomp.
NH <sub>2</sub>	Br	9-MeO-9-BBN <i>n</i> -BuLi <sup>152</sup>	PdCl <sub>2</sub> (dpp)	THF	75 °C	12 h	0%, SM reisolated
NHBoc	Br	9-MeO-9-BBN <sup>152</sup>	PdCl <sub>2</sub> (dpp)	THF	75 °C	12 h	3 %
<b>NH<sub>2</sub></b>	<b>I</b>	<b>NEt<sub>3</sub>, CuI<sup>156</sup></b>	<b>Pd(PPh<sub>3</sub>)Cl<sub>2</sub></b>	<b>DMF</b>	<b>r.t.</b>	<b>20 h</b>	<b>70 %</b>

Table 4: Reaction conditions for coupling reaction of AVE8062 synthesis

The Suzuki-Miyaura coupling conditions as described before for the synthesis of CA-4, triisopropylborate as the boron species and tetrakis(triphenylphosphine)palladium(0) as catalyst, resulted in reisolation of the starting materials. Also standard Heck reaction conditions with triphenylphosphine and palladium diacetate were tried but with not much

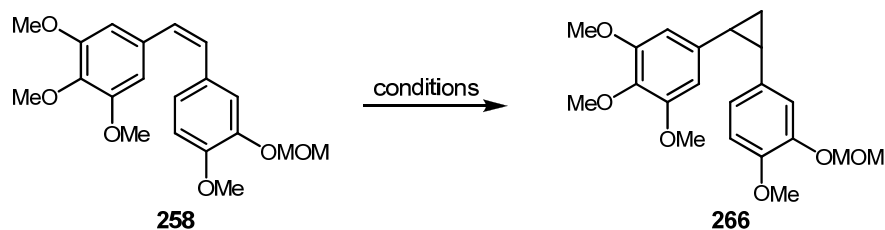
success.<sup>157</sup> We switched from the arylbromide to the more reactive aryl iodide and changed to Sonogashira coupling conditions with  $\text{NEt}_3$  as base;  $\text{CuI}$  and dichlorobis(triphenylphosphine)palladium(II) as catalyst.<sup>158</sup> Finally, we were able to isolate the coupling product **263** in good yield.



**Scheme 54: Synthesis of AVE8062**

As described in Scheme 54, coupling of the two aromatic fragments was followed by catalytic hydrogenation to afford **264**. In the following three steps first the Fmoc- and acetate-protected L-serine moiety was incorporated at the amino functionality of the *cis*-stilbene giving **265**. Furthermore, both protecting groups were cleaved under basic conditions with 2M NaOH and finally the hydrochloride was precipitated, affording the desired derivative AVE8062 (**7**).<sup>159</sup>

## 2.4. Synthesis of cyclopropane derivative (266)



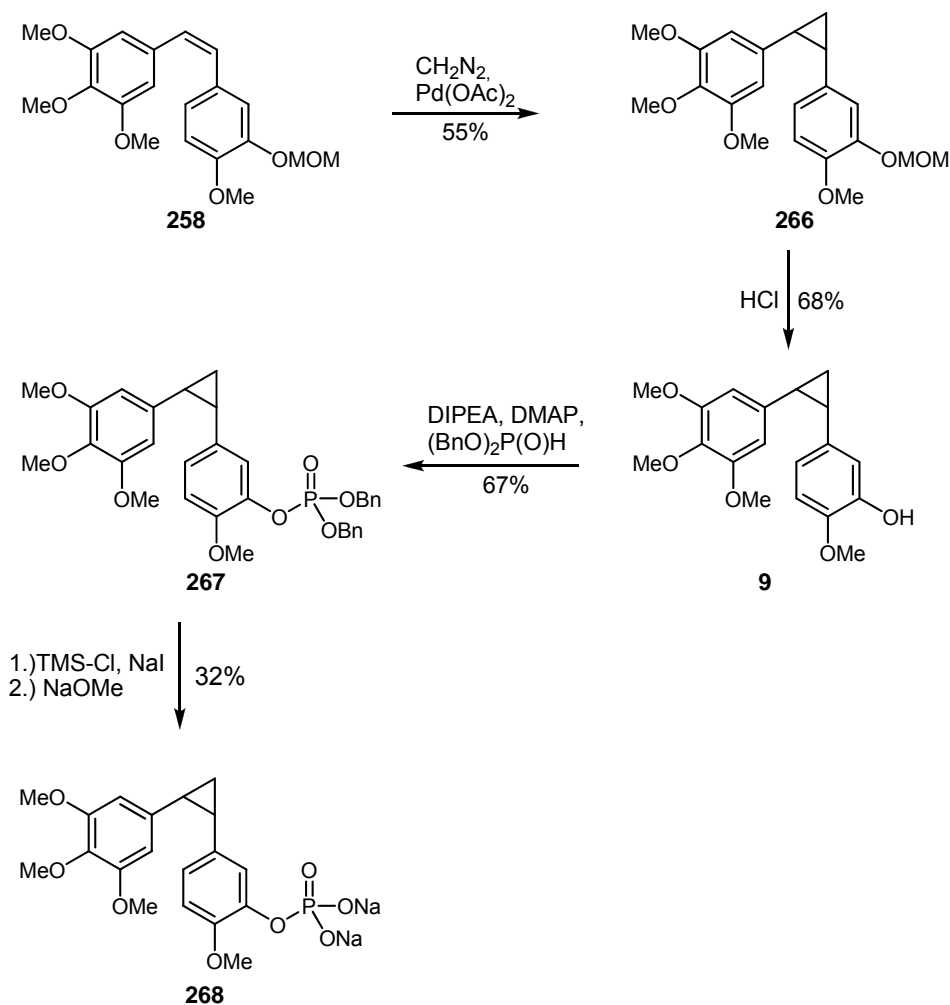
Scheme 55: Cyclopropanation reaction

Various conditions for the cyclopropanation (Scheme 55) of the double bond on the connecting carbon bridge of the MOM-protected CA-4 were investigated (Table 5).

Reagents	Solvent	T	Reaction time	Yield
CHCl <sub>3</sub> , benzyltriethylammonium chloride, NaOH <sup>160</sup>	-	50 °C	4 h	0%, decomposition
ZnEt <sub>2</sub> , CH <sub>2</sub> I <sub>2</sub> <sup>161</sup>	CH <sub>2</sub> Cl <sub>2</sub>	0 °C	12 h	0%, SM reisolated
ZnEt <sub>2</sub> , CH <sub>2</sub> I <sub>2</sub> <sup>161</sup>	CH <sub>2</sub> Cl <sub>2</sub>	r. t.	2 days	0%, SM reisolated
ZnEt <sub>2</sub> , CH <sub>2</sub> I <sub>2</sub> , TFA <sup>162</sup>	CH <sub>2</sub> Cl <sub>2</sub>	r. t.	12 h	0%, SM reisolated
CBrCl <sub>3</sub> , <i>n</i> -BuLi <sup>163</sup>	Et <sub>2</sub> O	r. t.	12 h	0%, SM reisolated
Mg, CCl <sub>4</sub> , TiCl <sub>4</sub> <sup>164</sup>	CICH <sub>2</sub> CH <sub>2</sub> Cl	0 °C	90 min	0%, SM reisolated
<b>CH<sub>2</sub>N<sub>2</sub>, Pd(OAc)<sub>2</sub><sup>165</sup></b>	<b>Et<sub>2</sub>O</b>	<b>0 °C</b>	<b>3 h</b>	<b>55%</b>

Table 5: Reaction conditions for the cyclopropanation reaction

Standard conditions for carbene formation, (chloroform, a phase-transfer-catalyst and NaOH as base<sup>160</sup>) resulted in decomposition of the starting material. The Simmons-Smith reaction<sup>161</sup> also did not afford the desired cyclopropane derivative and the starting material was recovered unchanged even when the Simmons-Smith reagent was activated with TFA.<sup>162</sup> Also the carbene formation with CBrCl<sub>3</sub> and *n*-BuLi<sup>163</sup> as well as the TiCl<sub>4</sub>-Mg-promoted dichlorocarbene transfer of CCl<sub>4</sub><sup>164</sup> did not show any reaction. The cyclopropanation with diazomethane and palladiumdiacetate as a catalyst<sup>165</sup> led to the desired cyclopropane derivative (**266**) with 55% yield.

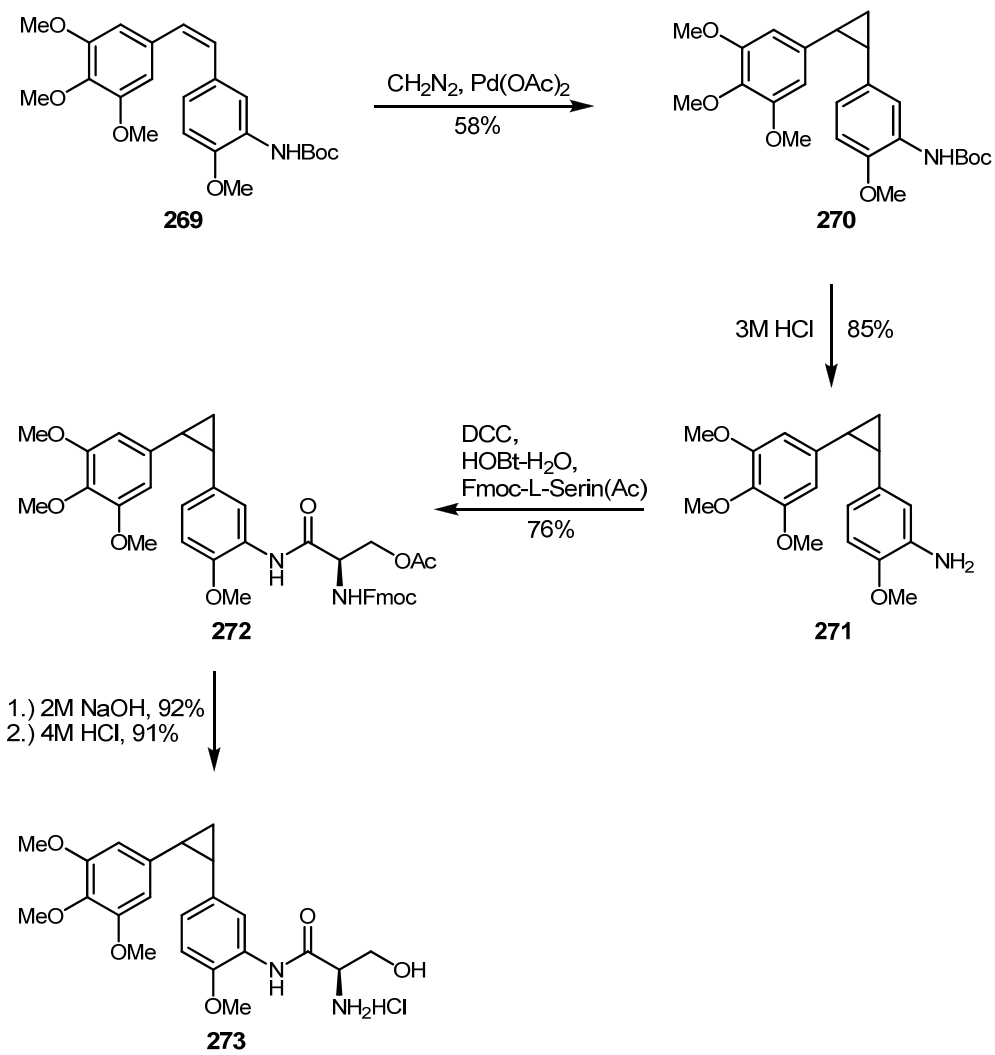


**Scheme 56: Synthesis of cyclopropane derivative 268**

The cyclopropanation was followed by the removal of the MOM-protecting-group under acidic condition, and the cyclopropyl derivative of CA-4 (**9**) was isolated. Subsequent derivatization of the free phenolic functionality with dibenzyl phosphite and transformation of the phosphate into the corresponding sodium salt was done to increase water solubility (Scheme 56).<sup>154</sup>

The cyclopropane derivative of AVE8062 was prepared as shown in Scheme 57. We started with the cyclopropanation, the reaction conditions were described earlier in that section, of the Boc-protected *cis*-stilbene (**269**). The cyclopropanation was also carried out with the unprotected compound. The reaction resulted in decomposition of the starting material. The protection group was cleaved, giving **271**, and the L-serine moiety was introduced following the same procedure as described for the synthesis of AVE8062. First the protected serine was incorporated (**272**) followed by deprotection and precipitation of the hydrochloride, affording the desired product **273**.<sup>159</sup>

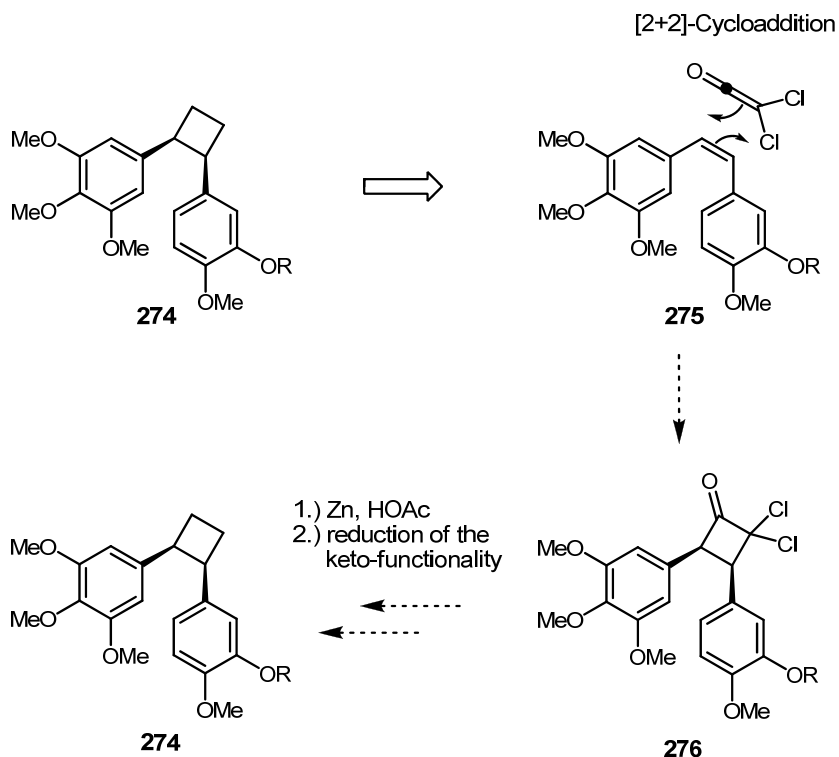




**Scheme 57: Synthesis of the cyclopropane derivative of AVE8062 (273)**

## 2.5. Synthesis of the cyclobutane derivative

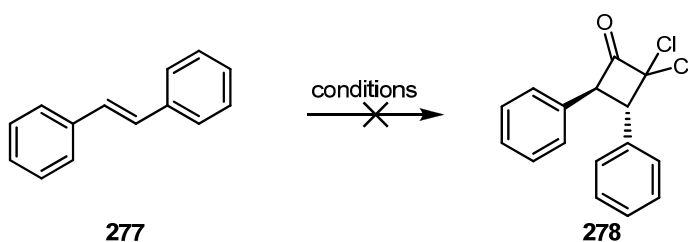
### 2.5.1. First approach – [2+2]-cycloaddition



Scheme 58: Synthesis of the cyclobutane derivative via [2+2]-cycloaddition

Key step in this approach (Scheme 58) is the [2+2]-cycloaddition followed by removal of the two chlorine atoms by zinc metal and subsequent reduction of the keto-functionality. Before reactions were carried out on the actual systems, conditions were optimized on model systems.

Standard dichloroketene-formation conditions on *trans*-stilbene were tested first (Scheme 59, Table 6).



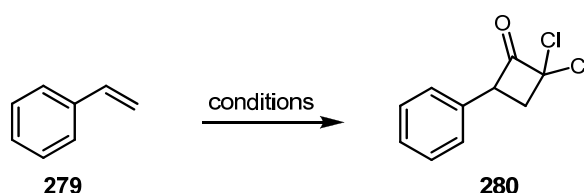
Scheme 59: [2+2]-cycloaddition on *trans*-stilbene

Reagents	Solvent	T	Reaction time	Yield
dichloroacetylchloride, NEt <sub>3</sub>	Et <sub>2</sub> O	0 C°	24 h	0%; SM reisolated
Zn, trichloroacetylchloride <sup>166</sup>	Et <sub>2</sub> O	0 C°	5 h	0%; SM reisolated
Zn, POCl <sub>3</sub> , trichloroacetylchloride <sup>167</sup>	Et <sub>2</sub> O	reflux	3 h	0%; SM reisolated
Zn-Cu, POCl <sub>3</sub> , trichloroacetylchloride <sup>167</sup>	Et <sub>2</sub> O	reflux	3 h	0%; SM reisolated

**Table 6: Reaction conditions [2+2]-cycloaddition, trans-stilbene**

We started with dichloroacetylchloride and NEt<sub>3</sub>, but no reaction was observed and the starting material was reisolated unchanged after the reaction. We switched to more reactive conditions and employed zinc-metal and trichloroacetylchloride<sup>166</sup>, but with no success. Also further activation with phosphorylchloride and zinc-copper-couple as metal species did not yield the desired material.<sup>167</sup>

Subsequently, we replaced our test system with styrol (Scheme 60, Table 7) and the reaction conditions tried earlier, zinc-copper-couple, POCl<sub>3</sub>, trichloroacetylchloride and diethylether as solvent,<sup>167</sup> afforded the desired product. We were able to isolate the desired cyclobutane derivative (**280**).

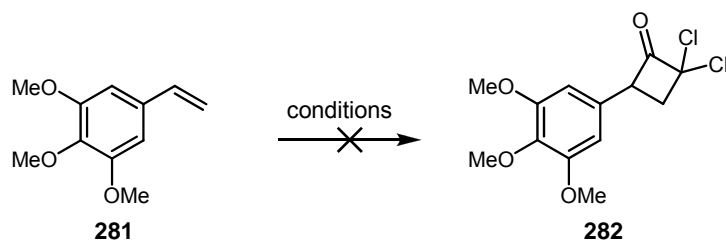


**Scheme 60: [2+2]-cycloaddition on styrol**

Reagents	Solvent	T	Reaction time	Yield
activated Zn, POCl <sub>3</sub> , trichloroacetylchloride <sup>167</sup>	Et <sub>2</sub> O	rt	45 min	90%

**Table 7: Reaction conditions [2+2]-cycloaddition, styrol**

However, the same reaction conditions led to decomposition of the third test system, the electron rich trimethoxystyrol (**281**, Scheme 61, Table 8).

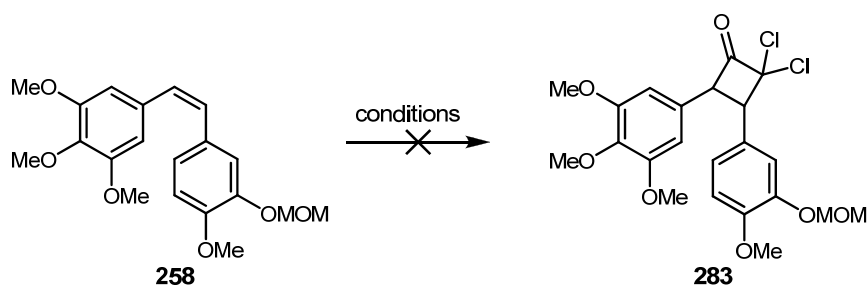


Scheme 61: [2+2]-cycloaddition on trimethoxystyrol

Reagents	Solvent	T	Reaction time	Yield
Zn-Cu (commercially available), trichloroacetylchloride <sup>167</sup>	Et <sub>2</sub> O	rt	2 h	decomposition
activated Zn, POCl <sub>3</sub> , trichloroacetylchloride <sup>167</sup>	Et <sub>2</sub> O	rt	2 h	decomposition

Table 8: Reaction conditions [2+2]-cycloaddition, trimethoxystyrol

Against great odds we tried the dichloroketene formation conditions on MOM-protected CA-4, but as expected with no success. The only reaction to occur was the cleavage of the MOM-group (Scheme 62, Table 9)

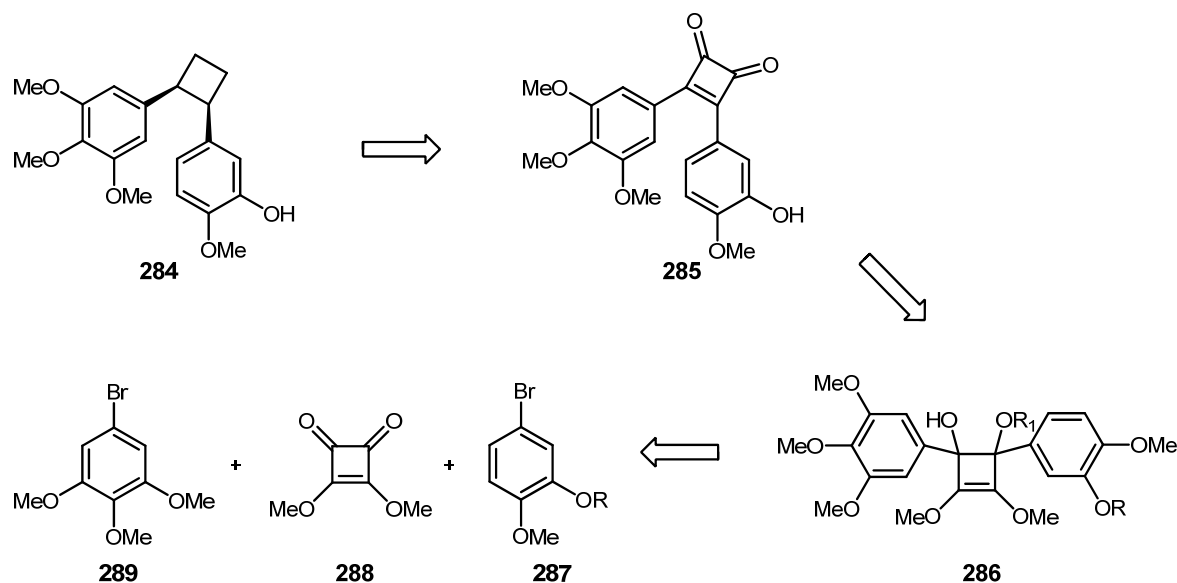


Scheme 62: [2+2]-cycloaddition on MOM-protected CA-4

Reagents	Solvent	T	Reaction time	Yield
Dichloroacetylchloride, NEt <sub>3</sub>	Et <sub>2</sub> O	0 C°	24 h	0%; SM reisolated
Zn, trichloroacetylchloride <sup>166</sup>	Et <sub>2</sub> O	0 C°	5 h	0%; SM reisolated
Zn-Cu, trichloroacetylchloride <sup>166</sup>	THF	0 °C	2 h	0%; SM reisolated
Zn, POCl <sub>3</sub> , trichloroacetylchloride <sup>167</sup>	Et <sub>2</sub> O	40 °C	3 h	0%; MOM-deprotection
Zn-Cu, POCl <sub>3</sub> , trichloroacetylchloride <sup>167</sup>	Et <sub>2</sub> O	40 °C	3 h	0%; MOM-deprotection, cis-trans-isomerization

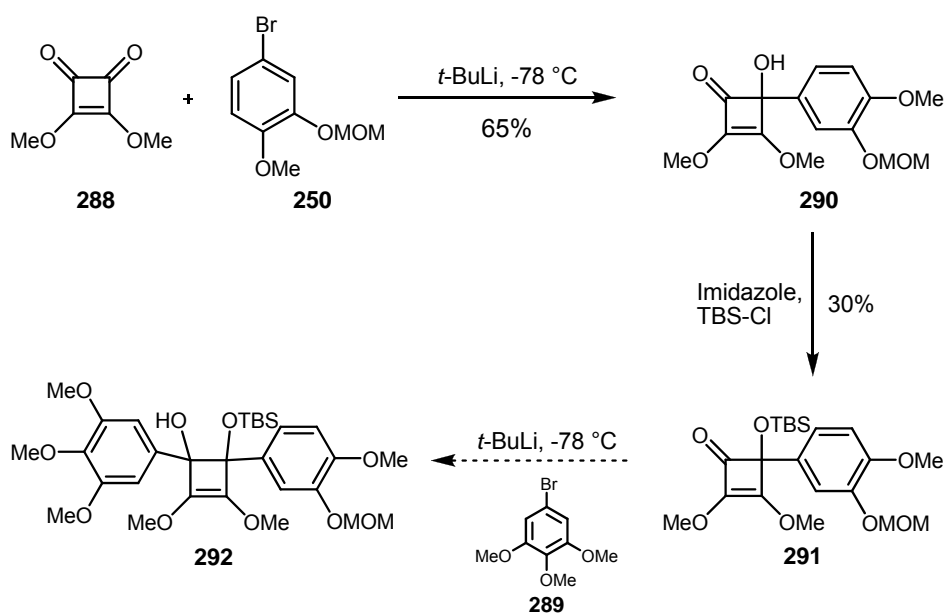
Table 9: Reaction conditions [2+2]-cycloaddition, MOM-protected CA-4

## 2.5.2. Second approach – Squaric acid



**Scheme 63: Retrosynthetic analysis of the squaric acid approach**

The synthetic strategy (Scheme 63) was the incorporation of the two aromatic rings (**287**, **289**) at the keto-functionalities of dimethylester of squaric acid (**288**), followed by elimination of two molecules of methanol with concentrated hydrochloric acid of the highly substituted cyclobutene derivative (**286**), as described in the literature, affording the diketo-compound (**285**).<sup>168,169</sup> Subsequent decarbonylation as well as hydrogenation of the double-bond of the cyclobutenyl-ring should give the desired cyclobutane derivative of CA-4 (**284**).



**Scheme 64: Squaric acid approach**

First, one equivalent of the MOM-protected aromatic derivative (**250**) was lithiated with *t*-BuLi at -78 °C in diethyl ether, after addition of dimethylsquarate the aromate was added, giving the resulting alcohol (**290**) with acceptable yield.<sup>168</sup> The tertiary alcohol was protected with TBS-chloride, affording (**291**).<sup>169</sup> But this approach failed at the next step. The plan was to repeat the reaction conditions for lithiating the second aromate, but we were not able to introduce that at the second keto-functionality of dimethylsquarate, affording **292**, so this approach was abandoned.

### 3. Biological evaluation

The biological activity of the compounds prepared within this work was evaluated on two human cancer cell lines. The biological activity study was carried out by cooperation partners at the University of Szeged.

HeLa cells are cervical epitheloid carcinoma cells and MCF 7 is a breast carcinoma cell line.

All tested compounds and their assigned numbers are listed in the following table.

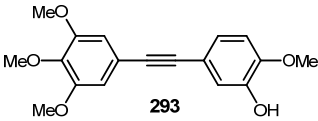
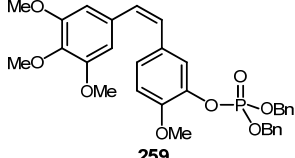
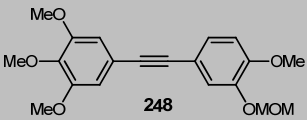
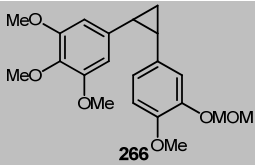
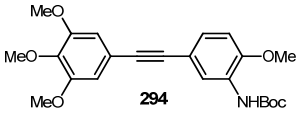
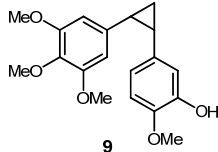
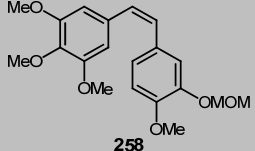
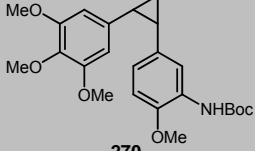
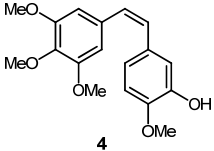
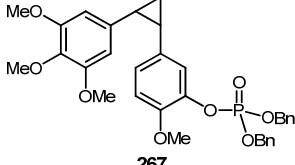
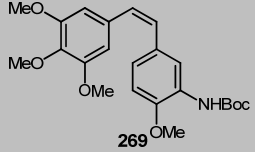
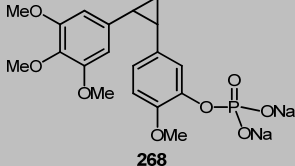
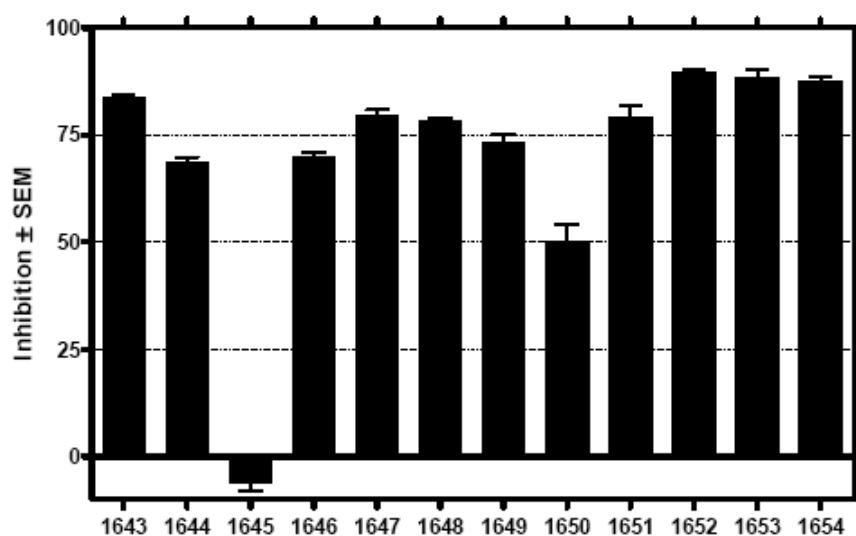
Assay-number	Compound	Assay-number	Compound
1643	 293	1649	 259
1644	 248	1650	 266
1645	 294	1651	 9
1646	 258	1652	 270
1647	 4	1653	 267
1648	 269	1654	 268

Table 10: Tested compounds

### 3.1. Results – HeLa cells

The concentration of the assays which were applied on the cell culture was 30  $\mu$ M. The inhibition of cell proliferation within a certain time is investigated. The bars in Scheme 65 demonstrate that all compounds with just one exception, the alkyne derivative **293** (assay # 1645) show potent biological activity. When the inhibition of a compound is less than 50% at 30  $\mu$ M it is considered as inactive. It seems very interesting that also the alkyne derivatives are active at that concentration.

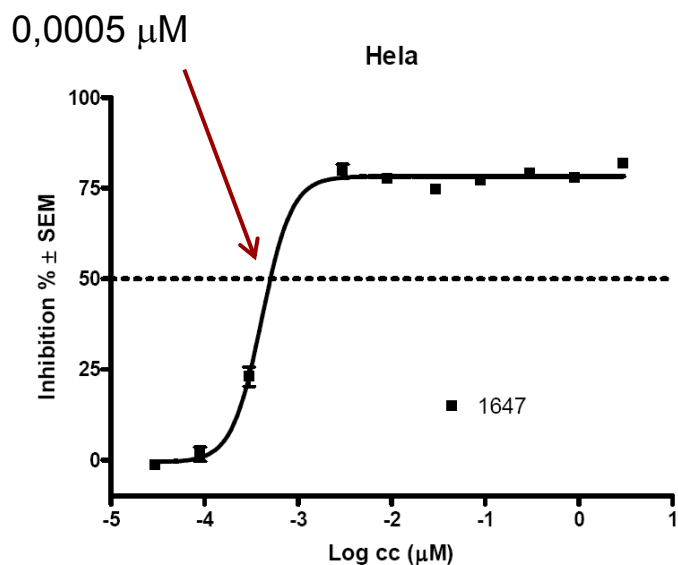


Scheme 65: HeLa screen

For more detailed investigations the test was repeated with lower concentration to describe the dose-response relationship and the half maximal inhibitory concentration ( $IC_{50}$ -value).

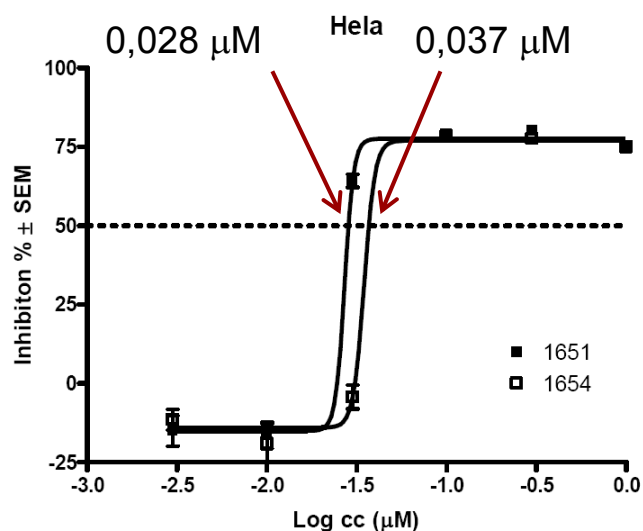
The graph in Scheme 66 demonstrates the  $IC_{50}$ -value for CA-4 (**4**, assay # 1647) for HeLa cells.





Scheme 66:  $\text{IC}_{50}$  value for CA-4 (HeLa cells)

In comparison to the result for CA-4, Scheme 67 shows the  $\text{IC}_{50}$ -values for the cyclopropane derivative (**9**, assay # 1651) of CA-4 and the appropriate diphosphate analog (**268**, assay # 1654).



Scheme 67:  $\text{IC}_{50}$ -value for the cyclopropane derivatives 1651 and 1654 (HeLa cells)

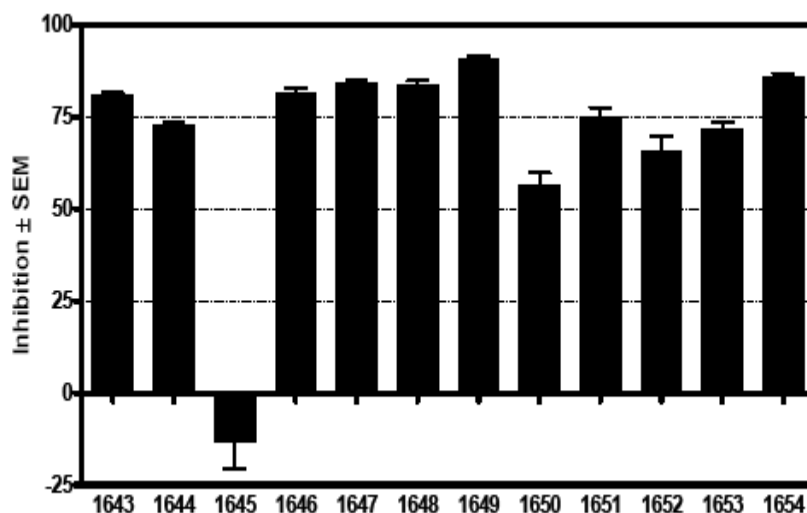
The  $\text{IC}_{50}$ -concentrations for all tested compounds on HeLa cells are listed in Table 11.

Assay-number	Compound-number	Calculated IC <sub>50</sub> value [ $\mu$ M] HeLa cells
1643	292	1.54
1644	248	26.81
1645	293	>30
1646	258	0.197
1647	4	0.0005
1648	269	1.17
1649	259	0.246
1650	266	23.96
1651	9	0.028
1652	270	10.07
1653	267	10.17
1654	268	0.037

Table 11: IC<sub>50</sub>-concentrations, HeLa cells

### 3.2. Results – MCF 7 cells

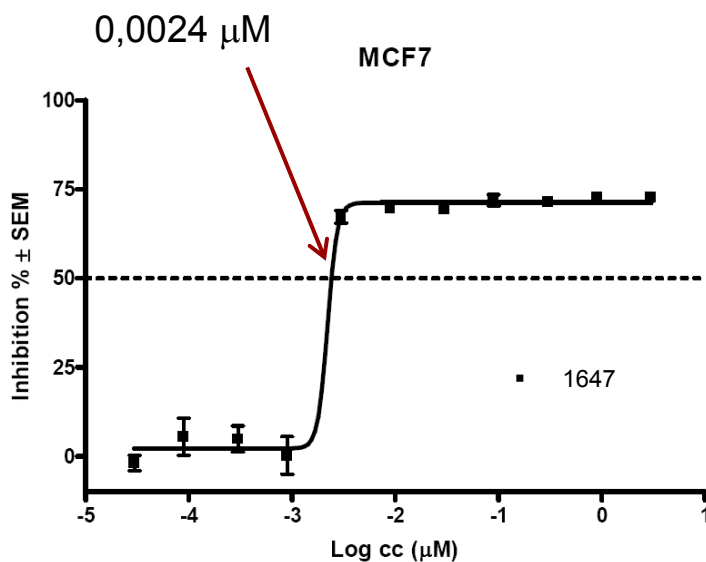
The same tests as described for HeLa cells were prepared for the MCF 7 cell line. Scheme 68 shows the results of the first screening with an assay concentration of 30  $\mu$ M.



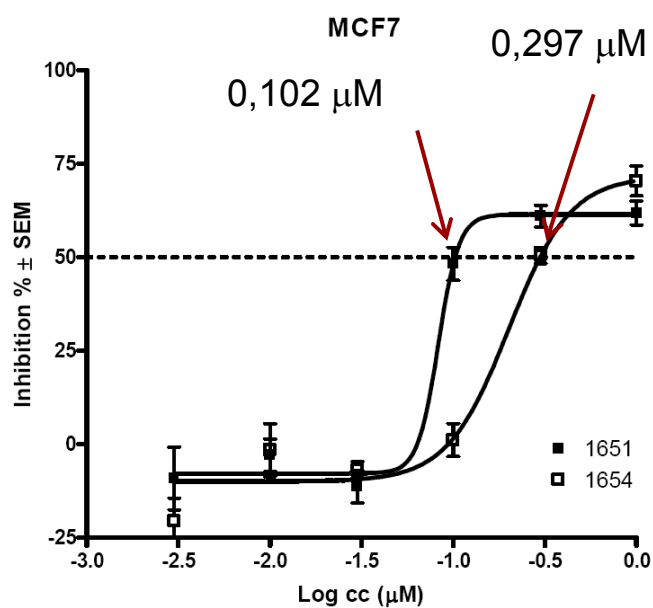
Scheme 68: MCF 7 screen

The result is very similar in comparison to HeLa cells, all compounds, except compound **293** (assay # 1645), show potent cytotoxicity against MCF 7 cells.

Again, the tests were repeated with lower concentrations to determine the  $IC_{50}$ -values. Scheme 69 presents the  $IC_{50}$ -concentration for CA-4 (**4**, assay # 1647) and in comparison Scheme 70 describes the values for the cyclopropane derivative (**9**, assay # 1651) and the diphosphate analog of CA-4 (**268**, assay # 1654).



Scheme 69:  $IC_{50}$  value for CA-4 (MCF 7 cells)



**Scheme 70: IC<sub>50</sub>-value for the cyclopropane derivatives 1651 and 1654 (MCF 7 cells)**

The IC<sub>50</sub>-values for all tested compounds on MCF 7 cells are listed in Table 12.

Assay-number	Compound-number	Calculated IC <sub>50</sub> value [ $\mu\text{M}$ ] MCF 7 cells
1643	<b>292</b>	1.64
1644	<b>248</b>	25.63
1645	<b>293</b>	>30
1646	<b>258</b>	0.269
1647	<b>4</b>	0.0024
1648	<b>269</b>	3.85
1649	<b>259</b>	1.17
1650	<b>266</b>	14.01
1651	<b>9</b>	0,102
1652	<b>270</b>	11.84
1653	<b>267</b>	10.77
1654	<b>268</b>	0,297

**Table 12: IC<sub>50</sub>-concentrations, MCF 7 cells**

## 4. Conclusion and Outlook

CA-4 is a biologically very active compound by binding to the colchicine binding site which lead to the inhibition of microtubule polymerization as well as showing antivascular effects by selectively shutting down the tumor blood flow. To avoid the disadvantage of rather low *in vivo* efficiency resulting from the isomerization of the *cis*-stilbene derivative to the thermodynamically more stable *trans*-isomer, our research group started the project for CA-4 analogs synthesis. The incorporation of carbocycles with different ring sizes on the connecting carbon-bridge of the natural compound prevents the system to undergo *cis-trans*-isomerization. The synthesis of the cyclopropane derivative of CA-4 (**9**) *via* the cyclopropanation reaction with diazomethane, and further analogs with incorporated moieties for better water solubility (**268**, **273**) were achieved within this diploma thesis. In cooperation with the Department of Pharmacodynamics and Biopharmacy of the University of Szeged we were able to investigate the biological activity against two human cancer cell lines (HeLa and MCF 7) of the compounds prepared within this work.

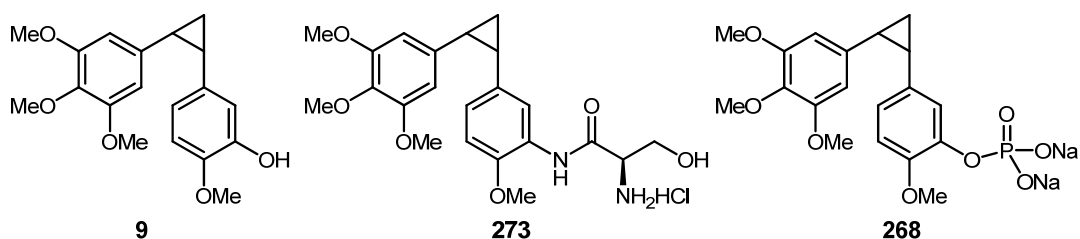
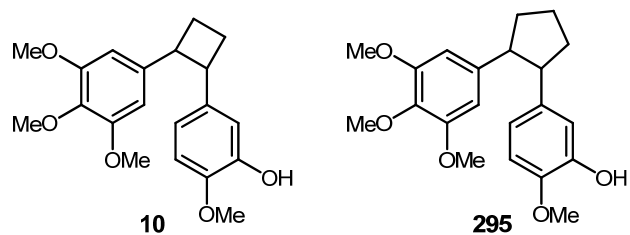


Figure 30: Biologically active compounds synthesized within this work

Cyclopropanes prepared during this study show almost the same activity as the natural product against these two human cancer cell lines and are active in the nanomolecular range. According to these excellent results our synthetic considerations were successful. The biological evaluations show also great promise relating to our continuative work, the synthesis of cyclobutane- and cyclopentane derivatives (**10**, **295**). Whereas initial studies towards the synthesis of the cyclobutane derivatives were already carried out and are described in this thesis.



**Figure 31: Cyclobutane- and cyclopentane derivative of CA-4**

The derivatives synthesized within this project also allow to investigate the fine-tuning of the dihedral angle of the two aromatic ring systems. Comparison of 3D-studies of the carbocyclic compounds the cyclobutyl analog is the most promising compound due to the similarity of the dihedral angle to that of the natural product.

## 5. Experimental part

### 5.1. General

#### Synthetic Methods

The following general procedures were used in all reactions unless otherwise noted. Reaction vessels were dried by repeated heating under vacuum (heat gun) followed by purging with dry argon. Oxygen- and moisture sensitive reactions were carried out under a slight argon overpressure (balloon) and in dry solvents. Sensitive liquids and solutions were transferred by double tipped needle or syringe through rubber septa. All reactions were stirred magnetically if not stated otherwise.

#### Solvents and Chemicals Purification

The used solvents and chemicals were, if necessary, purified and dried according to common procedures as follows. Dry solvents were stored under an argon atmosphere over molecular sieve (4Å).

Methylene chloride was distilled from P<sub>2</sub>O<sub>5</sub>, diethylether (Et<sub>2</sub>O) and tetrahydrofuran (THF) were freshly distilled from sodium/benzophenone under argon; Diisopropylamine (DIPA), diisopropylethylamine (DIPEA) and triethylamine (TEA), acetonitrile (MeCN), hexane and ethyl acetate were distilled from CaH<sub>2</sub>; toluene was refluxed over sodium and freshly distilled. All other solvents were HPLC grade.

#### Thin layer chromatography

All reactions were monitored using Merck silica gel 60-F<sub>254</sub> glass plates. The plates were developed with a mixture of hexane/ethyl acetate or toluene/ethyl acetate. Unless the compound was colored, UV-active spots were detected at longwave UV (254 nm) or shortwave (180 nm). Most plates were additionally treated with the following visualization reagent: CAN [H<sub>2</sub>SO<sub>4</sub> (conc., 22 mL), phosphormolybdic acid (20 g), Ce(SO<sub>4</sub>)<sub>2</sub> (0.5 g), 378 mL H<sub>2</sub>O)]

#### Column chromatography

Preparative column chromatography and flash chromatography was performed with silica gel 60 from Merck (0.040-0.063 μm, 240-400 mesh).

#### Analytic and preparative HPLC

For HPLC separations on analytical scale module systems from Jasco (PU-980, UV-975 detector, RI-930 RI detector, 250 x 4 mm column) were used. The adsorbent was

Superphere Si 60 (40  $\mu\text{m}$ , Merck) or Nucleosil 50 (4 $\mu\text{m}$ , Macherey-Nagel). The semipreparative and preparative scale was covered by module systems from Dynamax (SD-1 pump, UV-1 UV detector), Knauer (RI detector) and Shimadzu (LC-8A, SPD-20A UV/VIS Detector, LC-20AT Bus Module).

### **NMR-Spectroscopy**

NMR spectra were recorded either on a Bruker Avance AV 400, DRX 400, or DRX 600 MHz spectrometer. Unless otherwise stated, all NMR spectra were measured in  $\text{CDCl}_3$  solutions and referenced to the residual  $\text{CDCl}_3$  signal ( $^1\text{H}$ ,  $\delta=7.26$ ,  $^{13}\text{C}$ ,  $\delta=77.16$ ). All  $^1\text{H}$  and  $^{13}\text{C}$  shifts are given in ppm (s = singlet, d = doublet, dd = doublet of doublets, t = triplet, q = quartet, m = multiplet, b = broadened signal). Coupling constants  $J$  are given in Hz. Assignments of proton resonances were confirmed, when possible, by correlated spectroscopy (COSY, HSQC, HMBC, TOCSY, NOESY).

### **Mass Spectroscopy**

Mass spectra were measured on spectrometers from *Micro Mass*, *Fisions Instrument* and *Trio200*. Stated is the kind of ionization - in most cases EI, (**E**lectron **I**mpact); occasionally FAB, (**F**ast **A**tom **B**ombardment), - and electron activation energy (in eV). HRMS (**H**igh **R**esolution **M**ass **S**pectra) were taken with a *Finnigan* MAT 8230 with a resolution of 10000.

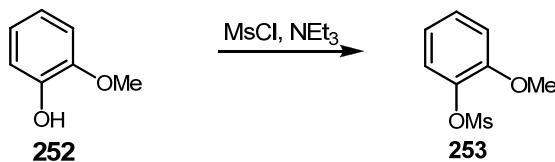
### **Infrared Spectroscopy**

IR were recorded using a Perkin-Elmer 1600 Series FTIR spectrometer and are reported in wave numbers ( $\text{cm}^{-1}$ ). All compounds were measured as a thin film on silicon single crystal plate.



## 5.2. Procedures

### 2-Methoxyphenyl methanesulfonate (**253**).



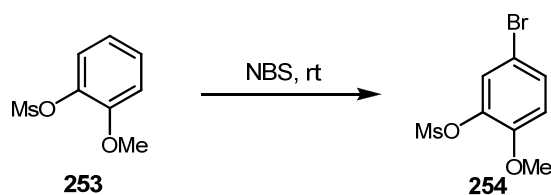
To a solution of guaicol (**252**, 100.5 mmol, 11.3 mL) and NEt<sub>3</sub> (150 mmol, 20.9 mL) in 100 mL CH<sub>2</sub>Cl<sub>2</sub> was added Ms-Cl (126 mmol, 9.75 mL) dropwise over 5 min (126 mmol, 9.75 mL) at 0 °C. The reaction mixture was allowed to stir at 0 °C for 90 min and further 12 hours at r.t. until total consumption of the starting material. The solution was quenched with 100 mL water and the organic layer was separated. The aqueous phase was extracted with CH<sub>2</sub>Cl<sub>2</sub> (2 x 100 mL) and the combined organic extracts were washed with saturated aq. NaHCO<sub>3</sub> (3 x 100 mL), water (2 x 150 mL) and brine (2 x 150 mL). The organic phase was dried over Na<sub>2</sub>SO<sub>4</sub> and the solvent was removed under reduced pressure affording 19.8 g (97%) of **253** as yellow oil without further purification.<sup>150</sup>

R<sub>f</sub> 0.38 (hexanes/ethyl acetate 2:1);

<sup>1</sup>H NMR (400 MHz, CDCl<sub>3</sub>) δ [ppm] 7.33-7.24 (m, 2H), 7.03-6.95 (m, 2H), 3.90 (s, 3H), 3.18 (s, 3H);

<sup>13</sup>C NMR (400 MHz, CDCl<sub>3</sub>) δ [ppm] 128.41, 124.75, 121.32, 113.10, 56.13, 38.40.

## 5-Bromo-2-methoxyphenyl methanesulfonate (**254**).



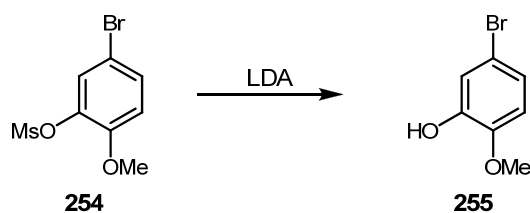
To a solution of **253** (49 mmol, 10 g) in 25 mL DMF was added NBS (64 mmol, 11.4 g) in 25 mL DMF. The reaction mixture was stirred at room temperature until total consumption of the starting material (48 h). The reaction was quenched with saturated aqueous  $\text{NH}_4\text{Cl}$  (200 mL). The resulting solution was diluted with diethyl ether (100 mL), the organic layer was separated and the aqueous phase was extracted with diethyl ether (4 x 100 mL). The combined organic extracts were washed with water (1 x 100 mL) and brine (1 x 100 mL), dried over  $\text{Na}_2\text{SO}_4$ , and the solvent was removed under reduced pressure affording 13.3 g of **254** as white crystals.<sup>150</sup>

$R_f$  0.53 (hexanes/ethyl acetate 2:1);

$^1\text{H}$  NMR (400 MHz,  $\text{CDCl}_3$ )  $\delta$  [ppm] 7.38 (d,  $J = 2.44$  Hz, 1H), 7.31 (dd,  $J = 8.80, 2.44$  Hz, 1H), 6.81 (d,  $J = 8.8$  Hz, 1H), 3.81 (s, 3H), 3.13 (s, 3H);

$^{13}\text{C}$  NMR (400 MHz,  $\text{CDCl}_3$ )  $\delta$  [ppm] 151.32, 139.02, 131.47, 128.02, 114.59, 112.76, 56.68, 38.93.

## 5-Bromo-2-methoxyphenol (**255**).



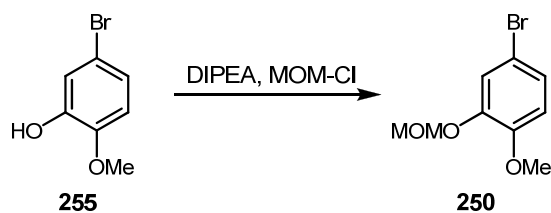
A THF-solution of LDA (1.5 M, 69.5 mL, 53.4 mmol) was added dropwise to a solution of **254** (35.6 mmol, 10 g) in 36 mL THF at 0 °C. After being stirred for 30 min the reaction mixture was quenched with 5% aq. HCl. The product was extracted with diethyl ether (3 x 100 mL). The ethereal extracts were washed successively with water (2 x 100 mL) and brine (2 x 100 mL), dried over Na<sub>2</sub>SO<sub>4</sub>, and the solvent was removed under reduced pressure. The residue was purified by flash chromatography (hexanes/ethyl acetate 5:1) affording **255** (6.7 g, 93%) as white crystals.<sup>150</sup>

R<sub>f</sub> 0.5 (hexanes/ethyl acetate 2:1);

<sup>1</sup>H NMR (400 MHz, CDCl<sub>3</sub>) δ [ppm] 7.07 (d, *J* = 2.27 Hz, 1H), 6.96 (dd, *J* = 8.59, 2.37 Hz, 1H), 6.71 (d, *J* = 8.59 Hz, 1H), 5.63 (s, 1H), 3.87 (s, 3H);

<sup>13</sup>C NMR (400 MHz, CDCl<sub>3</sub>) δ [ppm] 146.67, 146.02, 122.94, 117.99, 113.44, 112.00, 56.24.

#### 4-Bromo-1-methoxy-2-(methoxymethoxy)benzene (**250**).



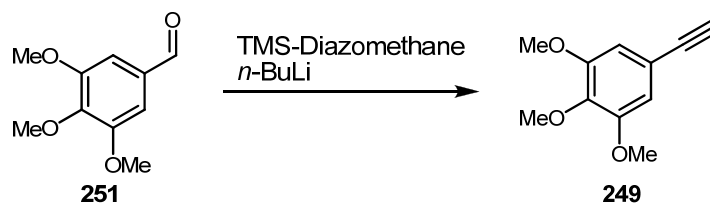
To a solution of **255** (9.9 mmol, 2 g) in 10 mL CH<sub>2</sub>Cl<sub>2</sub> at 0 °C was first added DIPEA (49.5 mmol, 8.6 mL) and then MOM-Cl (29.7 mmol, 2.3 mL). The reaction mixture was allowed to warm to room temperature and was stirred until total consumption of the starting material (48 h). The reaction was quenched with aqueous sat. NH<sub>4</sub>Cl. The organic layer was separated and the aqueous layer was extracted with CH<sub>2</sub>Cl<sub>2</sub> (2 x 10 mL). The combined organic extract was dried over Na<sub>2</sub>SO<sub>4</sub>, and the solvent was removed under reduced pressure. The residue was purified by flash chromatography (hexanes/ethyl acetate 19:1) affording **250** (2.33 g, 95%) as a colorless oil.

R<sub>f</sub> 0.53 (hexanes/ethyl acetate 5:1);

<sup>1</sup>H NMR (400 MHz, CDCl<sub>3</sub>) δ [ppm] 7.29 (d, *J* = 2.36 Hz, 1H), 7.09 (dd, *J* = 8.58, 2.36 Hz, 1H), 6.76 (d, *J* = 8.58 Hz, 1H), 5.21 (s, 2H), 3.85 (s, 3H), 3.51 (s, 3H);

<sup>13</sup>C NMR (400 MHz, CDCl<sub>3</sub>) δ [ppm] 149.24, 147.43, 125.24, 119.84, 113.16, 112.79, 95.77, 56.47, 56.22.

## 5-Ethynyl-1,2,3-trimethoxybenzene (**251**).



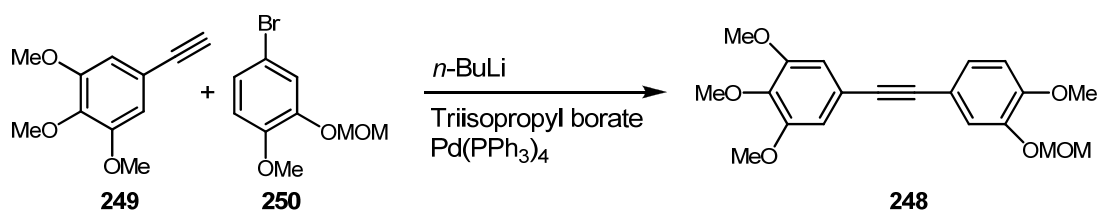
To a solution of TMS-diazomethane (6.3 mmol, 3.15 mL) in THF (7 mL) was added *n*-BuLi (2.5 M in hexanes, 6 mmol, 2.4 mL) at -78 °C. After the mixture had been stirred for 25 min a solution of **251** (5.1 mmol, 1 g) in THF (2.5 mL) was added. After stirring for an additional hour at -78 °C the reaction mixture was allowed to warm to r.t. The reaction was quenched with aqueous sat. NH<sub>4</sub>Cl. The aqueous layer was extracted with ethyl acetate (2 x 20 mL). The organic layers were dried over Na<sub>2</sub>SO<sub>4</sub> and concentrated *in vacuo*. The residue was purified by flash chromatography (hexanes/ethyl acetate 9:1 to 5:1) affording **249** (0.89 g, 90%) as light yellow crystals.<sup>170</sup>

R<sub>f</sub> 0.24 (hexanes/ethyl acetate 9:1);

<sup>1</sup>H NMR (400 MHz, CDCl<sub>3</sub>) δ [ppm] 6.73 (s, 2H), 3.85 (s, 9H), 3.03 (s, 1H);

<sup>13</sup>C NMR (400 MHz, CDCl<sub>3</sub>) δ [ppm] 153.21, 139.49, 117.17, 109.55, 83.85, 76.34, 61.09, 56.30.

**1,2,3-Trimethoxy-5-((4-methoxy-3-(methoxymethoxy)phenyl)ethynyl)-benzene (248).**



A solution of *n*-BuLi (2.5 M in hexanes, 4.64 mL, 11.6 mmol) was slowly added to a solution of **249** (11.1 mmol, 2.13 g) in 110 mL of the solvent mixture DME/THF in a 10:1 ratio (freshly distilled, degazed) under argon. After one hour at -78 °C triisopropylborate (11.02 mmol, 2.54 mL) was added. After stirring for additional two hours at -78 °C the temperature was raised to room temperature over 30 min. At the same time **250** (8.1 mmol, 2.0 g) and Pd(PPh<sub>3</sub>)<sub>4</sub> (0.081 mmol, 94 mg) were dissolved in 20 mL of the solvent mixture DME/THF 10:1, stirred for 10 min at room temperature and the solution was added to the reaction mixture of the alkyne.

After two days refluxing at 90 °C, the reaction mixture was cooled to room temperature and quenched with 100 mL water. The aqueous layer was extracted with ethyl acetate (3 x 100 mL), the organic phases were collected, dried over Na<sub>2</sub>SO<sub>4</sub> and the solvents were removed under reduced pressure. The residue was purified by flash chromatography (hexanes/ethyl acetate 19:1) affording **248** (1.63 g, 56%) as slightly yellow crystals.<sup>146</sup>

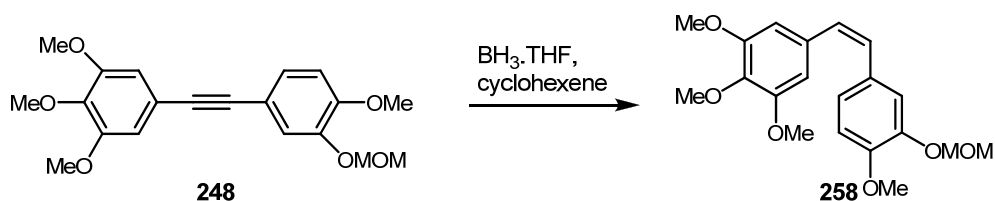
R<sub>f</sub> 0.3 (hexanes/ethyl acetate 5:1).

<sup>1</sup>H NMR (400 MHz, CDCl<sub>3</sub>) δ [ppm] 7.34 (d, *J* = 2.02 Hz, 1H), 7.19 (dd, *J* = 8.38, 2.02 Hz, 1H), 6.87 (d, *J* = 8.38 Hz, 1H), 6.76 (s, 2H), 5.25 (s, 2H), 3.91 (s, 3H), 3.89 (s, 6H), 3.87 (s, 3H), 3.54 (s, 3H);

<sup>13</sup>C NMR (400 MHz, CDCl<sub>3</sub>) δ [ppm] 153.22, 150.31, 146.39, 138.82, 126.42, 119.40, 118.62, 115.66, 111.71, 108.84, 95.63, 88.51, 88.20, 61.11, 56.42, 56.29, 56.07;

IR ν 2938 2837 1464 1154 1078 cm<sup>-1</sup>.

**(Z)-1,2,3-Trimethoxy-5-(4-methoxy-3-(methoxymethoxy)styryl)-benzene (258).**



Cyclohexene (5.7 mmol, 0.58 mL) was added to borane-tetrahydrofuran complex (1 M in hexanes, 3 mmol, 3 mL) at 0 °C. After stirring for 90 min at this temperature **248** (0.56 mmol, 200 mg) dissolved in 4 mL THF was added. The reaction mixture was stirred at 0 °C until total consumption of the starting material (60 min, TLC), before being quenched with 1 mL AcOH. After that 10 mL ethyl acetate were added and the mixture was washed with saturated aqueous  $\text{NaHCO}_3$  (2 x 15 mL), water (2 x 15 mL) and brine (1 x 10 mL) before drying over  $\text{Na}_2\text{SO}_4$ . The solvent was removed under reduced pressure and the residue was purified by flash column chromatography (hexanes/ethyl acetate, 19:1) affording 161 mg (80%) of **258**.<sup>153</sup>

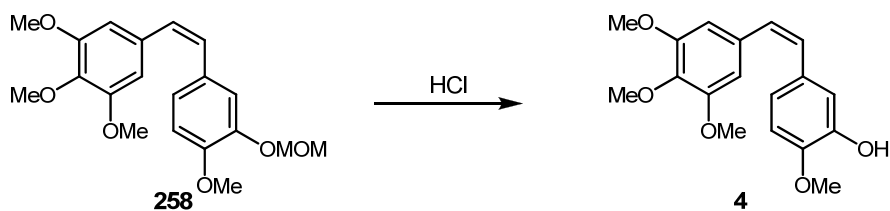
$R_f$  0.4 (hexanes/ethyl acetate 5:1);

$^1\text{H}$  NMR (400 MHz,  $\text{CDCl}_3$ )  $\delta$  [ppm] 7.07 (d,  $J = 2.05$  Hz, 1H), 6.92 (dd,  $J = 8.42, 2.03$  Hz, 1H), 6.78 (d,  $J = 8.42$  Hz, 1H), 6.50 (s, 2H), 6.46 (dd,  $J = 18.09, 11.98$  Hz, 2H), 5.06 (s, 2H), 3.84 (s, 3H), 3.83 (s, 3H), 3.70 (s, 6H), 3.41 (s, 3H);

$^{13}\text{C}$  NMR (400 MHz,  $\text{CDCl}_3$ )  $\delta$  [ppm] 153.07, 149.21, 146.12, 137.21, 133.00, 130.15, 129.60, 129.15, 123.64, 117.52, 111.50, 106.01, 95.65, 60.95, 56.16, 56.01;

IR  $\nu$  2937 2835 1579 1427 1078 1005  $\text{cm}^{-1}$ .

**(Z)-2-Methoxy-5-(3,4,5-trimethoxystyryl)phenol (CA-4, 4).**



To a solution of **258** (0.14 mmol, 50 mg) in 2 mL methanol 0.5 mL 3 M HCl were added. The reaction mixture was stirred for 24 h at room temperature. The solution was diluted with CH<sub>2</sub>Cl<sub>2</sub>. The organic layer was washed with water (2 x 8 mL), dried over Na<sub>2</sub>SO<sub>4</sub>, and the solvent was removed under reduced pressure. The residue was purified by HPLC affording 38 mg (95%) of **4**.<sup>171</sup>

R<sub>f</sub> 0.37 (hexanes/ethyl acetate 2:1);

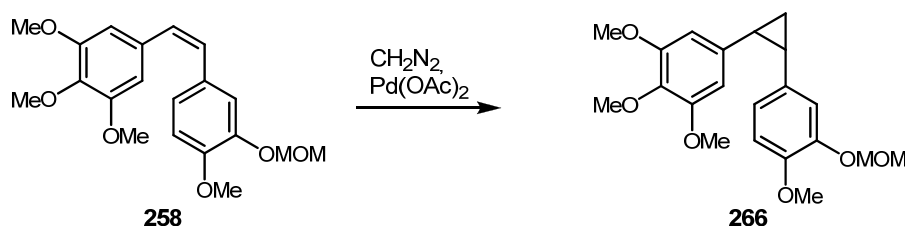
<sup>1</sup>H NMR (400 MHz, CDCl<sub>3</sub>) δ [ppm] 6.92 (d, *J* = 2.07 Hz, 1H), 6.80 (dd, *J* = 8.26, 2.07 Hz, 1 H), 6.73 (d, *J* = 8.26 Hz, 1H), 6.44 (dd, *J* = 12.17, 23.67 Hz, 2H), 5.52 (s, 1H), 3.86 (s, 3H), 3.84 (s, 3H), 3.69 (s, 6H);

<sup>13</sup>C NMR (400 MHz, CDCl<sub>3</sub>) δ [ppm] 153.01, 145.90, 145.39, 137.34, 132.84, 130.80, 129.62, 129.19, 121.25, 115.19, 110.47, 106.24, 61.06, 56.10, 56.08;

IR ν 3752 3422 3152 2837 1419 1274 1005 cm<sup>-1</sup>.



**1,2,3-Trimethoxy-5-(2-(4-methoxy-3-(methoxymethoxy)phenyl)-cyclopropyl)benzene (266).**



Diethyl ether (15 mL) and 25 mL saturated aq. NaOH were added in a conical flask and cooled to 0 °C. To this two phase system *N*-methyl-*N*-nitrosourea (8.25 mmol, 850 mg) was added affording a yellow solution of diazomethane which was dried over NaOH-platelets in a second conical flask before adding to a mixture of **258** (0.55 mmol, 200 mg) and  $\text{Pd}(\text{OAc})_2$  (0.0275 mmol, 6 mg) in 1 mL ether. The reaction mixture was stirred for 3 hours at 0 °C. The solution was filtered and the solvent was removed under reduced pressure. The residue was purified by flash chromatography (toluene/ethyl acetate, 19:1) affording 113 mg (55%) of **266**.<sup>165</sup>

$R_f$  0.29 (hexanes/ethyl acetate 5:1);

$^1\text{H}$  NMR (400 MHz,  $\text{CDCl}_3$ )  $\delta$  [ppm] 6.71 (s, 1H), 6.66 (s, 2H), 4.98 (dd,  $J = 11.62, 6.65$  Hz, 2H), 3.77 (s, 3H), 3.73 (s, 3H), 3.64 (s, 6H), 2.36 (m, 2H), 1.41 (ddd,  $J = 5.43, 8.78, 14.06$  Hz, 1H), 1.21 (m, 1H);

$^{13}\text{C}$  NMR (400 MHz,  $\text{CDCl}_3$ )  $\delta$  [ppm] 152.53, 147.93, 146.09, 136.01, 134.49, 131.32, 123.10, 117.34, 111.30, 106.09, 95.62, 60.82, 55.99, 55.92, 24.18, 23.80, 12.22;

IR  $\nu$  2944, 2838, 1585, 1233, 1124 1003  $\text{cm}^{-1}$ .

## 2-Methoxy-5-((3,4,5-trimethoxyphenyl)ethynyl)phenol (**293**).



Alkyne **248** (50 mg, 0.14 mmol) was dissolved in 2 mL of the solvent mixture MeOH:THF in a 1:1 ratio and 15 drops 3 M HCl were added. The reaction mixture was stirred at r.t. for 18 h. The solution was diluted with CH<sub>2</sub>Cl<sub>2</sub>. The layers were separated and the organic phase was washed with water (1 x 10 mL) and brine (1 x 10 mL). The organic layer was dried over Na<sub>2</sub>SO<sub>4</sub>, and the solvent was removed under reduced pressure. The residue was purified by HPLC affording **293** (45 mg, 90%) as colorless oil.

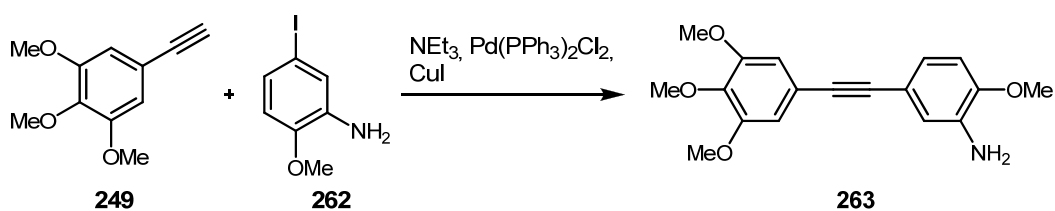
R<sub>f</sub> 0.5 (hexanes/ethyl acetate 1:1);

<sup>1</sup>H NMR (400 MHz, CDCl<sub>3</sub>) δ [ppm] 7.09 (d, *J* = 1.97 Hz, 1H), 7.05 (dd, *J* = 8.35, 1.97 Hz, 1H), 6.81 (d, *J* = 8.35 Hz, 1H), 6.75 (s, 2H), 5.67 (s, 1H), 3.90 (s, 3H), 3.87 (s, 6H), 3.86 (s, 3H);

<sup>13</sup>C NMR (400 MHz, CDCl<sub>3</sub>) δ [ppm] 153.19, 147.16, 145.51, 138.79, 124.33, 118.65, 117.64, 116.11, 110.65, 108.86, 88.55, 88.02, 61.08, 56.27, 56.06;

IR ν 3627, 3418, 2939, 2839, 1463, 1356 cm<sup>-1</sup>.

## 2-Methoxy-5-((3,4,5-trimethoxyphenyl)ethynyl)aniline (**263**).



A solution of **249** in 8 mL DMF was added slowly (5 min) to 5-iodo-2-methoxyaniline (**262**, 600 mg, 2.4 mmol), triethylamine (0.4 mL, 2.88 mmol),  $\text{Pd}(\text{PPh}_3)_2\text{Cl}_2$  (50 mg, 0.072 mmol), and copper iodide (24 mg, 0.12 mmol) in 20 mL DMF. The reaction mixture was stirred over night at room temperature. The reaction was quenched with water (30 mL). The organic layer was separated and the aqueous phase was extracted with ethyl acetate (3 x 20 mL). The combined organic extracts were washed with water (1 x 30 mL) and brine (1 x 30 mL), dried over  $\text{Na}_2\text{SO}_4$  and the solvent was removed under reduced pressure. The residue was purified by flash chromatography (hexanes/ethyl acetate 9:1, 1%  $\text{NEt}_3$ ) affording **263** (531 mg, 70%) as yellow crystals.<sup>156</sup>

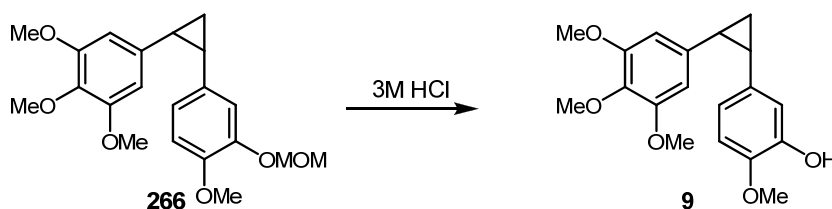
$R_f$  0.32 (hexanes/ethyl acetate 2:1);

$^1\text{H}$  NMR (400 MHz,  $\text{CDCl}_3$ )  $\delta$  [ppm] 6.81 (d,  $J = 8.33$  Hz, 1H), 6.78 (s, 3H), 6.73 (dd,  $J = 8.33, 2.02$  Hz, 1H), 4.87 (s, 2H), 3.82 (s, 6H), 3.79 (s, 3H), 3.68 (s, 3H);

$^{13}\text{C}$  NMR (400 MHz,  $\text{CDCl}_3$ )  $\delta$  [ppm] 152.89, 146.92, 138.06, 137.81, 119.92, 118.05, 115.87, 114.28, 110.49, 108.51, 89.46, 87.16, 60.11, 55.97, 55.31;

IR  $\nu$  3673, 3370, 2936, 1575, 1409, 1173  $\text{cm}^{-1}$ .

## 2-Methoxy-5-(2-(3,4,5-trimethoxyphenyl)cyclopropyl)phenol (**9**).



**266** (448 mg, 1.2 mmol) was dissolved in 10 mL of a solvent-mixture of MeOH/THF in a 1:1 ratio and 202  $\mu$ L 3 M HCl were added. The reaction mixture was stirred at room temperature for 18 hours. The solution was diluted with  $\text{CH}_2\text{Cl}_2$ . The layers were separated and the organic phase was washed with water (2 x 20 mL). The organic layer was dried over  $\text{Na}_2\text{SO}_4$  and the solvent was removed under reduced pressure. The residue was purified by HPLC affording **9** (269 mg, 68%) as colorless oil.

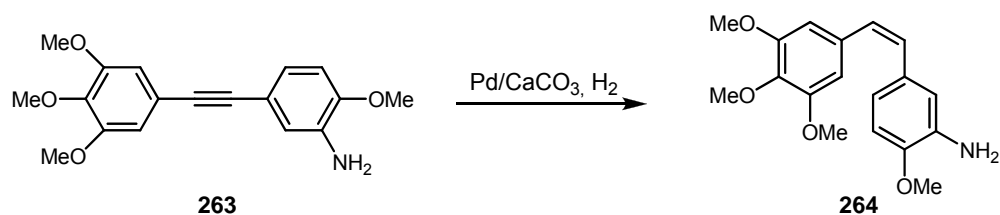
$R_f$  0.38 (hexanes/ethyl acetate 2:1);

$^1\text{H}$  NMR (400 MHz,  $\text{CDCl}_3$ )  $\delta$  [ppm] 6.66 (d,  $J = 2.26$  Hz, 1H), 6.62 (d,  $J = 8.32$  Hz, 1H), 6.46 (dd,  $J = 8.32, 2.26$  Hz, 2H), 6.12 (s, 2H), 5.43 (s, 1H), 3.80 (s, 3H), 3.75 (s, 3H), 3.65 (s, 6H), 2.40 (m, 1H), 2.31 (m, 1H), 1.41 (m, 1H), 1.21 (m, 1H);

$^{13}\text{C}$  NMR (400 MHz,  $\text{CDCl}_3$ )  $\delta$  [ppm] 152.55, 145.19, 144.89, 136.08, 134.76, 131.68, 120.78, 115.82, 110.31, 105.98, 60.95, 56.11, 56.03, 24.22, 24.10, 12.16;

IR  $\nu$  3413, 2937, 2838, 1737, 1514, 1416, 1007  $\text{cm}^{-1}$ .

**(Z)-2-Methoxy-5-(3,4,5-trimethoxystyryl)aniline (264).**



To a solution of catalyst (Pd/CaCO<sub>3</sub>, 0.032 mmol, 3.4 mg) in 2 mL ethyl acetate were added three drops of quinoline and 400 μL of cyclohexene. The solution was stirred for one hour at room temperature. Alkyne **263** (100 mg, 0.32 mmol) was dissolved in 1 mL ethyl acetate and was added to the reaction mixture. The solution was exposed to H<sub>2</sub> until total consumption of the starting material (3 h). The reaction mixture was filtered and the solvent was removed under reduced pressure. The residue was purified by flash chromatography (toluene/ethyl acetate 19:1, 1% NEt<sub>3</sub>) affording **264** (84 mg, 83%) as a yellow oil.

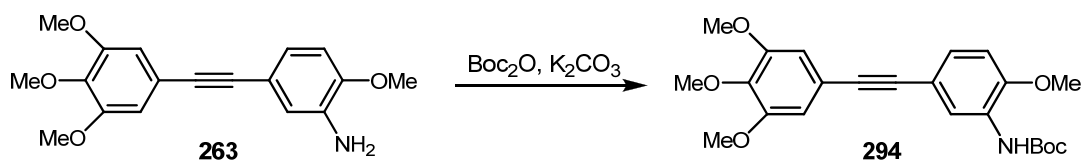
R<sub>f</sub> 0.27 (toluene/ethyl acetate 5:1);

<sup>1</sup>H NMR (400 MHz, CDCl<sub>3</sub>) δ [ppm] 6.93 (d, *J* = 8.27 Hz, 1H), 6.90 (s, 3H), 6.85 (dd, *J* = 8.02, 2.02 Hz, 1H), 4.99 (s, 2H), 3.92 (s, 6H), 3.92 (s, 6H), 3.91 (s, 3H), 3.80 (s, 3H);

<sup>13</sup>C NMR (400 MHz, CDCl<sub>3</sub>) δ [ppm] 154.14, 148.16, 139.30, 139.05, 121.16, 119.29, 117.11, 115.52, 111.73, 109.75, 90.70, 88.40, 61.35, 57.21, 56.56;

IR  $\nu$  3469, 3371, 2936, 1613, 1453, 1326, 1028 cm<sup>-1</sup>.

**Tert-butyl 2-methoxy-5-((3,4,5-trimethoxyphenyl)ethynyl)-phenylcarbamate (294).**



To a stirred solution of **293** (300 mg, 0.96 mmol) in 10 mL of a solvent mixture THF/ $\text{H}_2\text{O}$  in a 1:1 ratio was added  $\text{K}_2\text{CO}_3$  (794 mg, 5.76 mmol) at room temperature. After 10 min  $\text{Boc}_2\text{O}$  was added (838 mg, 3.84 mmol). The reaction mixture was stirred for two days at 60 °C. The reaction was quenched with 5% aqueous HCl. The two layers were separated and the aqueous phase was extracted with ethyl acetate (3 x 15 mL). The combined organic extracts were washed with water (1 x 20 mL) and brine (1 x 20 mL) and the solvent was removed under reduced pressure. The residue was purified by flash chromatography (hexanes/ethyl acetate 9:1), affording **294** as a colorless foam (356 mg, 90%).<sup>172</sup>

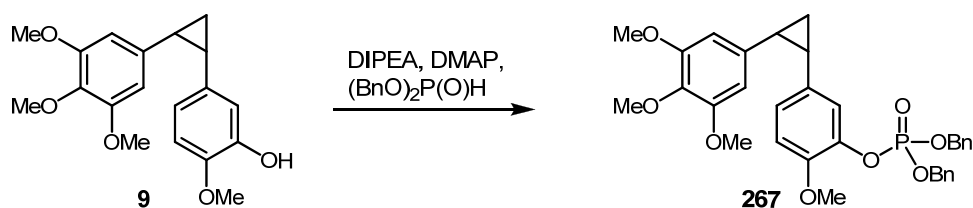
$R_f$  0.58 (hexanes/ethyl acetate 2:1);

$^1\text{H}$  NMR (400 MHz,  $\text{CDCl}_3$ )  $\delta$  [ppm] 8.32 (s, 1H), 7.16 (dd,  $J = 8.34, 2.02$  Hz, 1H), 7.09 (s, 1H), 6.81 (d,  $J = 8.34$  Hz, 1H), 6.75 (s, 2H), 3.89 (s, 3H), 3.88 (s, 6H), 3.86 (s, 3H), 1.54 (s, 9H);

$^{13}\text{C}$  NMR (400 MHz,  $\text{CDCl}_3$ )  $\delta$  [ppm] 153.19, 152.77, 147.69, 138.66, 128.25, 126.02, 121.09, 118.89, 116.03, 109.94, 108.83, 88.94, 88.02, 80.75, 61.11, 56.31, 55.91, 28.51;

IR  $\nu$  3436, 2938, 2839, 1726, 1527, 1128  $\text{cm}^{-1}$ .

## Dibenzyl-2-methoxy-5-(2-(3,4,5-trimethoxyphenyl)-cyclopropyl)-phenyl phosphate (**9**).



A solution of **9** (220 mg, 0.67 mmol) and CCl<sub>4</sub> (648  $\mu$ L, 6.7 mmol) in 4 mL acetonitrile was cooled to -10 °C and stirred for 10 min. Then DIPEA (228  $\mu$ L, 1.34 mmol) and DMAP (8 mg, 0.067 mmol) were added. After one minute dibenzylphosphite (221  $\mu$ L, 1 mmol) was added slowly and the mixture was stirred for additional 3 hours at -10 °C. After total consumption of the starting material the reaction was quenched with 0.5 M aqueous KH<sub>2</sub>SO<sub>4</sub> solution. The two layers were separated and the aqueous phase was extracted with ethyl acetate (3 x 15 mL). The combined organic extracts were washed with water (1 x 20 mL) and brine (1x 20 mL), and the solvents were removed under reduced pressure. The residue was purified by column chromatography (hexanes/ethyl acetate 3:1), affording **267** as a colorless oil (265 mg, 67%).<sup>91</sup>

R<sub>f</sub> 0.44 (hexanes/ethyl acetate 1:1);

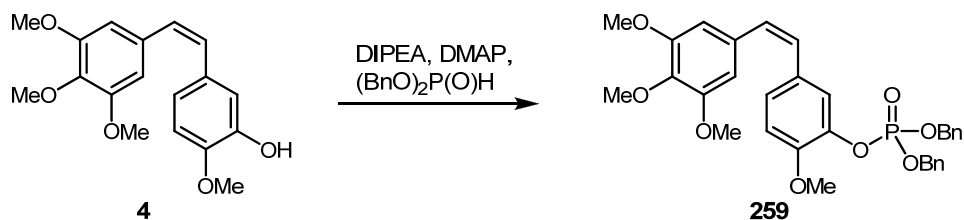
<sup>1</sup>H NMR (400 MHz, CDCl<sub>3</sub>)  $\delta$  [ppm] 7.35-7.28 (m, 10H), 7.04 (s, 1H), 6.65 (s, 2H), 6.09 (s, 2H), 5.16-5.05 (m, 4H), 3.72 (s, 3H), 3.68 (s, 3H), 3.62 (s, 6H), 2.41-2.29 (m, 2H), 1.45-1.37 (m, 1H), 1.22-1.14 (m, 1H);

<sup>13</sup>C NMR (400 MHz, CDCl<sub>3</sub>)  $\delta$  [ppm] 152.63, 148.91\*, 148.86, 139.29, 139.22, 136.13, 135.95\*, 135.87, 134.33, 131.33, 128.63, 128.57, 127.99, 122.83\*, 122.81, 112.26, 105.0, 69.91, 69.85, 60.89, 56.05, 24.32, 23.70, 12.18;

IR  $\nu$  2938, 2838, 1586, 1378, 1234, 1183, 1082 cm<sup>-1</sup>.

\*) denotes rotamer

**(Z)-Dibenzyl 2-methoxy-5-(3,4,5-trimethoxystyryl)phenyl phosphate (259).**



A solution of **4** (110 mg, 0.35 mmol) and  $\text{CCl}_4$  (338  $\mu\text{L}$ , 3.5 mmol) in 3 mL acetonitrile was cooled to  $-10\text{ }^\circ\text{C}$  and stirred for 10 min. Then DIPEA (118  $\mu\text{L}$ , 0.7 mmol) and DMAP (4 mg, 0.035 mmol) were added. After one minute dibenzylphosphite (116  $\mu\text{L}$ , 0.53 mmol) was added slowly and the mixture was stirred for an additional 3 hours at  $-10\text{ }^\circ\text{C}$ . After total consumption of the starting material the reaction was quenched with 0.5 M aqueous  $\text{KH}_2\text{SO}_4$  solution. The two layers were separated and the aqueous phase was extracted with ethyl acetate (3 x 10 mL). The combined organic extracts were washed with water (1 x 15 mL) and brine (1 x 15 mL), and the solvents were removed under reduced pressure. The residue was purified by column chromatography (hexanes/ethyl acetate 3:1), affording **259** as a colorless oil (115 mg, 57%).<sup>91</sup>

$R_f$  0.44 (hexanes/ethyl acetate 1:1);

$^1\text{H}$  NMR (400 MHz,  $\text{CDCl}_3$ )  $\delta$  [ppm] 7.38-7.27 (m, 10H), 7.18-7.14 (m, 1H), 7.07 (d,  $J = 8.32$  Hz, 1H), 6.79 (d,  $J = 8.32$  Hz, 1H), 6.49 (s, 2H), 6.43 (dd,  $J = 18.89, 12.17$  Hz, 2H), 5.16-5.10 (m, 4H), 3.80 (s, 3H), 3.77 (s, 3H), 3.68 (s, 6H);

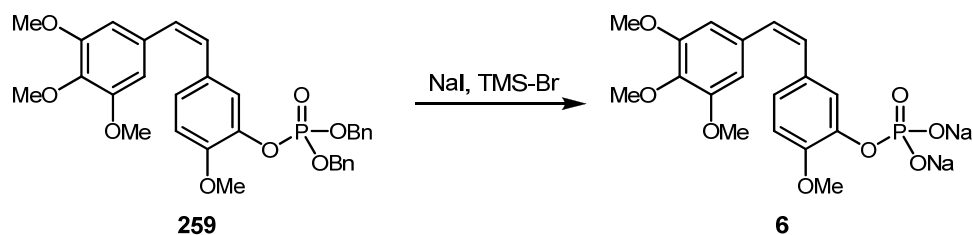
$^{13}\text{C}$  NMR (400 MHz,  $\text{CDCl}_3$ )  $\delta$  [ppm] 153.06, 149.93\*, 149.88, 139.62\*, 139.55, 137.34, 135.83, 135.76, 132.54, 130.27, 129.76, 128.63, 128.60, 128.55, 127.95, 126.65, 122.30\*, 122.27, 112.39, 106.05, 69.87, 69.81, 60.94, 56.05, 56.02;

IR  $\nu$  2938, 2838, 1579, 1279, 1127, 999  $\text{cm}^{-1}$ .

\*) denotes rotamer



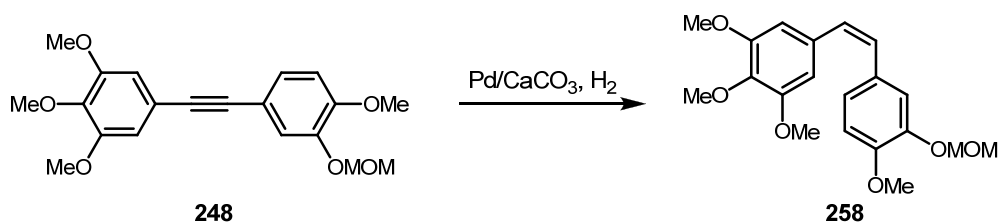
## Sodium (Z)-2-methoxy-5-(3,4,5-trimethoxystyryl)phenyl phosphate (6).



A mixture of **259** (100 mg, 0.17 mmol) and sodium iodide (99 mg, 0.66 mmol) in anhydrous acetonitrile was stirred at 0 °C and TMS-Br (86  $\mu$ L, 0.66 mmol) was added dropwise. The reaction mixture was stirred for 5 min at that temperature before it was quenched with water and extracted with ethyl acetate. The combined organic layers were dried over Na<sub>2</sub>SO<sub>4</sub>, filtered and the solvent was removed under reduced pressure. The residue was purified by flash column chromatography (CH<sub>2</sub>Cl<sub>2</sub>/MeOH 3:1, 1% AcOH) affording 30 mg (48%) of the free phosphorous acid. The free acid was dissolved in 1 mL MeOH and sodium methanolate (8 mg, 0.15 mmol) was added. The reaction mixture was stirred for 5 min, afterwards the solvent was removed under reduced pressure affording **6** (33 mg, 94%) as a white solid.

<sup>1</sup>H NMR (free phosphorus acid, 400 MHz, MeOD)  $\delta$  [ppm] 7.27 (s, 1H), 7.01 (d,  $J$  = 8.53 Hz, 1H), 6.92 (d,  $J$  = 8.53 Hz, 1H), 6.55 (s, 2H), 6.48 (dd,  $J$  = 18.45, 12.17 Hz, 2H), 3.82 (s, 3H), 3.74 (s, 3H), 3.66 (s, 6H).

**(Z)-1,2,3-Trimethoxy-5-(4-methoxy-3-(methoxymethoxy)styryl)-benzene (258).**



To a solution of catalyst (Pd/CaCO<sub>3</sub>, 0.14 mmol, 15 mg) in 10 mL ethyl acetate were added 10 drops of quinoline and 3 mL of cyclohexene. The solution was stirred for one hour at room temperature. Alkyne **248** (500 mg, 1.4 mmol) was dissolved in 5 mL ethyl acetate and was added to the reaction mixture. The solution was exposed to H<sub>2</sub> until total consumption of the starting material (3 h). The reaction mixture was filtered and the solvent was removed under reduced pressure. The residue was purified by flash chromatography (toluene/ethyl acetate 19:1) affording **258** (806 mg, 81%) as colorless oil.

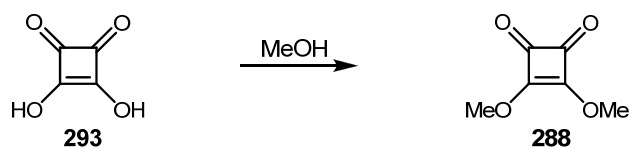
R<sub>f</sub> 0.4 (toluene/ ethyl acetate 5:1);

<sup>1</sup>H NMR (400 MHz, CDCl<sub>3</sub>) δ [ppm] 7.07 (d, *J* = 2.05 Hz, 1H), 6.92 (dd, *J* = 8.42, 2.03 Hz, 1H), 6.78 (d, *J* = 8.42 Hz, 1H), 6.50 (s, 2H), 6.46 (dd, *J* = 18.09, 11.98 Hz, 2H), 5.06 (s, 2H), 3.84 (s, 3H), 3.83 (s, 3H), 3.70 (s, 6H), 3.41 (s, 3H);

<sup>13</sup>C NMR (400 MHz, CDCl<sub>3</sub>) δ [ppm] 153.07, 149.21, 146.12, 137.21, 133.00, 130.15, 129.60, 129.15, 123.64, 117.52, 111.50, 106.01, 95.65, 60.95, 56.16, 56.01;

IR ν 2937 2835 1579 1427 1078 1005 cm<sup>-1</sup>.

### 3,4-Dimethoxycyclobut-3-ene-1,2-dione (**288**).



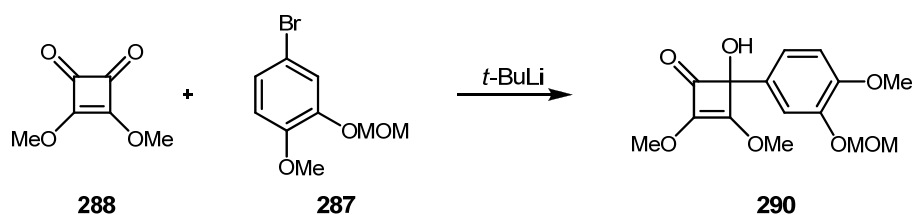
**293** (2 g, 17.5 mmol) in 156 mL methanol was refluxed for 72 hours. The solvent was removed under reduced pressure. The residue was purified by flash chromatography (hexanes/ethyl acetate 2:1) affording **288** (1.05 g, 42%) as white crystals.<sup>173</sup>

R<sub>f</sub> 0.5 (hexanes/ethyl acetate 1:1);

<sup>1</sup>H NMR (400 MHz, CDCl<sub>3</sub>) δ [ppm] 4.37 (s, 6H);

<sup>13</sup>C NMR (400 MHz, CDCl<sub>3</sub>) δ [ppm] 189.28, 184.60, 61.12.

**4-Hydroxy-2,3-dimethoxy-4-(4-methoxy-3-(methoxymethoxy)-phenyl)cyclobut-2-enone (290).**

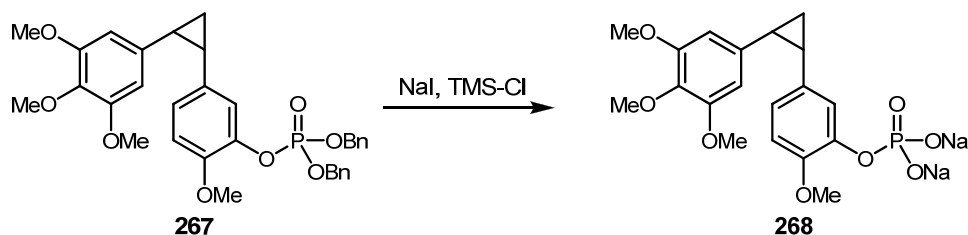


The aromatic fragment **287** (951 mg, 3.85 mmol) was dissolved in 15 mL diethyl ether. The reaction mixture was cooled to  $-78\text{ }^{\circ}\text{C}$  and *t*-BuLi (1.7 M solution, 8.05 mmol, 4.7 mL) was added. The resulting mixture was stirred for 30 min. The solution of the lithiated aromate was transferred *via* syringe to a solution of dimethyl squarate (**288**, 500 mg, 3.5 mmol) in 5 mL of the solvent mixture diethyl ether/THF in a 1:1 ratio at  $-78\text{ }^{\circ}\text{C}$ . The reaction mixture was stirred over night and was allowed to warm to room temperature. The reaction was quenched with sat.  $\text{NH}_4\text{Cl}$ , was extracted with ethyl acetate and the solvents were removed under reduced pressure. The residue was purified by flash chromatography (hexanes/ethyl acetate 9:1) affording **290** (704 mg, 65%) as colorless oil.<sup>168</sup>

$R_f$  0.33 (hexanes/ethyl acetate 2:1);

$^1\text{H NMR}$  (400 MHz,  $\text{CDCl}_3$ )  $\delta$  [ppm] 6.76 (d,  $J = 5.84\text{ Hz}$ , 1H), 6.74 (s, 1H), 6.45 (dd,  $J = 8.68, 2.88\text{ Hz}$ , 1H), 6.01-5.49 (bs, 1H), 5.19 (s, 2H), 3.81 (s, 3H), 3.50 (s, 3H), 2.95 (s, 3H), 2.88 (s, 3H).

**Sodium 2-methoxy-5-(2-(3,4,5-trimethoxyphenyl)cyclopropyl)-phenyl phosphate (268).**

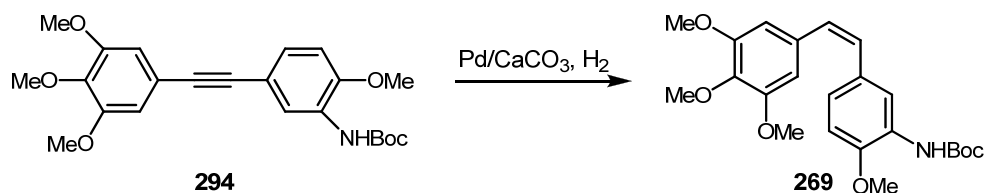


To a mixture of **267** (40 mg, 0.07 mmol) and NaI (42 mg, 0.28 mmol) in anhydrous acetonitrile was added TMS-Cl (35  $\mu$ L, 0.28 mmol) dropwise at room temperature. The reaction mixture was stirred for 3 hours, quenched with water and extracted with ethyl acetate. The organic layers were combined and the solvent was removed under reduced pressure. The residue was purified by flash chromatography (CH<sub>2</sub>Cl<sub>2</sub>/MeOH 5:1, 1% AcOH) affording the free phosphorous acid. The free acid was dissolved in 1 mL MeOH and sodium methanolate (1.2 mg, 0.023 mmol) was added. The reaction mixture was stirred for 5 min, afterwards the solvent was removed under reduced pressure affording **268** (10 mg, 32%) as a white solid.<sup>154</sup>

R<sub>f</sub> 0.1 (CH<sub>2</sub>Cl<sub>2</sub>/MeOH 3:1, 1% AcOH).

<sup>1</sup>H NMR (400 MHz, D<sub>2</sub>O)  $\delta$  [ppm] 7.39 (s, 1H), 6.82 (d, J=8.56 Hz, 1H), 6.83 (dd, J=8.56, 2.05 Hz, 1H), 6.42 (s, 2H), 3.79 (s, 3H), 3.73 (s, 6H), 3.70 (s, 3H), 2.63-2.53 (m, 1H), 2.52-2.44 (m, 1H), 1.53-1.44 (m, 2H).

**(Z)-tert-butyl 2-methoxy-5-(3,4,5-trimethoxystyryl)phenyl-carbamate (269).**



To a solution of catalyst (Pd/CaCO<sub>3</sub>, 0.097 mmol, 10 mg) in 4.5 mL ethyl acetate were added six drops of quinoline and 6 mL of cyclohexene. The suspension was stirred for one hour at room temperature. Alkyne **294** (400 mg, 0.97 mmol) was dissolved in 2 mL ethyl acetate and was added to the reaction mixture. The solution was exposed to H<sub>2</sub> until total consumption of the starting material (3 h). The reaction mixture was filtered and the solvent was removed under reduced pressure. The residue was purified by flash chromatography (toluene/ethyl acetate 19:1 to 9:1, 1% NEt<sub>3</sub>) affording **269** (1.68 g, 88%) as a yellow oil.

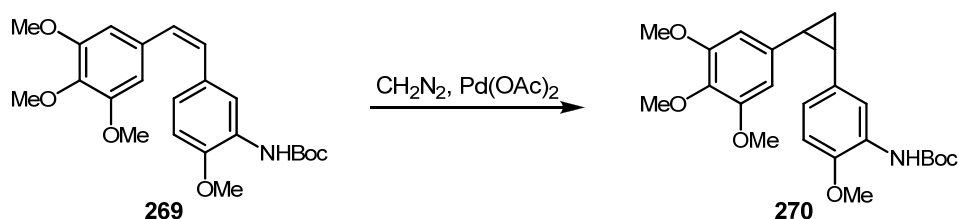
R<sub>f</sub> 0.51 (toluene/ethyl acetate 9:1);

<sup>1</sup>H NMR (400 MHz, CDCl<sub>3</sub>) δ [ppm] 8.08 (s, 1H), 7.25 (s, 1H), 6.92 (dd, *J* = 8.58, 2.02 Hz, 1H), 6.69 (d, *J* = 8.58 Hz, 1H), 6.53 (s, 2H), 6.46 (dd, *J* = 39.53, 12.06 Hz, 2H), 3.84 (s, 6H), 3.69 (s, 6H), 1.50 (s, 9H);

<sup>13</sup>C NMR (400 MHz, CDCl<sub>3</sub>) δ 153.0, 152.79, 146.74, 137.94, 133.04, 130.34, 130.07, 129.05, 128.37, 128.04, 123.10, 123.10, 118.96, 109.64, 106.25, 80.07, 61.04, 56.05, 28.47;

IR ν 3437, 2975, 1727, 1579, 1366, 1127, 1050 cm<sup>-1</sup>.

**Tert-butyl-2-methoxy-5-(2-(3,4,5-trimethoxyphenyl)-cyclopropyl)-phenyl-carbamate (270).**



Diethyl ether (25 mL) and 50 mL saturated aq. NaOH were added in a conical flask and cooled to 0 °C. To this two phase system *N*-methyl-*N*-nitrosourea (24 mmol, 2.47 g) was added affording a yellow solution of diazomethane which was dried over NaOH-platelets in a second conical flask before adding to a mixture of **269** (1.2 mmol, 500 mg) and  $\text{Pd}(\text{OAc})_2$  (0.12 mmol, 27 mg) in 3 mL diethyl ether. The reaction mixture was stirred for 20 min at 0 °C. The solution was filtered and the solvent was removed under reduced pressure. Afterwards the described procedure was repeated to afford complete conversion. The residue was purified by HPLC (toluene/ethyl acetat 19:1) affording 300 mg (58%) of **270** as a yellow oil.<sup>165</sup>

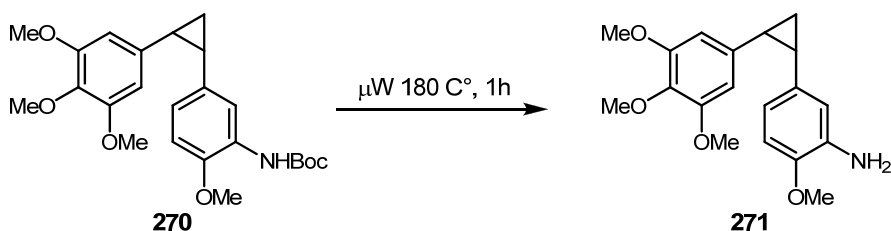
$R_f$  0.47 (toluene/ethyl acetate 9:1);

$^1\text{H}$  NMR (400 MHz,  $\text{CDCl}_3$ )  $\delta$  7.94 (s, 1H), 6.97 (s, 1H), 6.56 (d,  $J = 8.36$  Hz, 1H), 6.50 (dd,  $J = 8.36, 1.90$  Hz, 1H), 6.18 (s, 2H), 3.74 (s, 3H), 3.73 (s, 3H), 3.66 (s, 6H), 2.48-2.38 (m, 1H), 2.37-2.27 (m, 1H), 1.50 (s, 9H), 1.42-1.28 (m, 2H);

$^{13}\text{C}$  NMR (400 MHz,  $\text{CDCl}_3$ )  $\delta$  152.70, 152.44, 145.69, 135.87, 134.70, 130.87, 127.49, 122.59, 119.12, 109.39, 106.05, 80.13, 60.85, 55.94, 55.71, 28.43, 24.34, 24.32, 11.57;

IR  $\nu$  3436, 2975, 1724, 1509, 1367, 1156, 1049  $\text{cm}^{-1}$ .

## 2-Methoxy-5-(2-(3,4,5-trimethoxyphenyl)cyclopropyl)aniline (**271**).



**270** (300 mg, 0.7 mmol) was dissolved in 6 mL acetonitrile, transferred in a microwave reaction vessel and 1.5 g silica gel were added. The reaction mixture was placed in the microwave for 1 h at  $180\text{ }^\circ\text{C}$  (after 30 min the progress of the reaction was verified by TLC). The silica gel was filtered over a suction filter and was washed successfully with methanol. The solvent was removed under reduced pressure and the residue was purified by flash column chromatography (toluene/ethyl acetate 19:1) affording 190 mg (83%) of **271** as a yellow oil.

$R_f$  0.24 (toluene/ethyl acetate 5:1);

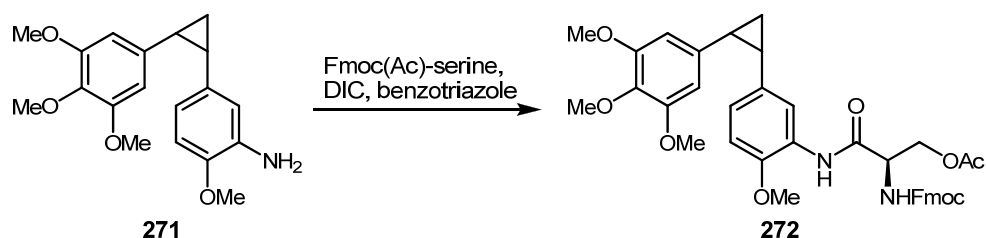
$^1\text{H}$  NMR (400 MHz,  $\text{CDCl}_3$ )  $\delta$  [ppm] 6.57 (d,  $J = 8.08$  Hz, 1H), 6.43 (d,  $J = 2.00$  Hz, 1H), 6.38 (dd,  $J = 8.08, 2.00$  Hz, 1H), 6.12 (s, 2H), 3.76 (s, 3H), 3.77 (s, 3H), 3.64 (s, 6H), 2.44-2.33 (m, 1H), 2.32-2.22 (m, 1H), 1.46-1.39 (m, 1H), 1.20-1.12 (m, 1H);

$^{13}\text{C}$  NMR (400 MHz,  $\text{CDCl}_3$ )  $\delta$  [ppm] 152.48, 145.85, 135.95, 135.71, 135.20, 130.93, 119.27, 116.53, 110.13, 105.86, 60.92, 55.99, 55.68, 24.17, 23.92, 12.62;

IR  $\nu$  3369, 2934, 1719, 1465, 1183,  $1008\text{ cm}^{-1}$ .



**(2R)-2-(((9H-fluoren-9-yl)methoxy)carbonylamino)-3-(2-methoxy-5-(2-(3,4,5-trimethoxyphenyl)cyclopropyl)phenylamino)-3-oxopropyl acetate (272).**



To a solution of **271** (200 mg, 0.3 mmol) in 6 mL anhydrous DMF, DIC (283  $\mu$ L, 1.83 mmol), Fmoc(Ac)-serine (676 mg, 1.83 mmol), and HOBt.H<sub>2</sub>O (218 mg, 1.83 mmol) were added, and the resulting reaction mixture was stirred for 16 h at room temperature. The reaction was quenched with water and extracted with diethyl ether (3 x 20 mL). The combined organic layers were subsequently washed with water (2 x 20 mL), dried over Na<sub>2</sub>SO<sub>4</sub> and the solvent was removed under reduced pressure. The crude product was purified by flash column chromatography (toluene/ethyl acetate 19:1 to 5:1) to give **272** (315 mg, 76%) as a white solid.<sup>159</sup>

R<sub>f</sub> 0.1 (hexanes/ethyl acetate 2:1),

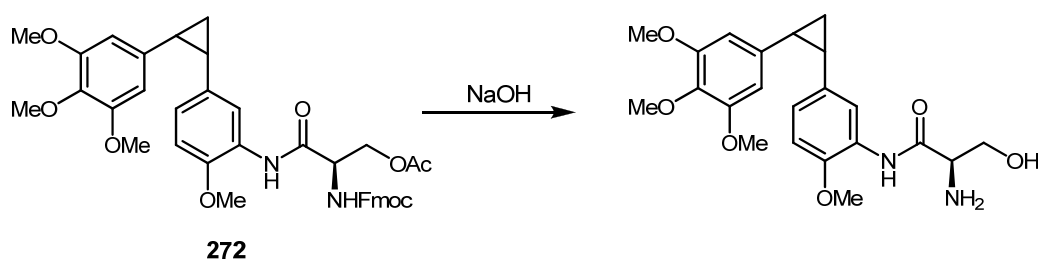
<sup>1</sup>H NMR (400 MHz, CDCl<sub>3</sub>)  $\delta$  [ppm] 8.34 (s, 1H), 8.19 (d, *J* = 7.08 Hz, 1H), 7.77 (d, *J* = 7.32 Hz, 2H), 7.60 (d, *J* = 7.32 Hz, 2H), 7.44-7.27 (m, 4H), 6.60 (s, 2H), 6.18 (d, *J* = 4.80 Hz, 2H), 5.69 (bs, 1H), 4.62 (bs, 1H), 4.54- 4.40 (m, 3H), 4.35-4.21 (m, 2H), 3.73 (s, 3H), 3.72 (s, 3H), 3.66 (s, 3H), 3.65 (s, 3H), 2.50-2.31 (m, 2H), 2.08 (s, 3H), 1.47-1.37 (m, 1H), 1.31-1.29 (m, 1H);

<sup>13</sup>C NMR (400 MHz, CDCl<sub>3</sub>)  $\delta$  [ppm] 170.57, 166.25, 152.39, 146.19, 143.55, 141.29, 135.83, 134.32\*, 134.26, 131.01\*, 130.99, 127.80, 127.10, 126.09, 124.96, 124.57, 121.02\*, 120.76, 120.03\*, 120.02, 109.41, 106.01\*, 105.90, 67.48, 63.89, 60.73, 55.85, 55.73, 47.08, 24.44\*, 24.31, 24.06\*, 24.00, 20.67, 11.45;

IR  $\nu$  3325, 2943, 2838, 1741, 1234, 1030 cm<sup>-1</sup>.

\*) denotes rotamer

**(2R)-2-Amino-3-hydroxy-N-(2-methoxy-5-(2-(3,4,5-trimethoxyphenyl)-cyclopropyl)phenyl)propanamide.**



The protected cyclopropyl derivative (**272**, 200 mg, 0.29 mmol) was dissolved in 4 mL of a solvent mixture of CH<sub>2</sub>Cl<sub>2</sub>/MeOH in a 1:1 ratio and 290  $\mu$ L of an aqueous solution of 2 M NaOH (0.58 mmol) were added to this biphasic mixture. The reaction mixture was stirred for 1 h and the reaction was diluted with water and extracted with CH<sub>2</sub>Cl<sub>2</sub> (8 x 15 mL). The combined organic layers were dried over Na<sub>2</sub>SO<sub>4</sub>, filtered and the solvent was removed *in vacuo*. The residue was purified by flash chromatography (CH<sub>2</sub>Cl<sub>2</sub>/MeOH 19:1) affording 110 mg (92%) of the seine derivative as a colorless oil.<sup>159</sup>

R<sub>f</sub> 0.63 (CH<sub>2</sub>Cl<sub>2</sub>/MeOH 5:1)

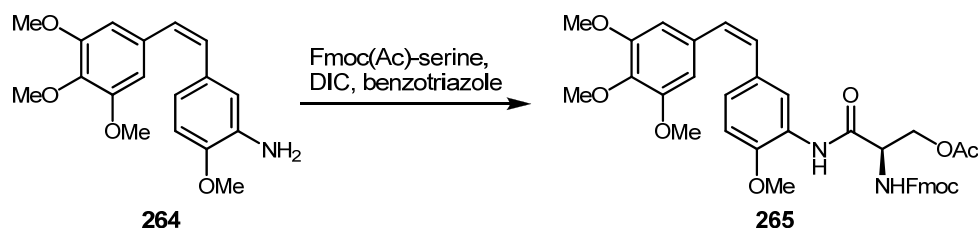
<sup>1</sup>H NMR (400 MHz, CDCl<sub>3</sub>)  $\delta$  [ppm] 9.75 (s, 1H), 8.19 (d, *J* = 20.87 Hz, 1H), 6.64 -6.58 (m, 2H), 6.20-6.16 (m, 2H), 3.98-3.90 (m, 1H), 3.79 (s, 3H), 3.77-3.74 (m, 1H), 3.73 (s, 3H), 3.66 (s, 3H), 3.65 (s, 3H), 3.56-3.50 (m, 1H), 2.49-2.29 (m, 2H), 2.11 (bs, 3H), 1.45-1.36 (m, 1H), 1.36-1.28 (m, 1H);

<sup>13</sup>C NMR (400 MHz, CDCl<sub>3</sub>)  $\delta$  [ppm] 171.68\*, 171.63, 152.32, 146.56\*, 146.52, 135.74, 134.50\*, 134.41, 130.80\*, 130.75, 126.45, 124.27\*, 124.09, 120.63\*, 120.22, 109.40\*, 109.36, 106.14\*, 105.94, 65.46\*, 65.40, 60.74, 56.60\*, 56.58, 55.85, 55.72, 24.37\*, 24.18, 24.05\*, 23.96, 11.51\*, 11.47;

IR  $\nu$  3306, 2938, 1510, 1234, 1027 cm<sup>-1</sup>.

\*) denotes rotamer

**(R,Z)-2-(((9H-fluoren-9-yl)methoxy)carbonylamino)-3-(2-methoxy-5-(3,4,5-trimethoxystyryl)phenylamino)-3-oxopropyl acetate (265).**



To a solution of **264** (200 mg, 0.63 mmol) in 6 mL anhydrous DMF, DIC (293  $\mu$ L, 1.89 mmol), Fmoc(Ac)-serine (698 mg, 1.89 mmol) and HOBt.H<sub>2</sub>O (225 mg, 1.89 mmol) were added and the resulting reaction mixture was stirred for 16 h at room temperature. The reaction was quenched with water and extracted with diethyl ether (3 x 20 mL). The combined organic layer was washed successfully with water (2 x 20 mL), dried over Na<sub>2</sub>SO<sub>4</sub> and the solvent was removed under reduced pressure. The crude product was purified by flash column chromatography (toluene/ethyl acetate 19:1 to 9:1) to give **265** (295 mg, 70%) as a white solid.<sup>159</sup>

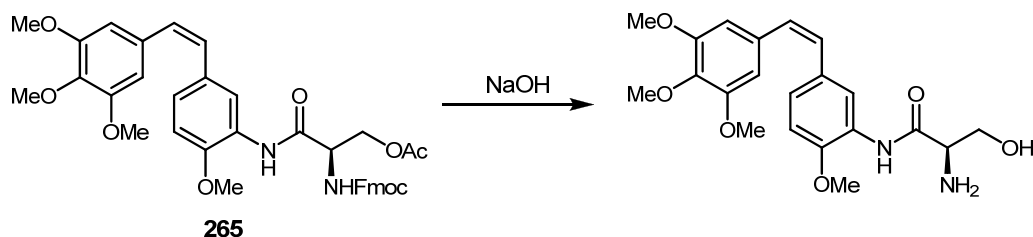
R<sub>f</sub> 0.1 (toluene/ethyl acetate 5:1);

<sup>1</sup>H NMR (400 MHz, CDCl<sub>3</sub>)  $\delta$  [ppm] 8.40 (s, 1H), 8.30 (d, *J* = 1.76 Hz, 1H), 7.76 (d, *J* = 7.56 Hz, 2H), 7.60 (d, *J* = 6.56 Hz, 2H), 7.44-7.36 (m, 2H), 7.36-7.27 (bs, 2H), 7.03 (dd, *J* = 8.60, 1.76 Hz, 1H), 6.71 (d, *J* = 8.60 Hz, 1H), 6.51 (s, 2H), 6.48 (dd, *J* = 21.44, 12.16 Hz, 2H), 5.83-5.68 (bs, 1H), 4.69-4.57 (bs, 1H), 4.55-4.41 (m, 3H), 4.38-4.28 (m, 1H), 4.28-4.21 (m, 1H), 3.84 (s, 3H), 3.79 (s, 3H), 3.69 (s, 6H), 2.09 (s, 3H);

<sup>13</sup>C NMR (400 MHz, CDCl<sub>3</sub>)  $\delta$  [ppm] 170.76, 166.54, 153.04, 147.28, 143.77, 143.68, 141.43, 137.30, 132.86, 130.34, 129.57, 129.47, 127.94, 127.24, 126.69, 125.17, 125.09, 121.02, 120.17, 109.75, 106.17, 67.64, 64.05, 61.00, 56.04, 55.00, 54.87, 20.83;

IR  $\nu$  3306, 2938, 1674, 1510, 1463, 1126 cm<sup>-1</sup>.

**(R,Z)-2-Amino-3-hydroxy-N-(2-methoxy-5-(3,4,5-trimethoxystyryl)-phenyl)-propanamide.**



**265** (200 mg, 0.3 mmol) was dissolved in 4 mL of a solvent mixture of CH<sub>2</sub>Cl<sub>2</sub>/MeOH in a 1:1 ratio and 0.3 mL of an aqueous solution of 2 M NaOH (0.6 mmol) was added to this biphasic mixture. The reaction mixture was stirred for 1 h and the reaction was diluted with water and extracted with CH<sub>2</sub>Cl<sub>2</sub> (8 x 15 mL). The combined organic layers were dried over Na<sub>2</sub>SO<sub>4</sub>, filtered and the solvent was removed in vacuo. The residue was purified by flash chromatography (CH<sub>2</sub>Cl<sub>2</sub>/MeOH 19:1) affording 73 mg (61%) of the serine derivative as a colorless oil.<sup>159</sup>

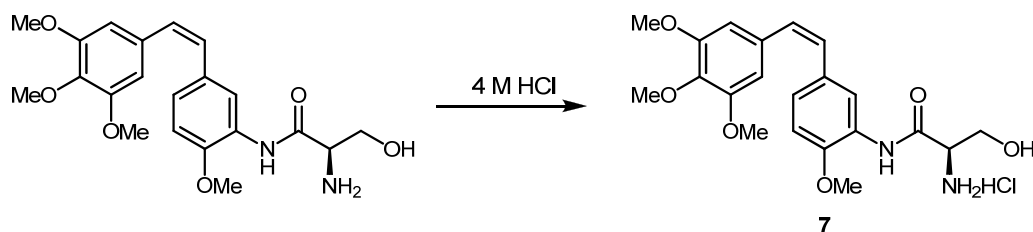
R<sub>f</sub> 0.72 (CH<sub>2</sub>Cl<sub>2</sub>/MeOH 5:1);

<sup>1</sup>H NMR (400 MHz, CDCl<sub>3</sub>) δ [ppm] 9.84 (s, 1H), 8.36 (d, *J* = 2.04 Hz, 1H), 7.01 (dd, *J* = 8.32, 2.04 Hz, 1H), 6.72 (d, *J* = 8.32 Hz, 1H), 6.51 (s, 2H), 6.48 (dd, *J* = 31.59, 12.14 Hz, 2H), 4.01-3.94 (m, 1H), 3.87 (s, 3H), 3.84 (s, 3H), 3.82-3.75 (m, 1H), 3.69 (s, 6H), 3.60-3.55 (m, 1H), 2.97-2.36 (bs, 1H), 1.95-1.51 (bs, 2H);

<sup>13</sup>C NMR (400 MHz, CDCl<sub>3</sub>) δ [ppm] 171.94, 153.03, 147.75, 130.00, 130.22, 129.86, 129.25, 127.07, 124.78, 120.72, 109.72, 109.78, 106.24, 65.68, 61.04, 56.75, 56.07, 56.02;

IR ν 3305, 2935, 1580, 1325, 1123, 1026 cm<sup>-1</sup>.

**(R,Z)-2-Amino-3-hydroxy-N-(2-methoxy-5-(3,4,5-trimethoxystyryl)-phenyl)-propanamide hydrochloride (AVE8062, 7).**



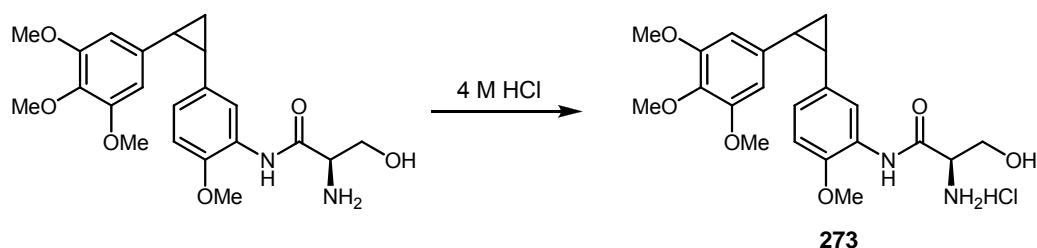
The serine derivative (20 mg, 0.05 mmol) was dissolved in 0.3 mL of methanol and 50  $\mu$ L 4 M HCl in dioxane were added. The resulting reaction mixture was stirred for 10 min. The solvent was removed under reduced pressure affording the desired hydrochloride **7** as a light yellow solid (20 mg, 91%).<sup>159</sup>

<sup>1</sup>H NMR (400 MHz, MeOD)  $\delta$  [ppm] <sup>1</sup>H NMR (400 MHz, CDCl<sub>3</sub>)  $\delta$  7.99 (d,  $J$  = 2.04, 1H), 7.07 (dd,  $J$  = 8.46, 2.04, 1H), 6.96 (d,  $J$  = 8.46, 1H), 6.55 (s, 2H), 6.50 (dd,  $J$  = 17.43, 12.13, 2H), 4.21 (m, 1H), 4.02-3.95 (m, 1H), 3.95-3.84 (m, 5H), 3.75 (s, 3H), 3.73-3.62 (m, 8H);

<sup>13</sup>C NMR (400 MHz, MeOD)  $\delta$  [ppm] <sup>13</sup>C NMR (400 MHz, CDCl<sub>3</sub>)  $\delta$  166.63, 154.19, 150.65, 138.25, 134.35, 131.24, 130.48, 130.34, 127.54, 127.30, 123.86, 111.73, 107.42, 61.77, 61.19, 56.47, 56.43\*, 56.39;

IR  $\nu$  3233, 2938, 1694, 1548, 1326, 1126, 1026 cm<sup>-1</sup>.

**(2R)-2-Amino-3-hydroxy-N-(2-methoxy-5-(2-(3,4,5-trimethoxyphenyl)-cyclopropyl)phenyl)propanamide hydrochloride (273).**



The serine derivative (20 mg, 0.05 mmol) was dissolved in 0.3 mL methanol and 50  $\mu$ L 4 M HCl in dioxane were added. The resulting reaction mixture was stirred for 10 min. The solvent was removed under reduced pressure affording the desired hydrochloride **273** as a light yellow solid (21 mg, 91%).<sup>159</sup>

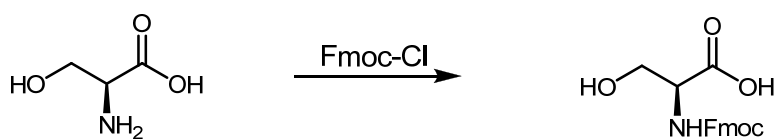
<sup>1</sup>H NMR (400 MHz, MeOD)  $\delta$  [ppm] <sup>1</sup>H NMR (400 MHz, CDCl<sub>3</sub>)  $\delta$  7.81 (s, 1H), 6.85-6.78 (m, 2H), 6.21 (d,  $J$  = 8.78 Hz, 2H), 4.20-4.14 (m, 1H), 4.0-3.93 (m, 1H), 3.92-3.78 (m, 4H), 3.68-3.61 (m, 12H), 2.51-2.35 (m, 2H), 1.46-1.31 (m, 2H);

<sup>13</sup>C NMR (400 MHz, MeOD)  $\delta$  [ppm] <sup>13</sup>C NMR (400 MHz, CDCl<sub>3</sub>)  $\delta$  166.50, 153.57, 149.46, 149.43\*, 136.33, 136.29\*, 136.26, 136.23\*, 131.84, 131.78\*, 127.31, 127.22\*, 126.93, 124.15, 124.09\*, 111.30, 111.28\*, 107.23, 107.05\*, 61.75, 61.05, 56.44\*, 56.38, 25.15, 25.11\*, 25.06, 24.99\*, 11.76, 11.66\*;

IR  $\nu$  3270, 2943, 1688, 1509, 1325, 1182, 1027 cm<sup>-1</sup>.

\*) denotes rotamer

**(S)-2-(((9H-fluoren-9-yl)methoxy)carbonylamino)-3-hydroxy-propanoic acid.**



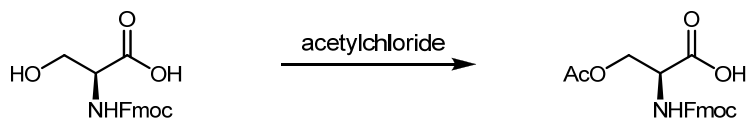
L-Serine (2.0 g, 19 mmol) and NaHCO<sub>3</sub> (4.0 g, 47.5 mmol) were dissolved in 40 mL H<sub>2</sub>O and cooled to 0 °C. Fmoc-Cl (4.9 g, 19 mmol) was dissolved in 40 mL dioxane and added dropwise to the aqueous solution. After addition was completed the ice bath was removed and the solution was stirred for 48 h. The solvent was removed under reduced pressure. The resulting suspension was diluted with H<sub>2</sub>O, washed with Et<sub>2</sub>O (2 x 100 mL) and the aqueous phase was acidified with 1 M citric acid to pH 3.5. The aqueous layer was extracted with ethyl acetate (3 x 50 mL). The combined organic phases were dried over Na<sub>2</sub>SO<sub>4</sub> and the solvent was removed under reduced pressure. The crude product was recrystallized from CH<sub>2</sub>Cl<sub>2</sub>-hexanes affording 4.57 g (65%) of the Fmoc-protected serine as a white solid.<sup>174</sup>

R<sub>f</sub> 0.68 (CH<sub>2</sub>Cl<sub>2</sub>/MeOH 3:1, 1% AcOH)

<sup>1</sup>H NMR (400 MHz, MeOD) δ [ppm] 7.82-7.76 (m, 2H), 7.72-7.58 (m, 2H), 7.42-7.35 (m, 2H), 7.34-7.27 (m, 2H), 4.46-4.19 (m, 4H), 3.96-3.76 (m, 2H);

<sup>13</sup>C NMR (400 MHz, MeOD) δ [ppm] 173.76, 158.57, 145.17, 142.53, 128.75, 128.14, 126.26, 126.20\*, 120.88, 68.15, 63.09, 57.71, 48.30.

**(S)-2-(((9H-fluoren-9-yl)methoxy)carbonylamino)-3-acetoxy-propanoic acid.**



Fmoc protected serine (2.58 g, 7.9 mmol) was added slowly to 8.4 mL (118.5 mmol) of acetyl chloride. The suspension was stirred for two hours at room temperature. Afterwards the excess of acetylchloride was removed under reduced pressure. The crude product was recrystallized from CH<sub>2</sub>Cl<sub>2</sub> affording 2.68 g (92%) of the Fmoc- and acetate-protected serine as a white solid.<sup>175</sup>

R<sub>f</sub> 0.9 (CH<sub>2</sub>Cl<sub>2</sub>/MeOH 3:1, 1% AcOH);

<sup>1</sup>H NMR (400 MHz, CDCl<sub>3</sub>) δ [ppm] 7.77 (d, *J* = 7.56 Hz, 2H), 7.50 (d, *J* = 7.08 Hz, 2H), 7.45-7.37 (m, 2H), 7.36-7.28 (m, 2H), 4.76-4.64 (m, 1H), 4.60-4.36 (m, 4H), 4.29-4.20 (m, 1H), 2.09 (s, 3H);

<sup>13</sup>C NMR (400 MHz, CDCl<sub>3</sub>) δ [ppm] 173.41, 170.86, 156.12, 143.83, 141.48, 127.96, 127.26, 125.18, 120.19, 67.58, 63.99, 53.34, 47.24, 20.83.



## References

- (1) Avendano, C.; Menendez, C. *Medicinal Chemistry of Anticancer Drugs*; Elsevier, 2008.
- (2) Boyle, P.; Levin, B. †World cancer report 2008, ‡ World Health Organization, 2008.
- (3) Newman, D. J.; Cragg, G. M.; Snader, K. M. *Natural Product Reports* **2000**, *17*, 215-234.
- (4) Pettit, G. R.; Cragg, G. M.; Herald, D. L.; Schmidt, J. M.; Lohavanijaya, P. *Canadian Journal of Chemistry-Revue Canadienne De Chimie* **1982**, *60*, 1374-1376.
- (5) Pettit, G. R.; Toki, B. E.; Herald, D. L.; Boyd, M. R.; Hamel, E.; Pettit, R. K.; Chapuis, J. C. *Journal of Medicinal Chemistry* **1999**, *42*, 1459-1465.
- (6) Lin, C. M.; Ho, H. H.; Pettit, G. R.; Hamel, E. *Biochemistry* **1989**, *28*, 6984-6991.
- (7) Chaudhary, A.; Pandeya, S. N.; Kumar, P.; Sharma, P.; Gupta, S.; Soni, N.; Verma, K. K.; Bhardwaj, G. *Mini-Reviews in Medicinal Chemistry* **2007**, *7*, 1186-1205.
- (8) Cushman, M.; Nagarathnam, D.; Gopal, D.; He, H. M.; Lin, C. M.; Hamel, E. *Journal of Medicinal Chemistry* **1992**, *35*, 2293-2306.
- (9) Hori, K.; Saito, S.; Kubota, K. *British Journal of Cancer* **2002**, *86*, 1604-1614.
- (10) Salmon, H. W.; Mladinich, C.; Siemann, D. W. *European Journal of Cancer* **2006**, *42*, 3073-3078.
- (11) Davis, P. D.; Dougherty, G. J.; Blakey, D. C.; Galbraith, S. M.; Tozer, G. M.; Holder, A. L.; Naylor, M. A.; Nolan, J.; Stratford, M. R. L.; Chaplin, D. J.; Hill, S. A. *Cancer Research* **2002**, *62*, 7247-7253.
- (12) Robinson, S. P.; McIntyre, D. J. O.; Checkley, D.; Tessier, J. J.; Howe, F. A.; Griffiths, J. R.; Ashton, S. E.; Ryan, A. J.; Blakey, D. C.; Waterton, J. C. *British Journal of Cancer* **2003**, *88*, 1592-1597.
- (13) Pettit, G. R.; Singh, S. B.; Niven, M. L.; Hamel, E.; Schmidt, J. M. *Journal of Natural Products* **1987**, *50*, 119-131.
- (14) Pettit, G. R.; Singh, S. B. *Canadian Journal of Chemistry-Revue Canadienne De Chimie* **1987**, *65*, 2390-2396.
- (15) Pettit, G. R.; Singh, S. B.; Boyd, M. R.; Hamel, E.; Pettit, R. K.; Schmidt, J. M.; Hogan, F. *Journal of Medicinal Chemistry* **1995**, *38*, 2994-2994.
- (16) Singh, S. B.; Pettit, G. R. *Journal of Organic Chemistry* **1989**, *54*, 4105-4114.
- (17) Pettit, G. R.; Singh, S. B.; Niven, M. L. *Journal of the American Chemical Society* **1988**, *110*, 8539-8540.
- (18) Kovacs, A.; Vasas, A.; Hohmann, J. *Phytochemistry* **2008**, *69*, 1084-1110.
- (19) Graening, T.; Schmalz, H. G. *Angewandte Chemie-International Edition* **2004**, *43*, 3230-3256.
- (20) Jordan, A.; Hadfield, J. A.; Lawrence, N. J.; McGown, A. T. *Medicinal Research Reviews* **1998**, *18*, 259-296.
- (21) Zhang, S. X.; Feng, J.; Kuo, S. C.; Brossi, A.; Hamel, E.; Tropsha, A.; Li, K. H. *Journal of Medicinal Chemistry* **2000**, *43*, 167-176.
- (22) Bai, R. L.; Covell, D. G.; Pei, X. F.; Ewell, J. B.; Nguyen, N. Y.; Brossi, A.; Hamel, E. *Journal of Biological Chemistry* **2000**, *275*, 40443-40452.
- (23) Andreu, J. M.; Timasheff, S. N. *Biochemistry* **1982**, *21*, 6465-6476.
- (24) Berg, U.; Deinum, J.; Lincoln, P.; Kvassman, J. *Bioorganic Chemistry* **1991**, *19*, 53-65.
- (25) Gatenby, R. A.; Gillies, R. J. *Nature Reviews Cancer* **2008**, *8*, 56-61.
- (26) Lowe, S. W.; Cepero, E.; Evan, G. *Nature* **2004**, *432*, 307-315.

- (27) Fidler, I. J. *Nature Reviews Cancer* **2003**, 3, 453-458.
- (28) Zeidman, I. *Cancer Research* **1957**, 17, 157-162.
- (29) Thiery, J. P. *Nature Reviews Cancer* **2002**, 2, 442-454.
- (30) Brabletz, T.; Jung, A.; Spaderna, S.; Hlubek, F.; Kirchner, T. *Nature Reviews Cancer* **2005**, 5, 744-749.
- (31) Greenblatt, M. S.; Bennett, W. P.; Hollstein, M.; Harris, C. C. *Cancer Research* **1994**, 54, 4855-4878.
- (32) Agapova, L. S.; Ivanov, A. V.; Sablina, A. A.; Kopnin, P. B.; Sokova, O. I.; Chumakov, P. M.; Kopnin, B. P. *Oncogene* **1999**, 18, 3135-3142.
- (33) Marshall, C. J. *Current Opinion in Cell Biology* **1996**, 8, 197-204.
- (34) Mollinedo, F.; Gajate, C. *Apoptosis* **2003**, 8, 413-450.
- (35) Margolis, R. L.; Wilson, L. *Nature* **1981**, 293, 705-711.
- (36) Jordan, M. A.; Wilson, L. *Nature Reviews Cancer* **2004**, 4, 253-265.
- (37) Panda, D.; Miller, H. P.; Wilson, L. *Biochemistry* **2002**, 41, 1609-1617.
- (38) Rodionov, V. I.; Borisy, G. G. *Science* **1997**, 275, 215-218.
- (39) Mitchison, T.; Kirschner, M. *Nature* **1984**, 312, 237-242.
- (40) Doxsey, S.; McCollum, D.; Theurkauf, W. *Annual Review of Cell and Developmental Biology* **2005**, 21, 411-434.
- (41) Hirokawa, N. *Science* **1998**, 279, 519-526.
- (42) Altmann, K. H.; Gertsch, J. *Natural Product Reports* **2007**, 24, 327-357.
- (43) Rai, S. S.; Wolff, J. *Journal of Biological Chemistry* **1996**, 271, 14707-14711.
- (44) Rao, S.; Krauss, N. E.; Heering, J. M.; Swindell, C. S.; Ringel, I.; Orr, G. A.; Horwitz, S. B. *Journal of Biological Chemistry* **1994**, 269, 3132-3134.
- (45) Rao, S.; Orr, G. A.; Chaudhary, A. G.; Kingston, D. G. I.; Horwitz, S. B. *Journal of Biological Chemistry* **1995**, 270, 20235-20238.
- (46) Svoboda, G. H.; Gorman, M.; Neuss, N.; Johnson, I. S. *Journal of Pharmaceutical Sciences* **1962**, 51, 707-&.
- (47) Joel, S. *Cancer Treatment Reviews* **1995**, 21, 513-525.
- (48) Gralla, R. J.; Gatzemeier, U.; Gebbia, V.; Huber, R.; O'Brien, M.; Puozzo, C. *Drugs* **2007**, 67, 1403-1410.
- (49) Aapro, M. S.; Conte, P.; Gonzalez, E. E.; Trillet-Lenoir, V. *Drugs* **2007**, 67, 657-667.
- (50) Mano, M. *Cancer Treatment Reviews* **2006**, 32, 106-118.
- (51) Hill, B. T. *Current Pharmaceutical Design* **2001**, 7, 1199-1212.
- (52) Jordan, M. A.; Thrower, D.; Wilson, L. *Cancer Research* **1991**, 51, 2212-2222.
- (53) Singer, W. D.; Jordan, M. A.; Wilson, L.; Himes, R. H. *Molecular Pharmacology* **1989**, 36, 366-370.
- (54) Newman, D. J.; Cragg, G. M. *Current Medicinal Chemistry* **2004**, 11, 1693-1713.
- (55) Newman, D. J.; Cragg, G. M. *Journal of Natural Products* **2004**, 67, 1216-1238.
- (56) Hirata, Y.; Uemura, D. *Pure and Applied Chemistry* **1986**, 58, 701-710.
- (57) Aicher, T. D.; Buszek, K. R.; Fang, F. G.; Forsyth, C. J.; Jung, S. H.; Kishi, Y.; Matelich, M. C.; Scola, P. M.; Spero, D. M.; Yoon, S. K. *Journal of the American Chemical Society* **1992**, 114, 3162-3164.
- (58) Newman, S. *Current Opinion in Investigational Drugs* **2007**, 8, 1057-1066.
- (59) Pettit, G. R.; Kamano, Y.; Herald, C. L.; Tuinman, A. A.; Boettner, F. E.; Kizu, H.; Schmidt, J. M.; Baczynskyj, L.; Tomer, K. B.; Bontems, R. J. *Journal of the American Chemical Society* **1987**, 109, 6883-6885.
- (60) Bai, R.; Pettit, G. R.; Hamel, E. *Biochemical Pharmacology* **1990**, 39, 1941-1949.
- (61) Cunningham, C.; Appleman, L. J.; Kirvan-Visovatti, M.; Ryan, D. P.; Regan, E.; Vukelja, S.; Bonate, P. L.; Ruvuna, F.; Fram, R. J.; Jekunen, A.; Weitman, S.; Hammond, L. A.; Eder, J. P. *Clinical Cancer Research* **2005**, 11, 7825-7833.

- (62) Talpir, R.; Benayahu, Y.; Kashman, Y.; Pannell, L.; Schleyer, M. *Tetrahedron Letters* **1994**, *35*, 4453-4456.
- (63) Loganzo, F.; Discafani, C. M.; Annable, T.; Beyer, C.; Musto, S.; Hari, M.; Tan, X. Z.; Hardy, C.; Hernandez, R.; Baxter, M.; Singanallore, T.; Khafizova, G.; Poruchynsky, M. S.; Fojo, T.; Nieman, J. A.; Ayril-Kaloustian, S.; Zask, A.; Andersen, R. J.; Greenberger, L. M. *Cancer Research* **2003**, *63*, 1838-1845.
- (64) Subbaraju, G. V.; Golakoti, T.; Patterson, G. M. L.; Moore, R. E. *Journal of Natural Products* **1997**, *60*, 302-305.
- (65) Panda, D.; Ananthnarayan, V.; Larson, G.; Shih, C.; Jordan, M. A.; Wilson, L. *Biochemistry* **2000**, *39*, 14121-14127.
- (66) Skoufias, D. A.; Wilson, L. *Biochemistry* **1992**, *31*, 738-746.
- (67) Mabeesh, N. J.; Escuin, D.; LaVallee, T. M.; Pribluda, V. S.; Swartz, G. M.; Johnson, M. S.; Willard, M. T.; Zhong, H.; Simons, J. W.; Giannakakou, P. *Cancer Cell* **2003**, *3*, 363-375.
- (68) Yoshimatsu, K.; Yamaguchi, A.; Yoshino, H.; Koyanagi, N.; Kitoh, K. *Cancer Research* **1997**, *57*, 3208-3213.
- (69) Wani, M. C.; Taylor, H. L.; Wall, M. E.; Coggon, P.; Mcphail, A. T. *Journal of the American Chemical Society* **1971**, *93*, 2325-&.
- (70) Schiff, P. B.; Fant, J.; Horwitz, S. B. *Nature* **1979**, *277*, 665-667.
- (71) Horwitz, S. B. *Nature* **1994**, *367*, 593-594.
- (72) Denis, J. N.; Correa, A.; Greene, A. E. *Journal of Organic Chemistry* **1990**, *55*, 1957-1959.
- (73) Nogales, E. *Annual Review of Biophysics and Biomolecular Structure* **2001**, *30*, 397-420.
- (74) Nogales, E.; Wolf, S. G.; Khan, I. A.; Luduena, R. F.; Downing, K. H. *Nature* **1995**, *375*, 424-427.
- (75) Derry, W. B.; Wilson, L.; Jordan, M. A. *Biochemistry* **1995**, *34*, 2203-2211.
- (76) Bollag, D. M.; Mcquaney, P. A.; Zhu, J.; Hensens, O.; Koupal, L.; Liesch, J.; Goetz, M.; Lazarides, E.; Woods, C. M. *Cancer Research* **1995**, *55*, 2325-2333.
- (77) Watkins, E. B.; Chittiboyina, A. G.; Jung, J. C.; Avery, M. A. *Current Pharmaceutical Design* **2005**, *11*, 1615-1653.
- (78) Low, J. A.; Wedam, S. B.; Lee, J. J.; Berman, A. W.; Brufsky, A.; Yang, S. X.; Poruchynsky, M. S.; Steinberg, S. M.; Mannan, N.; Fojo, T.; Swain, S. M. *Journal of Clinical Oncology* **2005**, *23*, 2726-2734.
- (79) Hofle, G.; Glaser, N.; Leibold, T.; Karama, U.; Sasse, F.; Steinmetz, H. *Pure and Applied Chemistry* **2003**, *75*, 167-178.
- (80) Kerbel, R. S. *Science* **2006**, *312*, 1171-1175.
- (81) Tozer, G. M.; Kanthou, C.; Baguley, B. C. *Nature Reviews Cancer* **2005**, *5*, 423-435.
- (82) Tozer, G. M.; Kanthou, C.; Parkins, C. S.; Hill, S. A. *International Journal of Experimental Pathology* **2002**, *83*, 21-38.
- (83) Dark, G. G.; Hill, S. A.; Prise, V. E.; Tozer, G. M.; Pettit, G. R.; Chaplin, D. J. *Cancer Research* **1997**, *57*, 1829-1834.
- (84) Tozer, G. M.; Prise, V. E.; Wilson, J.; Cemazar, M.; Shan, S. Q.; Dewhirst, M. W.; Barber, P. R.; Vojnovic, B.; Chaplin, D. J. *Cancer Research* **2001**, *61*, 6413-6422.
- (85) Kanthou, C.; Tozer, G. M. *Blood* **2002**, *99*, 2060-2069.
- (86) Cirila, A.; Mann, J. *Natural Product Reports* **2003**, *20*, 558-564.
- (87) Cushman, M.; Nagarathnam, D.; Gopal, D.; Chakraborti, A. K.; Lin, C. M.; Hamel, E. *Journal of Medicinal Chemistry* **1991**, *34*, 2579-2588.
- (88) Lin, C. M.; Singh, S. B.; Chu, P. S.; Dempcy, R. O.; Schmidt, J. M.; Pettit, G. R.; Hamel, E. *Molecular Pharmacology* **1988**, *34*, 200-208.

- (89) Nandy, P.; Banerjee, S.; Gao, H.; Hui, M. B. V.; Lien, E. J. *Pharmaceutical Research* **1991**, *8*, 776-781.
- (90) Bedford, S. B.; Quarterman, C. P.; Rathbone, D. L.; Slack, J. A.; Griffin, R. J.; Stevens, M. F. G. *Bioorganic & Medicinal Chemistry Letters* **1996**, *6*, 157-160.
- (91) Pettit, G. R.; Minardi, M. D.; Rosenberg, H. J.; Hamel, E.; Bibby, M. C.; Martin, S. W.; Jung, M. K.; Pettit, R. K.; Cuthbertson, T. J.; Chapuis, J. C. *Journal of Natural Products* **2005**, *68*, 1450-1458.
- (92) Pinney, K. G.; Mejia, M. P.; Villalobos, V. M.; Rosenquist, B. E.; Pettit, G. R.; Verdier-Pinard, P.; Hamel, E. *Bioorganic & Medicinal Chemistry* **2000**, *8*, 2417-2425.
- (93) Lawrence, N. J.; Rennison, D.; Woo, M.; McGown, A. T.; Hadfield, J. A. *Bioorganic & Medicinal Chemistry Letters* **2001**, *11*, 51-54.
- (94) Ohsumi, K.; Nakagawa, R.; Fukuda, Y.; Hatanaka, T.; Morinaga, Y.; Nihei, Y.; Ohishi, K.; Suga, Y.; Akiyama, Y.; Tsuji, T. *Journal of Medicinal Chemistry* **1998**, *41*, 3022-3032.
- (95) Wang, L.; Woods, K. W.; Li, Q.; Barr, K. J.; McCroskey, R. W.; Hannick, S. M.; Gherke, L.; Credo, R. B.; Hui, Y. H.; Marsh, K.; Warner, R.; Lee, J. Y.; Zielinski-Mozng, N.; Frost, D.; Rosenberg, S. H.; Sham, H. L. *Journal of Medicinal Chemistry* **2002**, *45*, 1697-1711.
- (96) Kim, Y.; Nam, N. H.; You, Y. J.; Ahn, B. Z. *Bioorganic & Medicinal Chemistry Letters* **2002**, *12*, 719-722.
- (97) Simoni, D.; Grisolia, G.; Giannini, G.; Roberti, M.; Rondanin, R.; Piccagli, L.; Baruchello, R.; Rossi, M.; Romagnoli, R.; Invidiata, F. P.; Grimaudo, S.; Jung, M. K.; Hamel, E.; Gebbia, N.; Crosta, L.; Abbadessa, V.; Di Cristina, A.; Dusonchet, L.; Meli, M.; Tolomeo, M. *Journal of Medicinal Chemistry* **2005**, *48*, 723-736.
- (98) Flynn, B. L.; Hamel, E.; Jung, M. K. *Journal of Medicinal Chemistry* **2002**, *45*, 2670-2673.
- (99) Sun, L. C.; Vasilevich, N. I.; Fuselier, J. A.; Hocart, S. J.; Coy, D. H. *Bioorganic & Medicinal Chemistry Letters* **2004**, *14*, 2041-2046.
- (100) Gurjar, M. K.; Wakharkar, R. D.; Singh, A. T.; Jaggi, M.; Borate, H. B.; Shinde, P. D.; Verma, R.; Rajendran, P.; Dutt, S.; Singh, G.; Sanna, V. K.; Singh, M. K.; Srivastava, S. K.; Mahajan, V. A.; Jadhav, V. H.; Dutta, K.; Krishnan, K.; Chaudhary, A.; Agarwal, S. K.; Mukherjee, R.; Burman, A. C. *Journal of Medicinal Chemistry* **2007**, *50*, 1744-1753.
- (101) Coulson, C. A.; Moffitt, W. E. *Journal of Chemical Physics* **1947**, *15*, 151-151.
- (102) Chakrabarti, P.; Seiler, P.; Dunitz, J. D.; Schluter, A. D.; Szeimies, G. *Journal of the American Chemical Society* **1981**, *103*, 7378-7380.
- (103) Walsh, A. D. *Nature* **1947**, *159*, 712-713.
- (104) Walsh, A. D. *Nature* **1947**, *159*, 165-165.
- (105) Kürti, L.; Czako, B. *Strategic Applications of Named Reactions in Organic Synthesis*; Elsevier, 2005.
- (106) Ponaras, A. A. *Tetrahedron Letters* **1976**, 3105-3108.
- (107) Chang, Y. H.; Campbell, D. E.; Pinnick, H. W. *Tetrahedron Letters* **1977**, 3337-3340.
- (108) Ueno, Y.; Chino, K.; Okawara, M. *Tetrahedron Letters* **1982**, *23*, 2575-2576.
- (109) Peterson, D. J.; Robbins, M. D. *Tetrahedron Letters* **1972**, 2135-&.
- (110) Sakurai, H.; Imai, T.; Hosomi, A. *Tetrahedron Letters* **1977**, 4045-4048.
- (111) Goering, H. L.; Trenbeath, S. L. *Journal of the American Chemical Society* **1976**, *98*, 5016-5017.
- (112) Merrill, R. E.; Allen, J. L.; Abramovitch, A.; Negishi, E. *Tetrahedron Letters* **1977**, 1019-1022.

- (113) Fitjer, L. *Synthesis-Stuttgart* **1977**, 189-191.
- (114) Truce, W. E.; Holliste, K.; Lindy, L. B.; Parr, J. E. *Journal of Organic Chemistry* **1968**, *33*, 43-&.
- (115) Klemmensen, P. D.; Kolindandersen, H.; Madsen, H. B.; Svendsen, A. *Journal of Organic Chemistry* **1979**, *44*, 416-420.
- (116) Hendrick, J. B.; Giga, A.; Wareing, J. *Journal of the American Chemical Society* **1974**, *96*, 2275-2276.
- (117) Gaoni, Y. *Journal of Organic Chemistry* **1982**, *47*, 2564-2571.
- (118) Genet, J. P.; Piau, F. *Journal of Organic Chemistry* **1981**, *46*, 2414-2417.
- (119) Singh, R. K.; Danishefsky, S. *Journal of Organic Chemistry* **1975**, *40*, 2969-2970.
- (120) Little, R. D.; Dawson, J. R. *Tetrahedron Letters* **1980**, *21*, 2609-2612.
- (121) Inouye, Y.; Inamasu, S.; Horiike, M.; Ohno, M. *Tetrahedron* **1968**, *24*, 2907-&.
- (122) Paulisse, R.; Teyssie, P.; Hubert, A. J. *Tetrahedron Letters* **1972**, 1465-&.
- (123) Donaldson, W. A. *Tetrahedron* **2001**, *57*, 8589-8627.
- (124) Pietruszka, J.; Widenmeyer, M. *Synlett* **1997**, 977-&.
- (125) Abdallah, H.; Gree, R.; Carrie, R. *Tetrahedron Letters* **1982**, *23*, 503-506.
- (126) Simmons, H. E.; Smith, R. D. *Journal of the American Chemical Society* **1958**, *80*, 5322-5324.
- (127) Furukawa, J.; Kawabata, N.; Nishimura, J. *Tetrahedron Letters* **1966**, 3353-&.
- (128) Molander, G. A.; Etter, J. B. *Journal of Organic Chemistry* **1987**, *52*, 3942-3944.
- (129) Charette, A. B.; Lebel, H. *Journal of Organic Chemistry* **1995**, *60*, 2966-2967.
- (130) Arai, I.; Mori, A.; Yamamoto, H. *Journal of the American Chemical Society* **1985**, *107*, 8254-8256.
- (131) Imai, T.; Mineta, H.; Nishida, S. *Journal of Organic Chemistry* **1990**, *55*, 4986-4988.
- (132) Charette, A. B.; Marcoux, J. F. *Synlett* **1995**, 1197-&.
- (133) Charette, A. B.; Brochu, C. *Journal of the American Chemical Society* **1995**, *117*, 11367-11368.
- (134) Balsells, J.; Walsh, P. J. *Journal of Organic Chemistry* **2000**, *65*, 5005-5008.
- (135) Denmark, S. E.; O'Connor, S. P. *Journal of Organic Chemistry* **1997**, *62*, 584-594.
- (136) Degroot, A.; Oudman, D.; Wynberg, H. *Tetrahedron Letters* **1969**, 1529-&.
- (137) Meijere, A. d. *Houben Weyl-Methods of organic chemistry*, 4th ed.; Thieme, 1996; Vol. E 17 b.
- (138) Brook, P. R.; Duke, A. J. *Journal of the Chemical Society-Perkin Transactions 1* **1973**, 1013-1019.
- (139) Fletcher, V. R.; Hassner, A. *Tetrahedron Letters* **1970**, 1071-&.
- (140) Dreibelbis, R. L.; Khatri, H. N.; Walborsky, H. M. *Journal of Organic Chemistry* **1975**, *40*, 2074-2079.
- (141) Fernandez, M. D.; Defrutos, M. P.; Marco, J. L.; Fernandezalvarez, E.; Bernabe, M. *Tetrahedron Letters* **1989**, *30*, 3101-3104.
- (142) Dauben, W. G.; Fonken, G. J. *Journal of the American Chemical Society* **1956**, *78*, 4736-4743.
- (143) Brycesmith, D.; Gilbert, A. *Tetrahedron* **1976**, *32*, 1309-1326.
- (144) Ors, J. A.; Srinivasan, R. *Journal of Organic Chemistry* **1977**, *42*, 1321-1327.
- (145) Annis, G. D.; Paquette, L. A. *Journal of the American Chemical Society* **1982**, *104*, 4504-4506.
- (146) Castanet, A. S.; Colobert, F.; Schlama, T. *Organic Letters* **2000**, *2*, 3559-3561.
- (147) Ramirez, F.; Mckelvie, N.; Desai, N. B. *Journal of the American Chemical Society* **1962**, *84*, 1745-&.
- (148) Corey, E. J.; Fuchs, P. L. *Tetrahedron Letters* **1972**, 3769-&.

- (149) Colvin, E. W.; Hamill, B. J. *Journal of the Chemical Society-Perkin Transactions 1* **1977**, 869-874.
- (150) Fujikawa, N.; Ohta, T.; Yamaguchi, T.; Fukuda, T.; Ishibashi, F.; Iwao, M. *Tetrahedron* **2006**, *62*, 594-604.
- (151) Lara-Ochoa, F.; Espinosa-Perez, G. *Tetrahedron Letters* **2007**, *48*, 7007-7010.
- (152) Fürstner, A.; Nikolakis, K. *Liebigs Annalen* **1996**, *7*.
- (153) Bui, V. P.; Hudlicky, T.; Hansen, T. V.; Stenstrom, Y. *Tetrahedron Letters* **2002**, *43*, 2839-2841.
- (154) Nam, N. H.; Kim, Y.; You, Y. J.; Hong, D. H.; Kim, H. M.; Ahn, B. Z. *Bioorganic & Medicinal Chemistry* **2003**, *11*, 1021-1029.
- (155) Lawrence, N. J.; Ghani, F. A.; Hepworth, L. A.; Hadfield, J. A.; McGown, A. T.; Pritchard, R. G. *Synthesis-Stuttgart* **1999**, 1656-1660.
- (156) Li, H. B.; Yang, H.; Petersen, J. L.; Wang, K. K. *Journal of Organic Chemistry* **2004**, *69*, 4500-4508.
- (157) Nwokogu, G. C. *Tetrahedron Letters* **1984**, *25*, 3263-3266.
- (158) Sonogashira, K.; Tohda, Y.; Hagihara, N. *Tetrahedron Letters* **1975**, 4467-4470.
- (159) Monk, K. A.; Siles, R.; Hadimani, M. B.; Mugabe, B. E.; Ackley, J. F.; Studerus, S. W.; Edvardsen, K.; Trawick, M. L.; Garner, C. M.; Rhodes, M. R.; Pettit, G. R.; Pinney, K. G. *Bioorganic & Medicinal Chemistry* **2006**, *14*, 3231-3244.
- (160) Jonnalagadda, S. S.; terHaar, E.; Hamel, E.; Lin, C. M.; Magarian, R. A.; Day, B. W. *Bioorganic & Medicinal Chemistry* **1997**, *5*, 715-722.
- (161) Long, J.; Yuan, Y.; Shi, Y. *Journal of the American Chemical Society* **2003**, *125*, 13632-13633.
- (162) Lorenz, J. C.; Long, J.; Yang, Z. Q.; Xue, S.; Xie, Y.; Shi, Y. *Journal of Organic Chemistry* **2004**, *69*, 327-334.
- (163) Miller, W. T.; Kim, C. S. Y. *Journal of the American Chemical Society* **1959**, *81*, 5008-5009.
- (164) Chien, C. T.; Tsai, C. C.; Tsai, C. H.; Chang, T. Y.; Tsai, P. K.; Wang, Y. C.; Yan, T. H. *Journal of Organic Chemistry* **2006**, *71*, 4324-4327.
- (165) Ozdemirhan, F. D.; Celik, M.; Atli, S.; Tanyeli, C. *Tetrahedron-Asymmetry* **2006**, *17*, 287-291.
- (166) Krepski, L. R.; Hassner, A. *Journal of Organic Chemistry* **1978**, *43*, 3173-3179.
- (167) Brocksom, T. J.; Coelho, F.; Depres, J. P.; Greene, A. E.; de Lima, M. E. F.; Hamelin, O.; Hartmann, B.; Kanazawa, A. M.; Wang, Y. Y. *Journal of the American Chemical Society* **2002**, *124*, 15313-15325.
- (168) Reed, M. W.; Pollart, D. J.; Perri, S. T.; Foland, L. D.; Moore, H. W. *Journal of Organic Chemistry* **1988**, *53*, 2477-2482.
- (169) Liebeskind, L. S.; Fengl, R. W.; Wirtz, K. R.; Shawe, T. T. *Journal of Organic Chemistry* **1988**, *53*, 2482-2488.
- (170) van de Sande, M.; Gais, H. J. *Chemistry-a European Journal* **2007**, *13*, 1784-1795.
- (171) Nerdinger, S.; Kendall, C.; Cai, X.; Marchart, R.; Riebel, P.; Johnson, M. R.; Yin, C. F.; Henaff, N.; Eltis, L. D.; Snieckus, V. *Journal of Organic Chemistry* **2007**, *72*, 5960-5967.
- (172) Peterson, M. A.; Nilsson, B. L. *Synthetic Communications* **1999**, *29*, 3821-3827.
- (173) Fu, N.; Allen, A. D.; Kobayashi, S.; Tidwell, T. T.; Vukovic, S.; Matsuoka, T.; Mishinia, M. *Journal of Organic Chemistry* **2008**, *73*, 1768-1773.
- (174) Brimble, M. A.; Kowalczyk, R.; Harris, P. W. R.; Dunbar, P. R.; Muir, V. J. *Organic & Biomolecular Chemistry* **2008**, *6*, 112-121.
- (175) Horton, D. *Organic Syntheses, Vol 5* **1973**, *5*, 1.

## Abstract

CA-4 is a biologically very active compound by binding to the colchicine binding site which lead to the inhibition of microtubule polymerization as well as showing antivasular effects by selectively shutting down the tumor blood flow. To avoid the disadvantage of rather low *in vivo* efficiency resulting from the isomerization of the *cis*-stilbene derivative to the thermodynamically more stable *trans*-isomer, our research group started the project for CA-4 analogs synthesis. The incorporation of carbocycles with different ring sizes on the connecting carbon-bridge of the natural compound prevents the system to undergo *cis-trans*-isomerization. The synthesis of the cyclopropane derivative of CA-4 (**9**) *via* the cyclopropanation reaction with diazomethane, and further analogs with incorporated moieties for better water solubility (**268**, **273**) were achieved within this diploma thesis. In cooperation with the Department of Pharmacodynamics and Biopharmacy of the University of Szeged we were able to investigate the biological activity against two human cancer cell lines (HeLa and MCF 7) of the compounds prepared within this work.

## Zusammenfassung

Der Naturstoff Combretastatin A-4 (CA-4) wurde 1982 erstmals, gemeinsam mit verwandten Verbindungen aus einer afrikanischen Weidenart, *Combretum caffrum*, isoliert. Die Verbindung zeigt sehr starke antimetabolische Wirkung gegen einige menschliche Krebszelllinien. CA-4 bindet an Tubulin an der Colchicin-Bindungsstelle und unterdrückt somit das Polymerisationsgleichgewicht der Mikrotubuli in der Zelle. Dieser Prozess führt zum Zell-Zyklus-Arrest beim Übergang von Meta- zur Anaphase und letztendlich zur Apoptose.

CA-4 zeigt in lebenden Systemen zwei große Nachteile. Einerseits kommt es zur Isomerisierung der cis-Doppelbindung zum thermodynamisch stabileren *trans*-Isomer, welches keine biologische Aktivität zeigt, und andererseits ist der Naturstoff sehr schlecht wasserlöslich. Um diese beiden Nachteile zu umgehen wurden in den vergangenen Jahren unzählige Derivate synthetisiert mit dem Ziel die biologische Wirksamkeit im Vergleich zum Naturstoff zu erhöhen.

Ziel dieser Arbeit war die Synthese von CA-4 Derivaten durch Modifikation der cis-Doppelbindung. Die Einführung von Carbozyklen mit unterschiedlicher Ringgröße verhindert die cis-trans-Isomerisierung.

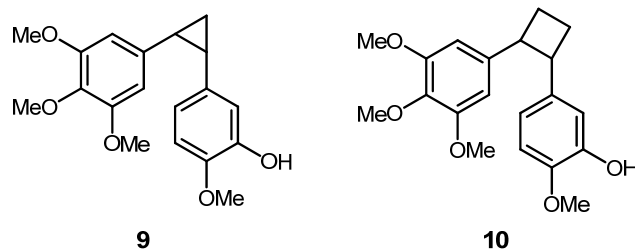


Abbildung 1: CA-4 Derivate

Die Synthese des Cyclopropan-Derivates über die Cyclopropanierung mit Diazomethan als Schlüsselschritt ist im Laufe dieser Diplomarbeit gelungen. Alle End- und Zwischenprodukte wurden in Kooperation mit dem Institut für Pharmakodynamik und Biopharmazie an der Universität Szeged an zwei verschiedenen Zelllinien (HeLa und MCF 7) auf ihre biologische Aktivität getestet.



# Curriculum Vitae

## PERSÖNLICHE ANGABEN

---

- Vor- und Zuname: Rita Fürst
- Geburtsdatum: 12. Mai 1984
- Geburtsort: Oberpullendorf
- Nationalität: Österreich

## SCHULE & AUSBILDUNG:

---

- 03/2008 Beginn der Diplomarbeit „**Synthesis and Biological Evaluation of Novel Combretastatin A-4 Analogs**“ unter der Betreuung von O. Univ.-Prof. Dr. Johann Mulzer
- 10/2006 Abschluss des ersten Studienabschnittes mit ausgezeichnetem Erfolg
- 10/2003 Diplomstudium Chemie Universität Wien
- 06/2003 Matura bestanden mit ausgezeichnetem Erfolg
- 09/1998 – 06/2003 Gymnasium für Studierende der Musik / Oberstufe Oberschützen
- 09/1994 – 06/1998 Evangelisches Realgymnasium / Unterstufe Oberschützen